A COMPARATIVE STUDY OF CENTRAL CARDIOVASCULAR DYNAMICS IN VERTEBRATES

by

BRIAN LOWELL LANGILLE

B.Sc., University of British Columbia, 1969

M.Sc., University of British Columbia, 1970

A THESIS SUBMITTED IN PARTIAL FULFILLMENT OF THE REQUIREMENTS FOR THE DEGREE OF

DOCTOR OF PHILOSOPHY

in the Department

of

ZOOLOGY

We accept this thesis as conforming to the required standard

THE UNIVERSITY OF BRITISH COLUMBIA

September, 1975

In presenting this thesis in partial fulfilment of the requirements for an advanced degree at the University of British Columbia, I agree that the Library shall make it freely available for reference and study. I further agree that permission for extensive copying of this thesis for scholarly purposes may be granted by the Head of my Department or by his representatives. It is understood that copying or publication of this thesis for financial gain shall not be allowed without my written permission.

Department of Zoology

The University of British Columbia
2075 Wesbrook Place
Vancouver, Canada
V6T 1W5

Date Oct 21, 1975

Abstract

The dynamic properties of blood flow through the heart and arterial systems have been examined in representative species of fish, amphibia, birds and mammals. In the amphibian examined, the bullfrog Rana catesbeiana, the conus arteriosis was found to perform no active valving function and hence was not responsible for shunting blood to, or away from, the lungs in response to lung ventilation or apnoea. Conus volume changes generated a small fraction of cardiac stroke volume although a low impedance of the pulmocutaneous vasculature resulted in a preferential distribution of this blood to the gas exchanger circulations. The pressure pulse took a negligible fraction of the cardiac cycle to traverse the arterial tree and peripherally recorded pressures were similar in profile to central pressures, these results indicating that wave transmission effects were small. Impedance analysis of pressure and flow data suggested that a two element lumped parameter (windkessel) model accurately describes arterial pressure-flow relationships in the bullfrog. Arterial haemodynamics in the cod, Gadus morhua was examined in terms of a hydraulic model of the 'in series' gill and systemic circulations. Results indicate that the dorsal aorta is not a rigid conduit and the compliance of this vessel has a marked effect on the pulsatility of blood flow through

the gills.

In the duck, Anas platyrhynchos pressure and flow profiles have been mapped throughout the central circulation. Mean systemic arterial pressure (143 ± 2 mm Hg) and cardiac output (219 ± 7 ml/min per kg) were high compared with mammals of similar size although pulmonary pressures were not high, perhaps because of the unique structure of the avian lung. 75% of total systemic flow was distributed to wing, flight muscles and head by the brachiocephalic arteries. Unlike the situation in the bullfrog wave transmission phenomena had a pronounced effect on arterial pressure and flow signals and impedance data were characterised by features commonly ascribed to the effects of wave reflection. Therefore it is concluded that the windkessel is not a realistic model of the avian arterial system.

Pressures generated in both ventricles of the rabbit heart were influenced by contraction of the opposite ventricle although the influence of right ventricular contraction on left ventricular pressure was negligible during normal cardiac function and only became marked when the right ventricular volumes were large or left ventricular volumes were small. Comparison of the effects of vasomotion and artificially induced discrete reflections confirmed that pulse wave transmission effects in mammalian arteries are dominated by reflections from the arteriolar beds. Although studies of a hydraulic model

confirmed the viability of transmission line theories on the effects of spatial variations in arterial wall elasticity, close examination suggests that this 'elastic taper' does not have a dominant effect on wave propagation.

TABLE OF CONTENTS

General Introduction 1

Section I. Central Blood Flow in the Bullfrog, *Rana Catesbeiana*

Introduction 18

Methods 24

Results 29

Discussion 53

Section II. The Single Circulation in the Cod, *Gadus morhua*

Introduction 60

Methods 64

Results 68

Discussion 76

Section III. Central Cardiovascular Dynamics of Ducks

Introduction 81

Methods 83

Results 93

Discussion 103

Section IV. The Effects of 'Elastic Taper' and Reflections on Wave Propagation in Mammalian Arteries

Introduction 109

Methods 113

Results 123

Discussion 133

Section V. Mechanic Interaction Between the Ventricles of the Mammalian Heart

Introduction 140

Methods 143

Results 147

Discussion 156

General Discussion 160

Summary 163

Bibliography 166

Appendix 182

Bibliography 185

LIST OF FIGURES

Figure 1.	Blood flow pathways in vertebrates.	3
Figure 2.	Central and peripheral arterial pressure profiles from the rabbit.	9
Figure 3.	Impedance curves for windkessel models with different time constants.	12
Figure 1-1.	Intraventricular cavity of the frog heart.	30
Figure 1-2.	The conus arteriosis and spiral valve of the frog heart.	31
Figure 1-3.	Frozen sections of the conus arteriosis and spiral valve.	33
Figure 1-4.	Blood pressures in the ventricle, conus arteriosis and arterial arches of the bullfrog.	35
Figure 1-5.	Blood pressures in the systemic arch, pulmocutaneous arch and ventricle of the bullfrog.	36
Figure 1-6.	Arch pressures in the bullfrog during synchronous contraction of the ventricle and conus arteriosis.	39
Figure 1-7.	Effect of prolonged coronary ligation on central pressures in the bullfrog.	41
Figure 1-8.	Test of valve competency in the relaxed frog heart.	42

Figure 1-9. Systemic and pulmocutaneous arch pressures and flows in the bullfrog. 45

Figure 1-10. Arch pressures and flows before and during apnoea. 47

Figure 1-11. Input impedance of the systemic circulation of the frog. 49

Figure 1-12. Input impedance of the pulmocutaneous circulation in the bullfrog during lung ventilation and during apnoea. 50

Figure 1-13. Central and peripheral arterial pressures in the bullfrog. 52

Figure 2-1. Ventral and dorsal aortic blood flows in the cod. 70

Figure 2-2. Dorsal aortic pressure and flow in the cod. 71

Figure 2-3. Effect of 'dorsal aortic' compliance on pressures and flows in a hydraulic model of the fish circulation. 73

Figure 2-4. Gill and systemic flow relationships predicted by an electrical analogue of the fish circulation. 74

Figure 3-1. Technique for measuring arterial pulse wave velocity in the duck. 87

Figure 3-2.	Pressures and flows in the central circulation of the duck.	94
Figure 3-3.	Overlap diagram of pressures and flows recorded in the duck.	95
Figure 3-4.	Central and peripheral arterial pressures in the duck.	97
Figure 3-5.	Effect of adrenaline on the pulmonary arterial flow profile in the duck.	100
Figure 3-6.	Input impedances to the systemic and pulmonary circulations of the duck.	101
Figure 4-1.	Apparatus for measuring elasticity .	114
Figure 4-2.	Elastic modulus vs. position in a hydraulic model.	124
Figure 4-3.	Pressure wave amplification in an elastically tapered tube.	125
Figure 4-4.	Transfer function for the pressure wave propagated along an elastically tapered tube.	127
Figure 4-5.	Central and peripheral pressures recorded in the rabbit aorta. The effect of vasoactive drugs.	129
Figure 4-6.	The effects of vasoactive drugs on the transfer function of arterial pressure wave propagation.	131

Figure 5-1. Ventricular pressures and rates of change of pressures in the rabbit during aortic occlusion. 148

Figure 5-2. Ventricular pressures during sinusoidal infusion of saline into the left ventricle. 150

Figure 5-3. The effect of pulmonary outflow occlusion on ventricular pressures and rates of change of pressures. 152

Figure 5-4. Inter-ventricular pressure transference in the excised heart in rigor mortis. 154

Figure A-1. Manometer frequency response determined by the Fourier transform technique. 183

LIST OF TABLES

Table 1. Values for cardiovascular parameters measured in cod. 69

ACKNOWLEDGEMENTS

I wish to thank Dr. D.R. Jones for his enthusiastic supervision of this research and particularly for his efforts in acquainting me with experimental techniques of cardiovascular biophysics.

I am also grateful to Colin Parkinson and Daphne Hards for their technical assistance and to Mr. Eric Minch for assistance with the computer analysis of data in Section IV.

Bill Milsom and Nigel West contributed a number of helpful suggestions on the presentation of my results.

Finally I am most grateful to Lorraine Langille for proof-reading and typing the thesis and for her support and encouragement throughout the course of this study.

All in vivo experiments on the cod in Section II were performed by D.R. Jones, D.J. Randall and G. Shelton although these workers do not necessarily agree with the conclusions I have drawn from their results.

Many of the experiments in Sections I and III were performed jointly with D.R. Jones although D.R. Jones does not necessarily agree with my interpretation of the results of these experiments.

GENERAL INTRODUCTION

In all but the smallest, most primitive organisms diffusion alone is inadequate for the supply of oxygen and nutrients to, and the removal of metabolic wastes from, the tissues; therefore most animals utilize some sort of convective transport system. In almost all vertebrates this system consists of a central pump, the heart, which drives a liquid transport medium, the blood, continuously around a closed vascular system. The vascular system distributes blood to specialized exchangers (e.g. gills, lungs, gut), where local diffusion supplies nutrients and oxygen to the blood, and to the tissues where these nutrients are absorbed. Metabolic wastes transferred to the blood from the tissues are removed by again passing the blood through exchanger systems (e.g. kidney). Transfer at the tissues takes place across a fine network of microscopic capillary vessels, an arrangement that distributes blood supply to the deepest regions of the tissues and permits fine control of blood flow distribution in the interests of maintaining homeostasis. Thus an understanding of cardiovascular function requires a knowledge of the transport properties of the blood (e.g. blood-gas association, dissociation characteristics), the mechanism of transfer across capillary walls, the regulation of the functions of the cardiovascular system and the mechanical

aspects of pumping blood through a complex network of blood vessels. It is with the last of factors that the present study is concerned.

A major difficulty of a comparative study of haemodynamics in vertebrates is the marked variability in cardiovascular form and function which has accompanied vertebrate phylogenetic development. Such variations are intimately related to the different environments which vertebrate species inhabit and in this respect adaptions to different modes of respiratory gas exchange are particularly important. Fig. 1 illustrates a schematic view of the manner in which blood is distributed to the gas exchanger and tissue circulation in vertebrates. The arrangement in fishes of a direct, 'in series' connection between the gill and systemic circulations with no intervening pump poses unique questions about the dynamic interaction between these two systems and although Satchell (1971) has outlined some of the associated problems no experimental investigations have been published. Instead experimental studies deal mainly with net cardiac output (Murdaugh et al., 1965; Mott, 1957) and comparisons of arterial blood pressures proximal and distal to the gills (Stevens and Randall, 1967). While such measurements supply valuable information on cardiovascular adjustments to exercise (Stevens and Randall, 1967 a and b) and changing environmental factors (Holeton and Randall, 1967) they

Figure 1. Blood flow pathways in fish, amphibia, mammals (and birds) and reptiles.

fishes

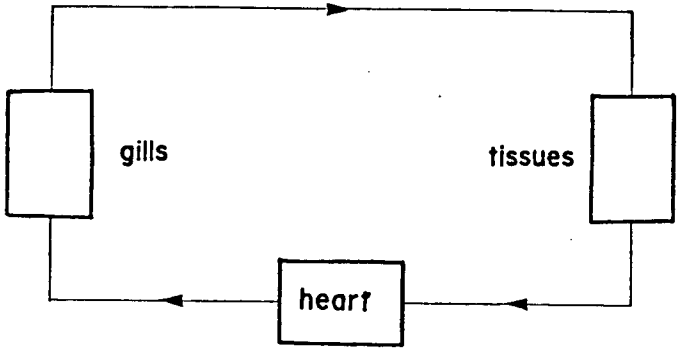

amphibia

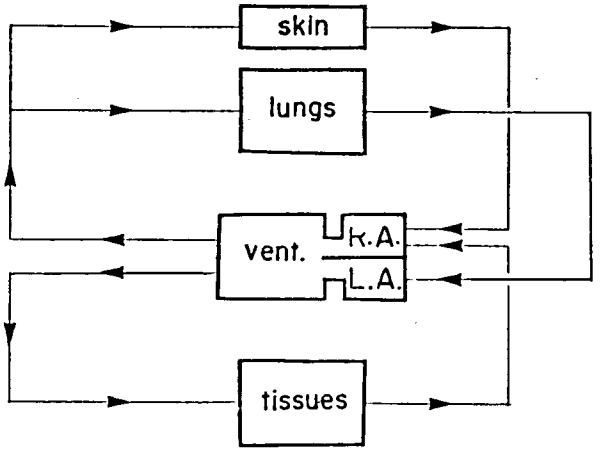

mammals

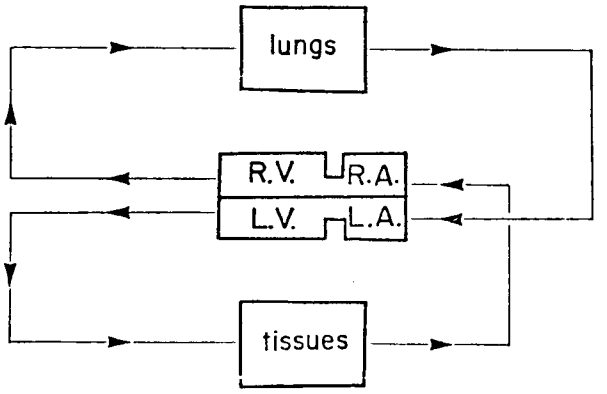

crocodilia

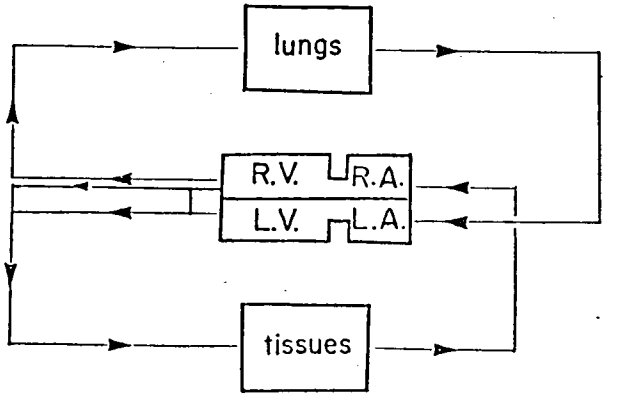

non-crocodilian reptiles

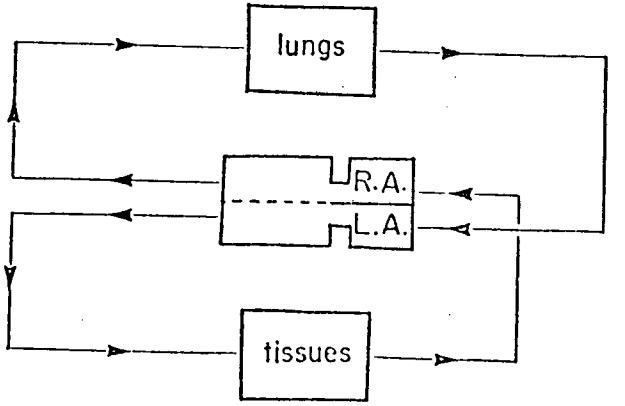

provide limited information on the dynamics of blood flow. The temptation to apply principles of blood flow in single vascular beds to the combined gill and systemic circulations of the fish is dangerous and has led to erroneous arguments on the nature of the pressure gradient across the gills (Holeton and Randall, 1967).

In amphibia blood in the single ventricle travels to either the gas exchanger (lungs, skin) or the tissue circulations rather than sequentially through both, an arrangement which allows shunting of blood to or away from the lungs in response to changes in oxygen availability (Shelton, 1970; Emilio and Shelton, 1972). In birds and mammals blood flow again passes sequentially through the tissues and the lungs although in this case a second pump, the right ventricle, drives blood around the lung circulation. The existence of two completely divided circulations requires that the output of the two pumps be equal if volume loading of one circulation is to be avoided and no shunting to or from the lungs is possible. The situation in the non-crocodilian reptiles (Chelonia and Squamata) is somewhat intermediate between that of amphibia and mammals with the ventricle being partially divided. It may be that, like amphibia, these reptiles shunt blood to or from the lungs in response to changing conditions but White (1968) feels that, at least when these animals are resting and breathing air, there

is effective separation of cardiac cavities and the situation approaches that of mammals. In crocodilian reptiles the two ventricles are completely divided and although the left aorta arises from the right ventricle it anastomoses with the right aorta via the foramen Pinizzae and normally high systemic pressures transmitted through the foramen prevent right ventricular ejection into this vessel. Nonetheless the possibility of blood shunting remains if under certain circumstances right ventricular pressures reach those of the left ventricle.

Obviously an analysis of cardiovascular dynamics in any vertebrate species must involve consideration of the pumping characteristics of the heart, the dynamic properties of the vascular beds and the interaction between these two factors. Examinations of cardiac function in lower vertebrates have traditionally been based on purely anatomical studies (the study of Sabatier, 1873 is a classic examination of anatomy of vertebrate hearts whereas that of Sharma, 1957 is a modern application of the same approach). However the advancement of sophisticated techniques for measuring blood pressures, flow rates and flow patterns in the past two decades has resulted in many studies of both anatomy and physiology which, in some cases, have disproven theories based on purely anatomical investigations (for example see de Graff, 1957). In fishes this approach has established that the conus arteriosis of

elasmobranchs (sharks and skates), a contractile chamber between the ventricle and the ventral aorta, serves a type of active valving function (Satchell and Jones, 1967) while the similarly situated bulbus arteriosis of teleost fishes, is a simple elastic chamber which serves to depulsate ventricular ejection (Johansen, 1962; Randall, 1968). The complex nature of blood flow through the partially divided amphibian and reptilian hearts has been elucidated by correlating the cyclical volume changes of the cardiac chambers with pressure recordings (Shelton and Jones, 1965(b)) and by following dye streams (Simons, 1957) and radio-opaque madia (Johansen 1971, White, 1968) through the heart. Despite such advances many problems remain. Even the mechanics of the mammalian heart, although widely studied, is in many ways poorly established and some of the problems encountered in analyzing the function of this pair of interconnected, asymmetrical, muscular pumps which contract in a complex fashion may be technically insurmountable at the present time.

The complex nature of cardiac contraction in most vertebrate means that attempts to assess many aspects of blood flow through the cardiac chambers are limited to qualitative descriptions. On the other hand the nearly one-dimensional flow of blood in cylindrically symmetrical vessels of the arterial tree makes a more quantitative approach feasible and

two such approaches have been applied to the study of blood flow in mammalian arteries. According to the first approach the high pressures produced by cardiac ejection (systole) cause a synchronous expansion of the arterial tree and thus the arteries hold an increased volume of blood during this phase of the cycle. During diastole passive contraction of these vessels drives this stored blood through the terminal capillary beds to maintain peripheral flow between cardiac ejections; thus the arterial circulation is viewed as an elastic reservoir connected to outflow resistance vessels. Otto Frank (1899) proposed the first quantitative analysis of this model which is now universally referred to as the 'elastic resevoir' or 'windkessel' model. According to Frank the dynamics of the blood flow in arteries could be defined completely by the compliance of the arterial system, K, and the resistance of the peripheral beds, R. (K is the change in volume of the arterial elastic resevoir divided by the increment in pressure which caused this change and R is the ratio of pressure to volume flow rate produced when a static pressure is applied to the system). Analysis of this model led to the relation

$$Q = P/R + K\frac{\partial P}{\partial t} \qquad (1)$$

where Q = volume flow rate of blood into the system

P = arterial pressure

$\frac{\partial P}{\partial t}$ = rate of change of arterial pressure .

This equation specifies the relationship between arterial pressure and flow and was of immediate interest to cardiologists since it implies that cardiac output could be calculated from routine arterial pressure measurements provided the physical parameters, K and R, could be determined. However attempts to apply this analysis to the mammalian circulation were not highly productive and it was recognized that a major limitation of this theory was the implicit assumption that the pressure changes generated by cardiac ejection occur simultaneously throughout the system (McDonald, 1974). In reality each heart beat sends out a pulse wave which travels through the arterial system and arrives at different sites at different times and consequently instantaneous flow rate predicted by equation (1) would depend on the site at which arterial pressure was recorded. In addition, a number of other features of arterial haemodynamics could not be reconciled with the windkessel model. Not only does the pressure pulse arrive later at sites more distal to the heart but it exhibits marked changes in waveform as pulse pressure increases considerably (up to 100%) and secondary waves appear in the diastolic portion of the pulse (Fig. 2). Furthermore pressure-flow relationships at the input to the system could not be predicted from a windkessel approach.

A major advantage of the windkessel model was that the mathematical analysis was relatively simple and all of the

Figure 2. Pressures recorded in the root of the aorta (smaller profile) and the distal abdominal aorta (larger profile) of the rabbit.

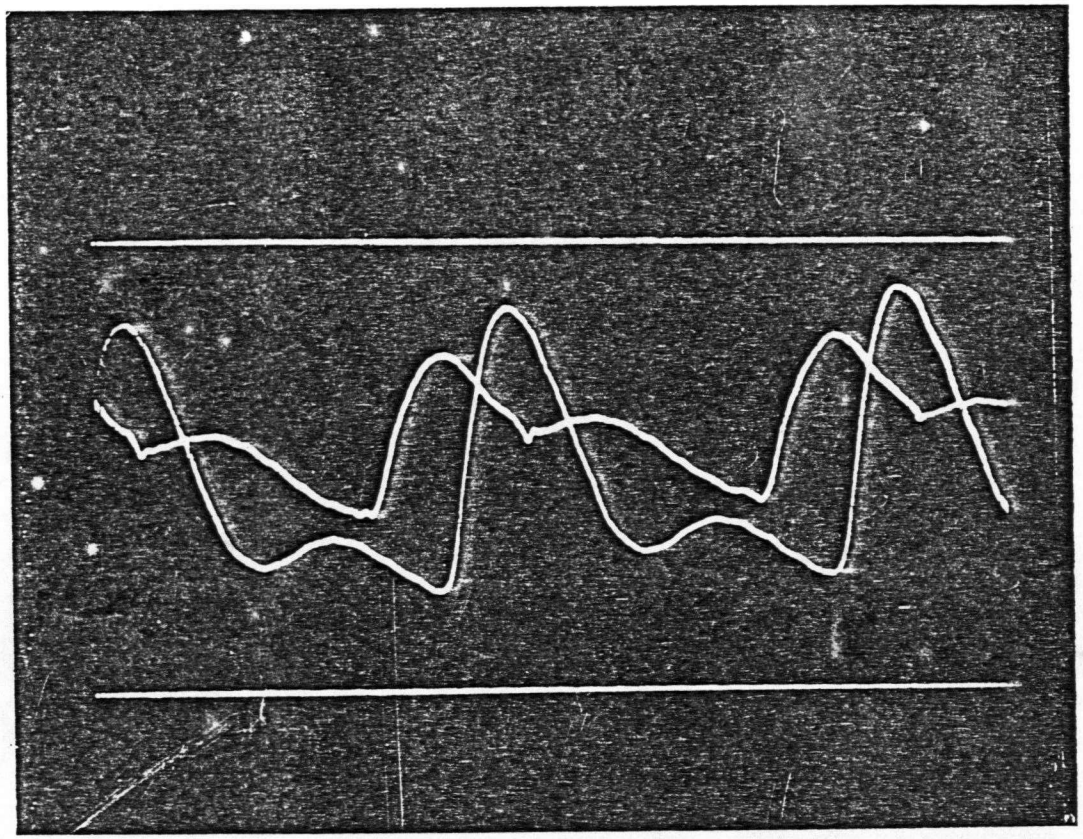

75 mm Hg

0·5 SEC

complex elastic and geometric properties of the arterial system were lumped into two parameters, the compliance of the major arteries and the resistance of the peripheral beds. However analysis of wave propagation through the system requires a more complex approach. Firstly, the analysis of wave phenomena is only mathematically tractable if sinusoidal waves are involved and consequently complex (non-sinusoidal) arterial pressure and flow waves must be represented by Fourier series. According to Fourier's theorem any complex waveform of constant frequency can be represented by its mean value plus a sum of sinusoidal waves of various amplitudes oscillating at the frequency of the complex wave and at multiples of this frequency. Thus if heart rate is 1 beat per second then the arterial pressure or flow wave can be expressed as the mean pressure or flow plus a sum of sinusoidal waves of frequencies of 1,2,3,... cycles per second. These sinusoidal waves are referred to as the 1st, 2nd, 3rd,... harmonics of the complex wave and under certain assumptions which are generally considered acceptable in the cardiovascular system (Attinger et al., 1965; McDonald, 1974) each harmonic of pressure is related only to the corresponding harmonic of flow and vice versa. Generally, no more than the first five to ten harmonics make measurable contributions to arterial pressure and flow waves. The advantage of the Fourier analysis approach is that by analyzing the response of the arterial system to

sinusoidal driving pressures the response to an arbitrary oscillation in pressure can be derived. A further implication of Fourier's theory is that when a system is driven by a complex oscillation it is necessary to understand the response of the system both at the frequency of the driving force and at the frequencies of the higher harmonics.

The dependence of sinusoidal pressure-flow relationships on frequency is most succinctly expressed in terms of vascular impedance curves. Impedance modulus is the ratio of the amplitude of the pressure wave to that of the flow wave and impedance phase describes the degree to which the pressure oscillation leads the flow oscillation (in simple terms, the amount by which crests (and troughs) of the two waves are out of synchrony). Because the viscous and inertial properties of the blood and the compliance of the arterial wall effect blood flow to a different degree at different frequencies impedance is highly dependent on frequency. Fig. 3 illustrates a set of impedance curves applying to windkessel models of different time constants, (The time constant of a windkessel, the product of resistance and compliance, is a measure of how long it takes the arterial elastic resevoir to discharge through the peripheral resistance if further cardiac ejection is prevented.) Also included in Fig. 3 is a sample of the type of impedance curve commonly recorded in the aortic root of mammals.

Figure 3. Impedance curves for windkessel systems (solid curves) of various time constants (T) as well as for the systemic circulation of the dog (dashed profile - after O'Rourke and Taylor, 1967).

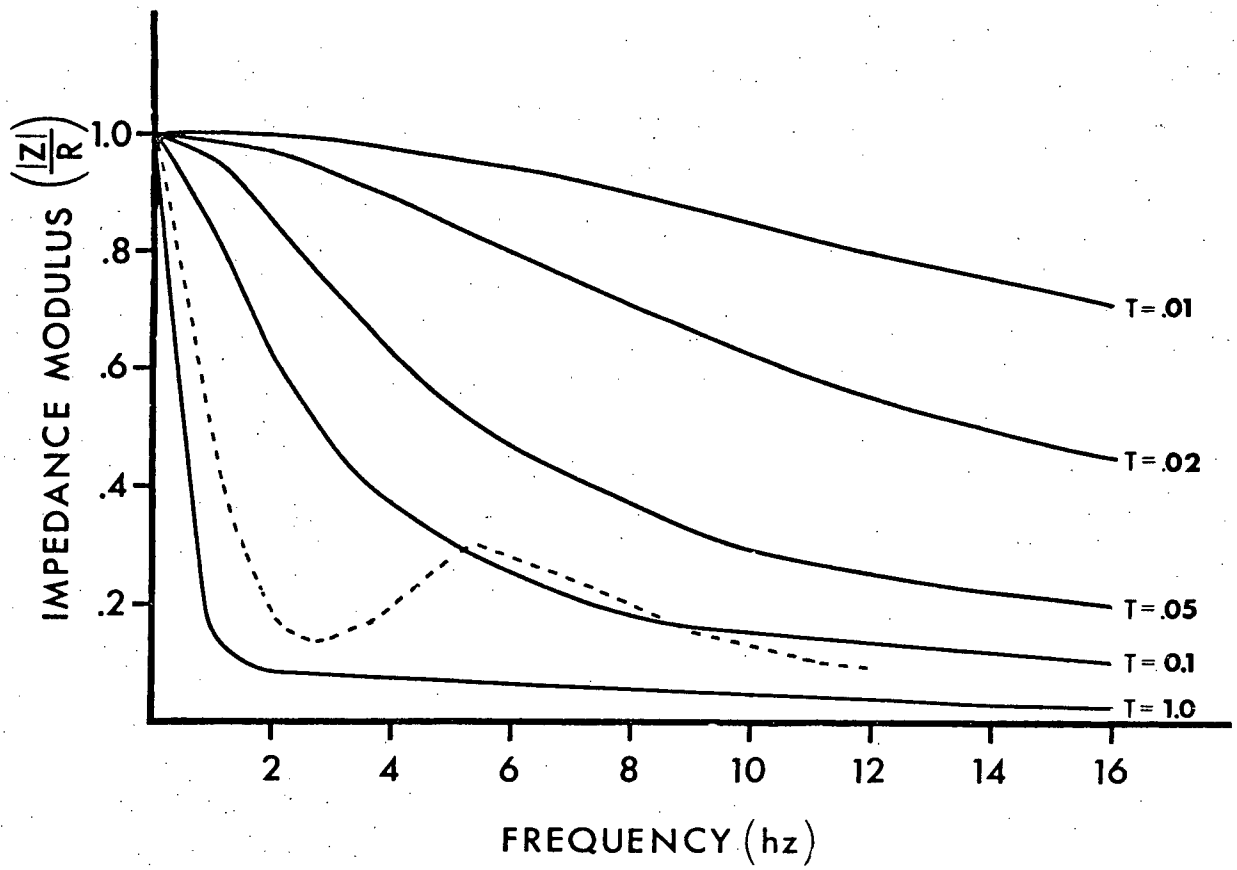
IMPEDANCE MODULUS (|Z|/R)
1.0
.8
.6
.4
.2
T = .01
T = .02
T = .05
T = 0.1
T = 1.0
2
4
6
8
10
12
14
16
FREQUENCY (hz)

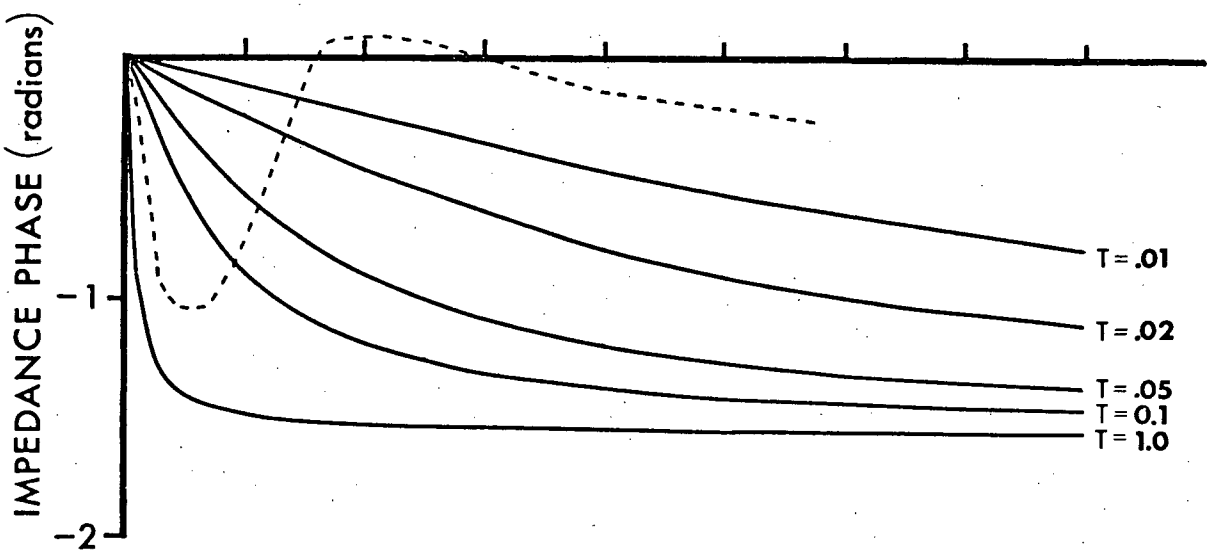
IMPEDANCE PHASE (radians)
-1
-2
T = .01
T = .02
T = .05
T = 0.1
T = 1.0

The Fourier series approach was employed by Womersley (1958) who performed a sophisticated mathematical analysis of wave propagation through a viscous fluid contained in a visco-elastic tube. The analysis involved simultaneous solution of the momentum equations for the fluid and the membrane equations of the tube and experimental studies by McDonald (1955, 1974) demonstrated that Womersley's results were applicable to short, uniform lengths of arteries. Although a quantitative synthesis of wave propagation throughout the arterial tree was not possible a number of generalizations could be made. Womersley predicted that branch sites and other discontinuities in the arterial tree would give rise to reflected waves which are directed back towards the heart. More recent theories (Taylor, 1964, 1965(a)) suggest that the increase in wall stiffness with distance from the heart (Bergel, 1961; Learoyd and Taylor, 1966) produce effects which may augment those of reflections although experimental verification of this theory has not yet been presented. Thus the picture which emerges is one of wave propagation through an interconnected system of tubes of spatially varying properties with reflected waves being sent back towards the heart from reflection sites scattered throughout the system. The pattern of pressure signals recorded at different sites in the arterial tree of mammals is well predicted by a wave transmission model and can be attributed largely to

interference between outgoing and reflected waves (O'Rourke, 1967; McDonald, 1974). The pattern of vascular impedance both at the input to the systemic circulation (Fig. 3) and at more peripheral beds is also compatible with this model (McDonald, 1974).

The above considerations indicate why most investigators feel that windkessel models have outlived their usefulness in studies of mammalian circulations, however there may be good reason to suspect that such models may be applicable to some non-mammalian systems. Taylor (1964) measured arterial pressure at different sites within the aortae of turkeys and finding no evidence of wave transmission effects he speculated that a windkessel model may apply to the circulations of birds. In addition, many small poikilotherms exhibit lower heart rates than similarly sized mammals and unless major arteries are long, which will not be the case in smaller species, or arterial pulse wave velocities are low, the transit time of the pulse through the arterial system may be negligible compared with the cardiac cycle. If this is the case then wave transmission effects will be minor and simpler models may be applied. On the other hand an 'a priori' assumption that pulse wave velocities and hence arterial compliances, in these species are within the mammalian range seems questionable. It has been suggested (Taylor, 1964) that arterial systems exhibit an optimal compliance which

represents a balance between reducing blood flow pulsatility and decreasing the time required to accomplish regulatory changes in pressure. (Obviously in a highly compliant system more blood must be shifted from the venous to arterial circulation in order to elevate pressure.) The lower heart rates prolong the time over which the arteries recoil and discharge and hence flow pulsatility may be high if vessels are not highly distensible. In addition the less active life-style of many poikilotherms, compared with most mammals of similar size, may indicate that rapid blood pressure regulation is of a lower priority.

In the present study the dynamics of blood flow through the hearts and arterial systems of a number of vertebrates has been investigated with special emphasis placed on the interpretation of species differences in terms of haemodynamic models. In the first section the circulation of the amphibian, Rana catesbeiana, is examined in order to describe the function of the partially divided cardiac chambers and to establish the dynamic properties of the arterial systems that these chambers supply. Since amphibia often experience rapid shifts from a terrestrial to an aquatic environment pronounced cardiovascular adjustments to different modes of respiration must be made. Consequently the effect of lung ventilation on the dynamic properties of the arterial circulation has also been examined.

In the second section the implications of the 'in series' gill and tissue circulations of the fish have been analyzed in terms of theoretical and hydraulic models in an attempt to clarify the physical interaction between these two systems. Model predictions are assessed in terms of pressure and flow data from *in vivo* investigations of the circulation of the cod, *Gadus morhua*.

A marked paucity of information on haemodynamics in birds prompted the detailed examination of central cardiovascular dynamics of the duck, *Anas platyrhynchos*, in Section III. Pressure and flow profiles have been mapped throughout the central circulation and the relationships between pressure and flow have been examined in terms of proposed windkessel (Taylor, 1964) and wave transmission models. Section IV includes a test of theories of the effects of spatial variations in arterial wall elasticity (elastic taper) as well as an evaluation of the importance these effects in the mammalian systemic circulation compared with those of discrete wave reflections.

Although the mammalian heart is completely divided and there is total separation of flow to the lung and systemic circulations it cannot be inferred that the nature of ejection from each ventricle is independent of the function of the opposite ventricle. In the final section the mammalian heart is examined for mechanical interaction between the two ventricles during cardiac contraction. In addition to examining suggestions

that left ventricular contraction influences pressures generated by the right ventricle evidence is presented that, in some circumstances, right ventricular contraction significantly influences left ventricular pressure.

SECTION I

Central Blood Flow in the Bullfrog, Rana Catesbeiana

Introduction

In terms of gross morphological structure the central circulation of the frog is intermediate between that of fishes and higher vertebrates. The frog heart retains the four basic chambers found in the fish heart; the sinus venosus, auricle, ventricle and conus arteriosis (or bulbus, in teleost fishes), whereas, the distributing arteries more closely follow the pattern of higher vertebrates with the third, fourth and sixth aortic arches persisting as the carotid, systemic and pulmonary (pulmocutaneous) arteries. The pulmocutaneous circulation is completely separated from the systemic circuits and the lungs return oxygenated blood to the left side of a completely divided auricle although this separation of oxygenated and oxygen-poor blood is lost in the ventricle, which, like the ventricle of fishes, is undivided. Here the term 'oxygen-poor' is used since right atrial blood includes blood returning from the skin gas exhanger and thus the term 'venous blood' or 'de-oxygenated blood' would seem inappropriate. Nonetheless, in anura lung ventilation predominates (Hutchison, et al, 1968; Jones 1972(b)) and marked PO_2 gradiants between the two atria are observed (DeLong, 1962, Johansen and Ditadi, 1966). The

absence of a totally divided heart obviates the necessity encountered by higher vertebrates of an equal distribution of blood to the lung and body circulations and thus allows amphibians to shunt blood to or from the lungs in response to the wide ranges of O_2 availability which they encounter (Shelton, 1970; Emilio and Shelton, 1972). A drawback to this arrangement is that there is no physical separation of oxygenated and oxygen-poor blood within the heart and if mixing of these two blood-streams occurs then oxygen delivery to the tissues is compromised. The degree of mixing of blood within the amphibian heart has been the subject of a number of studies (DeLong, 1962; Haberich, 1965; Johansen and Ditadi, 1966; Toews et al., 1971) and it is generally felt that at least partial separation is maintained. The amphibian ventricle is a highly trabeculate structure and it is believed that atrial contraction drives blood directly into the fine channels in the ventricular wall and thus gross stirring is prevented. The pattern of blood flow during ejection, particularly during passage through the conus arteriosis, is more controversial. The conus arteriosis is a separate contractile chamber of the heart which beats at the cardiac frequency, although contraction is delayed until late in ventricular systole (Brady, 1964) and lasts until late in diastole (Shelton and Jones, 1968). It is divided into two channels, the cavum aorticum and the cavum pulmocutaneum, by

a spiralling central wall, the spiral valve, which separates systemic and pulmocutaneous outflows. However, the valve is attached to the conus wall only along one edge and its function and the degree of flow separation it affords has been the subject of controversy (Noble, 1925; Vandervael, 1933; Foxon, 1947; Simons, 1959). Early anatomical studies (Brucke, 1852; Sabatier, 1873) led to the 'classical theory' according to which the ventricle first ejects blood into a low pressure pulmocutaneous arch then, as ventricular pressure exceeds the higher systemic pressure, deflection of the spiral valve occludes pulmocutaneous outflow and the ventricle ejects the remainder of the stroke volume into the systemic and carotid arches. In the last two decades, however, it has been well established that pressures in both the systemic and pulmocutaneous circuits closely follow ventricular pressure throughout ventricular ejection and hence no sequential distribution of blood could be occurring. Originally it was also held that conus contraction served to extend cardiac ejection until late in diastole and thus depulsate inflow into the arterial circulations (Johansen, 1963). However, direct measurement of relative volume changes of the conus and ventricle throughout the cardiac cycle indicate that the conus contribution to cardiac output is quite small (Shelton and Jones, 1965). Thus the functional significance of conus contraction remains obscure.

Despite the demise of the classical theory the view that rapid deflections of the spiral valve within the conus play an important role in central blood distribution has persisted. Although pulmocutaneous arch pressure falls to a significantly lower level than systemic pressure and hence should be exceeded earlier by the rising front of the ventricular pressure pulse, Shelton and Jones (1965(b)) were unable to detect a time difference between the onset of pressure rise in the two arches. Consequently they concluded that the spiral valve occluded the cavum pulmocutaneum until systemic ejection started. Morris (1974) proposed that contraction of the conus actively displaced the spiral valve to initiate this occlusion during late ventricular ejection. He argued that the timing of this event was regulated by the pH of the coronary blood supply, pulmocutaneous outflow occlusion occurring earlier when blood pH (and presumably O_2 availability) was low and later when pH was high and thus the conus acted as a central 'variable shunt' to regulate blood flow distribution during periods of apnoea, presumably in addition to the controls afforded by regulated vaso-activity in peripheral vascular beds (Shelton, 1970; Emilio and Shelton, 1972). That the coronary circulation has persisted only in the conus arteriosis of the frog heart suggests an important functional significance and since Jones and Shelton (1965(b)) failed to observe obvious detrimental effects of acute

ligation of the coronary supply of frogs under controlled conditions the suggestion that it plays a role in regulatory adjustments to changing environments merits further investigation. On the other hand the absence of marked pressure gradients between the ventricle and pulmocutaneous arch during late systole argues against Morris' theory. Since an understanding of the mechanics of the conus arteriosis is essential not only to an accurate description of cardiac function but also to the explanation of the characteristics of blood pressure and flow within the arterial beds supplied by the heart the present study includes an attempt to present a coherent picture of conus function. Particular attention has been paid to the significance of conus contraction and its timing with respect to other cardiac events, the function of the spiral valve and the role of the coronary circulation.

Although the nature of blood flow through the frog heart has attracted considerable attention few studies have investigated the dynamics of blood flow within the arterial systems supplied by this pump and attempts to analyze arterial pressure-flow relationship in amphibia have, to date, been based upon relatively simple cardiovascular models such as the windkessel (Jones and Shelton, 1972) in which haemodynamic relationships can be defined completely in terms of the peripheral resistance of the terminal beds and a lumped compliance for the arterial

system. As discussed in the "General Introduction" such models cannot account for the wave transmission phenomena associated with mammalian haemodynamics but may be suitable for examination of blood flow in some lower vertebrates, particularly small poikilotherms such as the frog. In the present study an assessment is made of wave transmission effects and the applicability of cardiovascular models to the amphibian arterial systems. The cardiovascular responses to lung ventilation are also examined in terms of these models.

METHODS

Pressure and flow recordings

Experiments were performed on 26 bullfrogs (Rana catesbeiana) weighing from 200 to 550 g. The frogs were anaesthetized by immersion in Sandoz MS 222 anaesthesia (1-2 g/L) and restrained on their backs and the heart and arterial arches were exposed by a midline incision through the sternum. The lungs were cannulated through an incision in the left abdominal wall which was subsequently sutured around the cannula and the animal was ventilated with a Harvard 670 positive pressure respirator, although some animals breathed spontaneously when the pump was shut off. The frogs were allowed to recover to a more lightly anaesthetized state which was maintained by frequently wetting the skin with the anaesthetic solution.

Physiological Studies

Pressures were recorded in the ventricle, conus arteriosis and right systemic and left pulmocutaneous arches with Bio-tec BT-70 and Hewlett-Packard 267 BC pressure transducers connected to the blood vessels with 10 cm lengths of PE 50 tubing. Dynamic calibration of the manometers and recording systems was performed by applying a step change in pressure to the tips of the manometer cannulae and recording the free vibrations of the

system. Since the natural frequency of the system always exceeded 50 Hz, far in excess of the frequency of the physiological signals recorded, no correction for manometer distortion was required.

Blood flows were recorded in the left systemic and right pulmocutaneous arches with Biotronix BL 610 electromagnetic flowmeters utilizing cuff-type extra-corporeal flow probes. Flow probes were calibrated by excising a portion of the artery to which they were attached and perfusing this vessel under pressure with physiological saline. The saline was collected in a calibrated cylinder and the time taken for a given volume to pass through the vessel was recorded with a stopwatch. The volume flow rate thus determined was compared with the output voltage of the flowmeter. Flowmeter outputs during isotonic saline perfusion differ from outputs during blood perfusion by at most 2% (Pierce et al., 1964; Greenfield et al., 1966). Care was taken to site pressure and flow probes the same distance from the conus in both the systemic and pulmocutaneous arches and in all cases this distance was from 0.5 to 1.5 cm. In some experiments a stimulator attached to the conus via two fine copper wires sewn into conus wall was triggered by the QRS wave of the ECG so that the ventricle and conus contracted simultaneously. Normally conus contraction is not initiated until late in ventricular systole (Brady, 1964) and it was

hoped that these experiments would provide insight into the importance of this delay.

Data was recorded on a Techni-Rite TR888 chart recorder writing on rectilinear co-ordinates and in most cases was simultaneously recorded on an Akai 280DSS four channel tape recorder. F.M. adaptors (A.R. Vetter and Co.) frequency modulated the data for storage on the audio recorder and demodulated the output when the recorder was in the playback mode. Vascular impedance at the input to both the systemic and pulmocutaneous circulations was determined by playing tape recorded pressure and flow signals into an A-D converter interfaced with a LAB 8/E computer (Digital Equipment) which performed a Fourier analysis of the pressure and flow signals and printed out the ratio of pressure to flow (impedance modulus) and the phase difference between pressure and flow (impedance phase) for each of the first ten harmonics.

These experimentally determined impedance curves were compared with curves calculated from a windkessel model according to the equations

$$\text{impedance modulus} = R \Big/ \sqrt{1 + (2\Pi f T)^2}$$

$$\text{impedance phase} = -\arctan(2\Pi f T)$$

where R is the vascular resistance (mean arterial pressure divided by mean flow), f is frequency and T is the time constant of the windkessel which is determined from the diastolic

portion of the pressure profile according to the equation

$$T = t / \ln(P_0/P(t))$$

where t is the duration of diastole, P(t) is pressure at the end of diastole and P_0 is pressure at the beginning of diastole.

Pressures alone were recorded from the ventricle, conus and both arterial arches in four frogs in order to precisely determine the time relationships between events of the cardiac cycle. In a further two animals pressure was recorded in a systemic arch and the sciatic artery in order to examine the transit time and distortion of the pressure pulse as it travelled through the arterial system.

In four frogs the sternum was opened with a small incision directly ventral to the atrio-ventricular junction and a ligature was placed around the coronary artery. The wound was then closed and the frog left to recover for one week. At this time the chest was reopened and arch, ventricular and conus pressures recorded to assess the effects of long term coronary occlusion on conus performance.

Anatomical Studies

The conus was opened with a ventral midline incision and the cut edges were drawn back and trimmed to permit direct observation of the spiral valve, the inflow and outflow regions of the conus and the cavum aorticum and cavum pulmo-cutaneum. In addition serial sections of the conus were

prepared. The ventricle and conus were quickly dissected from three frogs, washed in saline and fixed in Bouin's solution. The hearts were set in wax and serial sections made (5 μ/ section). The procedure was not wholly successful as fixation caused marked shrinkage of the spiral valve however, the sections did allow close examination of the site of attachment of the spiral valve to the conus wall as a function of position along the conus and also provided confirmation of some observations made during dissection. The shrinkage problem was avoided in later preparations by having frozen sections of fresh conus preparations prepared by the department histologist (12 μ/ section).

Results

Anatomical Studies

Detailed descriptions of the functional anatomy of the frog heart are available in the literature (Brucke, 1852; Sabatier, 1873; de Graaf, 1957; Sharma, 1957; Sharma, 1961) and with a few exceptions the present studies confirmed that these descriptions apply to R. catesbeiana. Briefly, blood is pumped into the ventricle from the two atria and passes immediately into many deep trabeculae in the sponge-like ventricular wall (Fig. 1-1). During ejection blood directed ventral to the spiral valve flows to the left dorsal opening of the pulmocutaneous circulation at the anterior end of the conus (Fig. 1-2). Systemic outflow passes dorsal to the posterior end of the spiral valve and exits through the systemic opening at the left ventral aspect of the anterior conus. Any deflections of the spiral valve must serve to compress or close off one of these two outflow tracts. The two branches of the truncus arteriosis into which the conus empties each contain two internal walls which keep separate flows to the carotid, systemic and pulmocutaneous arches. The atrio-ventricular junction is guarded by two similar valves and by smaller left and right lateral pocket valves. Both conus outflow tracts are guarded by watch-pocket valves.

Figure 1-1. View of the intra-ventricular cavity exposed by a lateral incision from apex to base.

Figure 1-2. Ventral view of the heart of the bullfrog before (A) and after (B) cutting away the ventral conus wall to expose the spiral valve, V, ventricle; C.A., conus arteriosis; T.A., Truncus arteriosis; Sp. V., spiral valve.

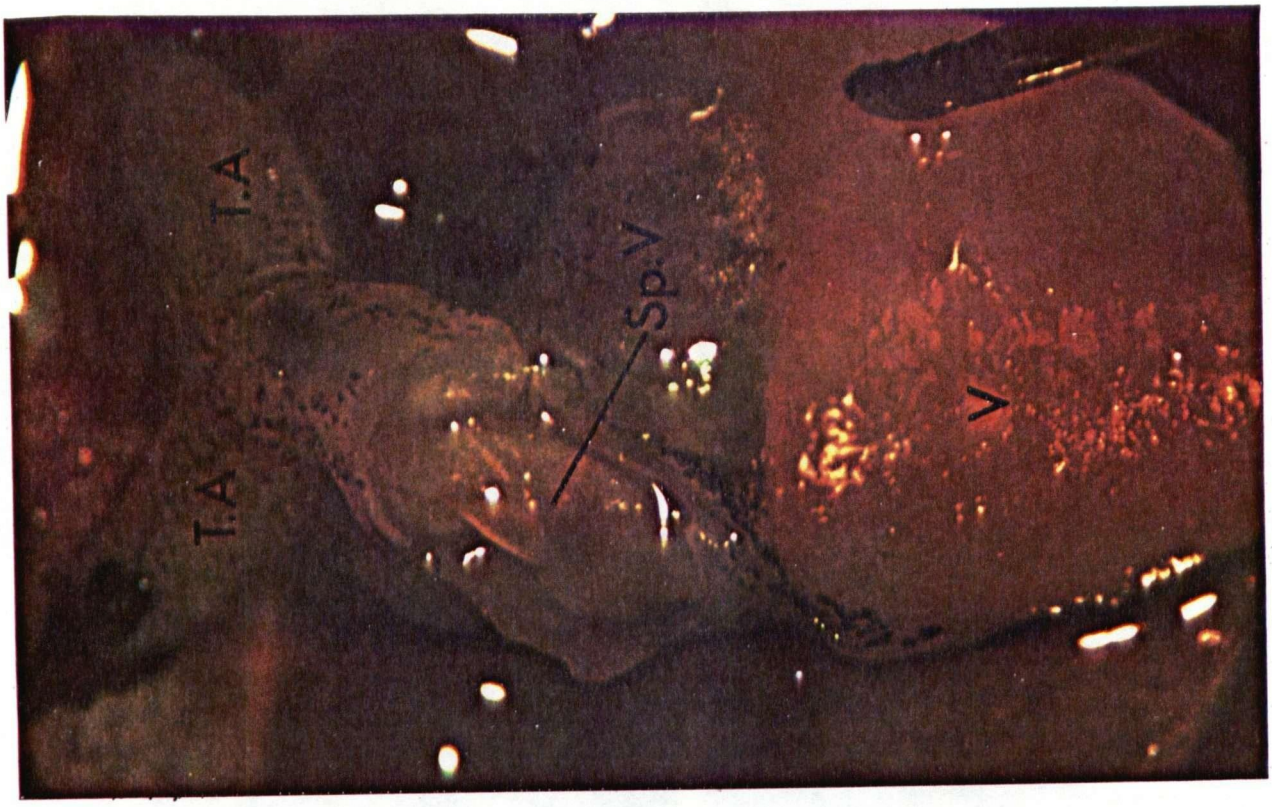
T.A
T.A
Sp.V
V

C.A
V

The most significant contrast between the present study and previous work lies in defining the properties of the spiral valve. Previously the valve has been described as having a very thin attachment to the conus wall and a wide head (de Graaf, 1957; Sharma, 1957). The functional implications of such a structure are best stated by Sharma (1957), "The shape of the spiral valve, its hing-like attachment and disposition, a slight curvature in form, its hammer-headed top-heavy head... all indicate that the spiral valve moves...". Similar results were obtained in the present investigation when standard histological preparations were employed. It was obvious, however when comparing the resulting slides with the spiral valve in fresh preparations, that marked shrinkage had occurred during preparation of the sections. When frozen section techniques were employed a different picture arose. Although the spiral valve resembles the above description in the posterior region of the conus it is a much sturdier structure in the anterior region of the conus and an obverse cross section of the valve is not observed here (Fig. 1-3). Thus any displacement of this spiral valve would appear to result from a bending of the valve rather than a flapping movement from a hinge-like attachment.

Figure 1-3. Lateral cross-sections of the conus arteriosis prepared using frozen section techniques. Slides are equally spaced samples chosen from 12μ serial sections. Sections display the valve as seen from an upstream viewpoint at sites which move progressively downstream from sections A to E. pd.v, pad-like valve; p.o.v., pulmocutaneous outflow valves; sp.v, spiral valve. The pad-like valve is not a true valve but is just a protruberance from the proximal, right dorsal conus wall. Magnification is 30x.

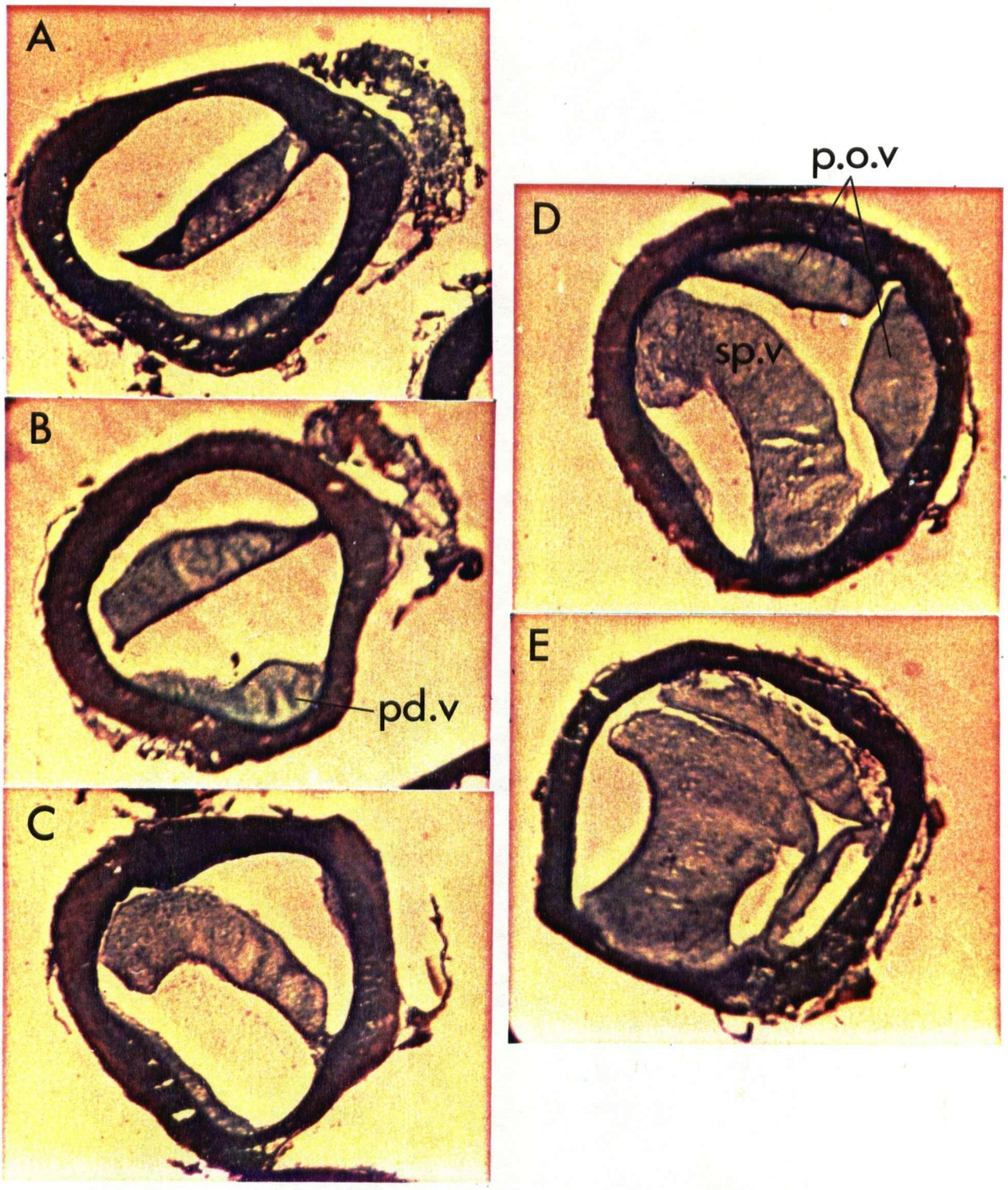
A
B
pd.v
C
p.o.v
D
sp.v
E

Blood pressures from ventricle, conus and arterial arches

The pressure pulses recorded in the central circulation of Rana catesbeiana (Fig. 1-4 and 1-5) confirmed the general shape of pulses reported for other amphibia (Shelton and Jones, 1968). Pressure in the ventricle displayed an initial sharp rise followed by a more gradual rise to peak pressure. Ventricular contraction lasted approximately half the cardiac cycle before being terminated by a rapid return to near-zero pressures. Often, ventricular diastolic pressure did not show a distinct hump indicating auricular contraction as has been recorded in other amphibia (Shelton and Jones, 1968). Pressure in the conus arteriosis followed ventricular pressure until late systole but when ventricular pressure dropped rapidly conus pressure exhibited an inflexion and conus contraction maintained pressure at arterial levels, clearly indicating closure of the pylangial valves (between the ventricle and conus). Late in the cardiac cycle the conus relaxed and pressure fell but at normal heart rates never dropped to ventricular pressure before the next contraction.

During the phase when ventricular pressure was rising diastolic pressure in the pulmocutaneous arches was exceeded before systemic pressure and pulmocutaneous pressure showed an initial sharp rise (Fig. 1-5). Some 50 msec later ventricular pressure exceeded systemic pressure and,as the synangial valves between the conus and systemic channels of the truncus opened

Figure 1-4. Blood pressures (mm Hg) in the ventricle, conus arteriosis, pulmocutaneous arch and systemic arch.

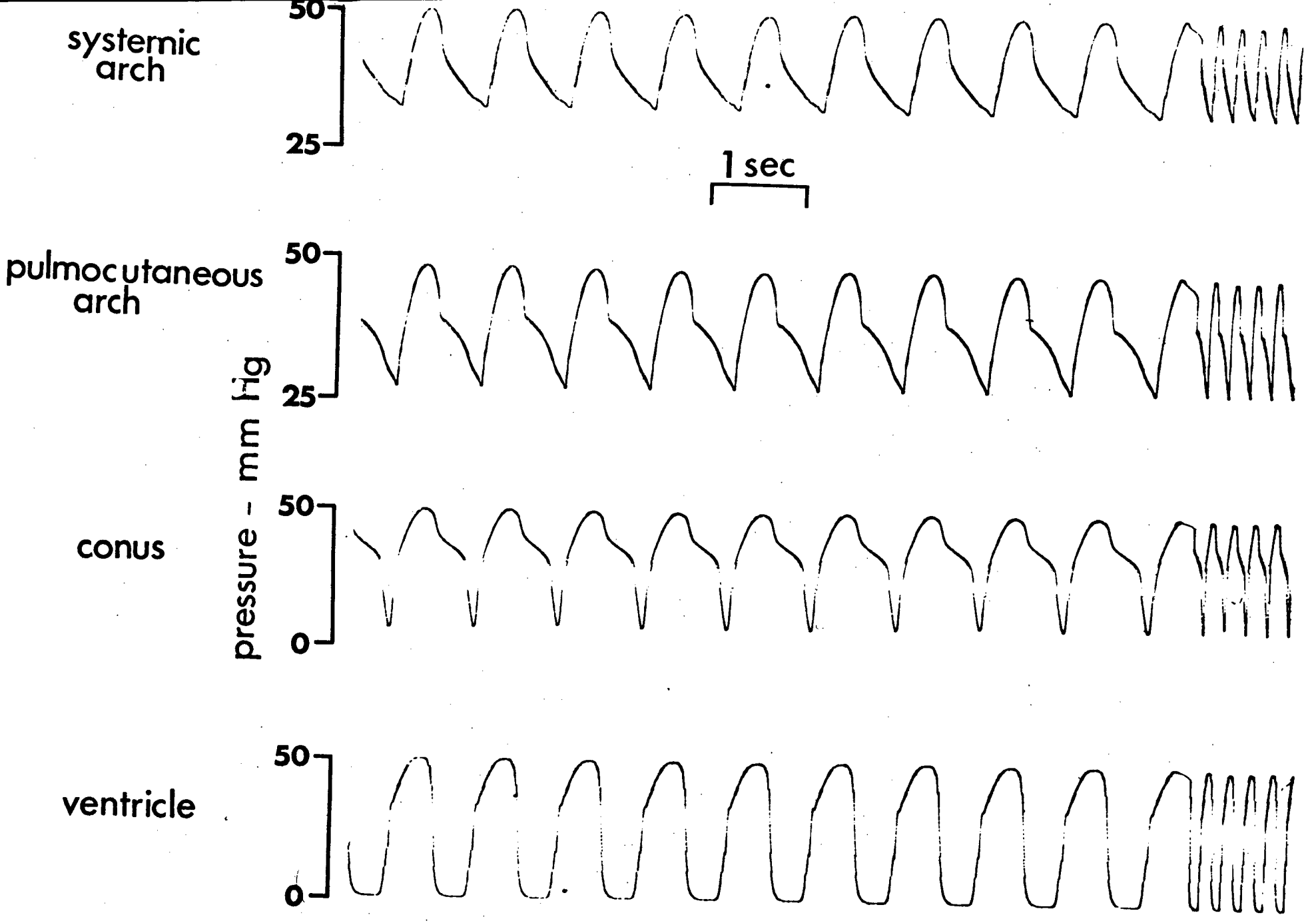
systemic arch
50
25
1 sec
pulmocutaneous arch
50
25
pressure - mm Hg
conus
50
0
ventricle
50
0

Figure 1-5. Blood pressures recorded in the systemic arch, pulmocutaneous arch and ventricle. Vertical lines link co-incident events at the onset of ejection into the pulmocutaneous and systemic circulations. Arrows indicate spontaneous breathing movements and concomitant changes in pressures.

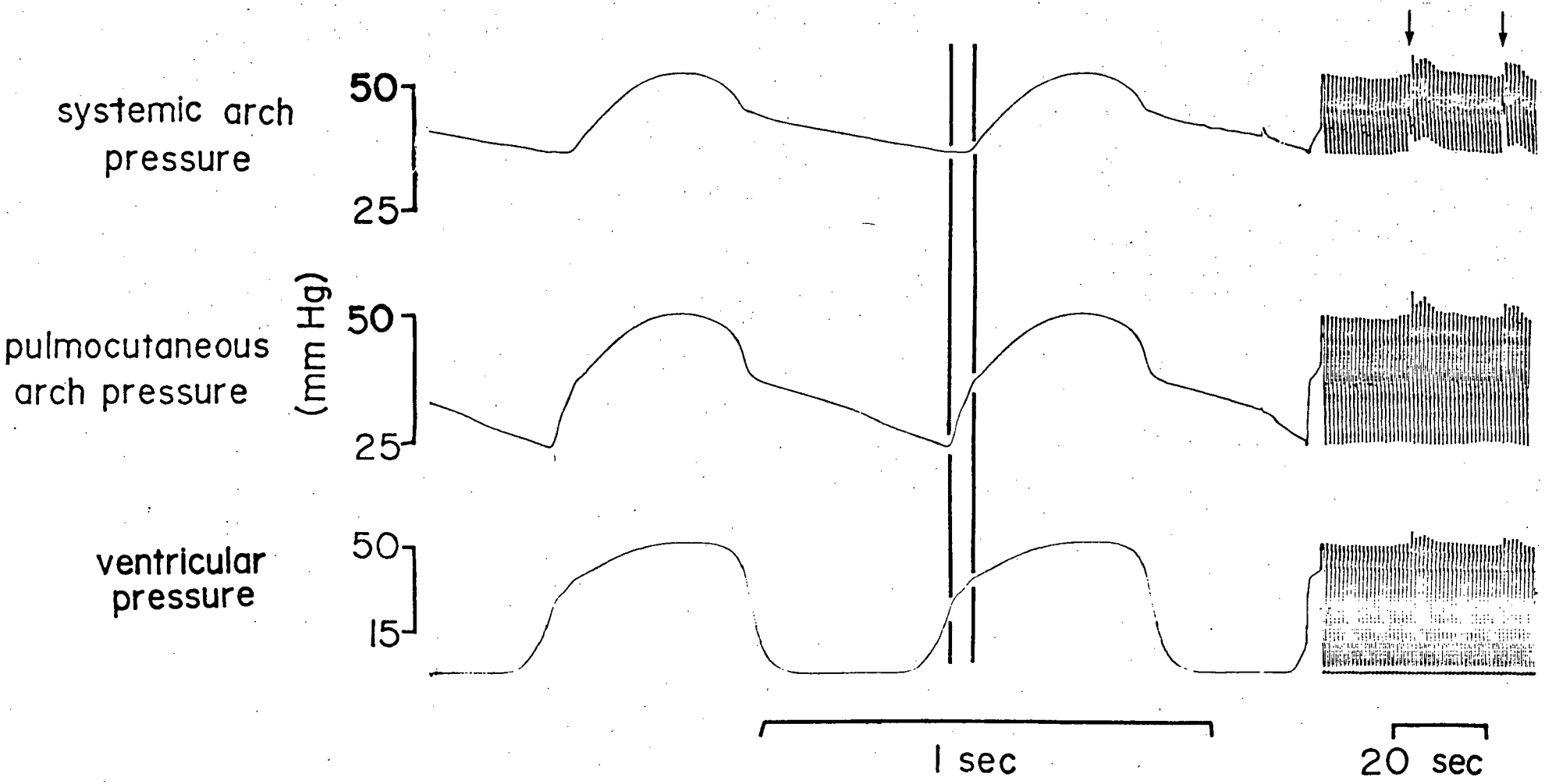
systemic arch pressure
50
25
pulmocutaneous arch pressure
(mm Hg)
50
25
ventricular pressure
50
15
1 sec
20 sec

and systemic pressure started to rise, a marked inflexion in the pressure profiles in the ventricle, conus and pulmocutaneous arches was observed and subsequent pressure rises were more gradual (Fig. 1-4 and 1-5). Throughout the remainder of ventricular ejection all pressures followed ventricular pressure.

The effect of conus contraction on arch pressures is slight because of the small ejection volume of this chamber and is most often evident only as a small notch signalling conus relaxation. In the present study this conus component was observed in both arches although during lung ventilation it frequently did not appear in the systemic arch pressure trace, a response attributed to marked lung vasodilation which may decrease outflow resistance to the lung-skin circuit to the extent that the conus is no longer capable of reaching systemic pressures. Although there must be a resultant elevation in conus ejection to the pulmocutaneous system, pressure in the pulmocutaneous arch often showed a reduced conus component and this is attributed to the marked fall in pulmocutaneous vascular impedance during lung ventilation (discussed later) which reduces pressure increments produced by a given inflow. The observation of a conus component on the pressure profile in both systemic and pulmocutaneous arches, is in agreement with the earlier report of de Graaf (1957) but at variance with the

findings of Shelton and Jones (1965(a)) who rarely observed any evidence of a conus contribution to pulmocutaneous outflow. Diastolic decline of pulmocutaneous pressure was more rapid than that of systemic pressure although when both pressures displayed a conus component this more rapid decline was restricted to late diastole. Consequently pulse pressures were always greater in the pulmocutaneous circulation although, as previously reported (Jones and Shelton, 1972), this difference was diminished during apnoea. Fig. 1-5 also illustrates the immediate effects of lung ventilation on central pressures. Spontaneous breathing movements (see arrows) in frogs not artifically ventilated resulted in elevated ventricular pressures which caused an increase in mean systemic pressure with little change in pulse pressure whereas in the pulmocutaneous arches both mean and pulse pressure increased distinctly. This increase in pulmocutaneous pulse pressure had previously been investigated in Xenopus laevis (Shelton, 1970) and found to result from lung vasodilation which causes a drop in the time constant of the pulmocutaneous circulation, i.e. an increase in the rate of decline of diastolic pressure.

Elimination of the ventricle to conus conduction delay by stimulating the conus in phase with ventricular depolarization had a marked effect on arch pressure profiles (Fig. 1-6). In particular there is a sharp decrement in peak pulmo-

Figure 1-6. Result of stimulating the conus contraction in time with ventricular contraction (stimulator triggered from QRS wave of the ECG). The decrement in pulmocutaneous arch pressure during systole and co-incident rise in systemic pressure clearly indicate occlusion of the pulmocutanious outflow.

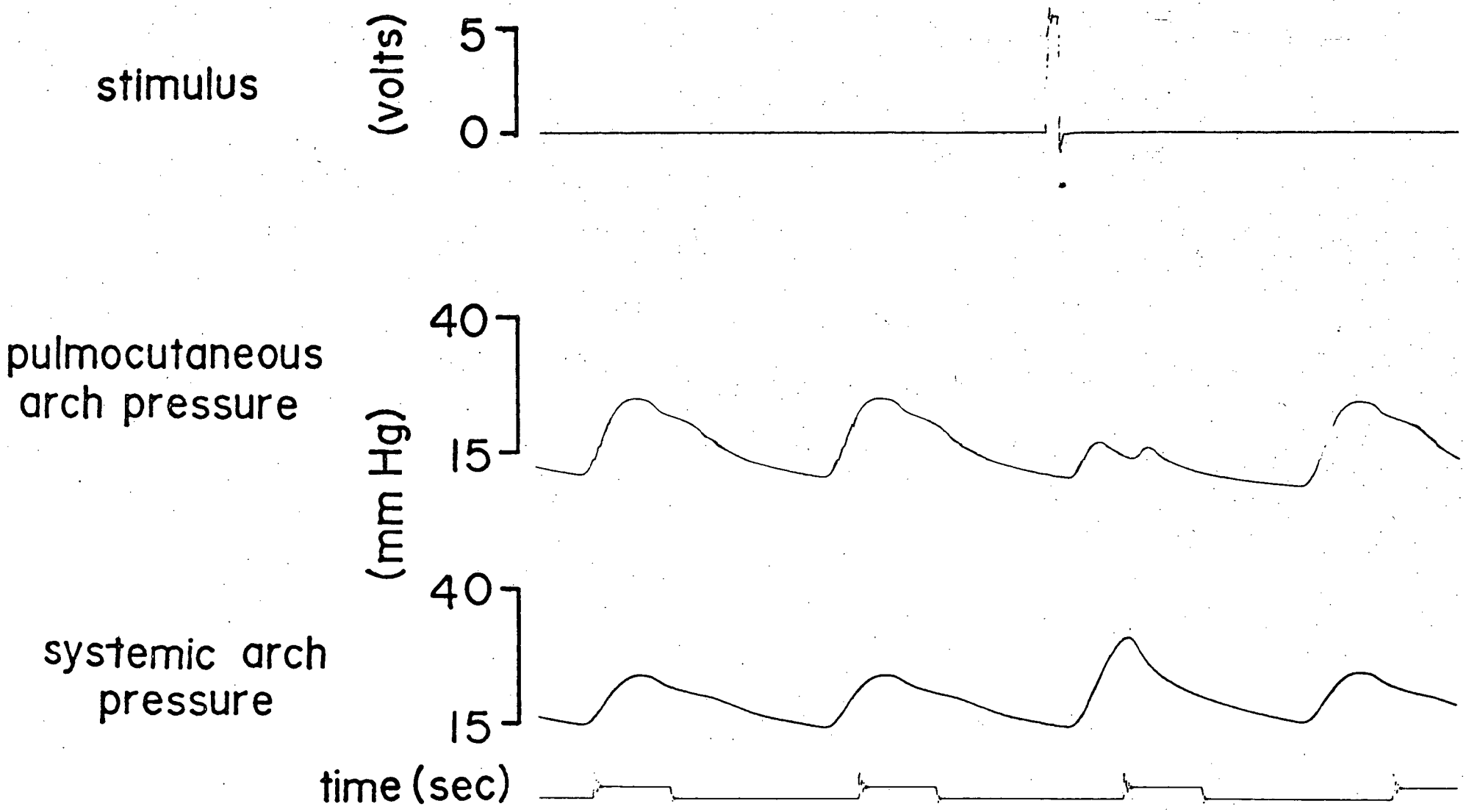
stimulus
(volts)
5
0
pulmocutaneous
arch pressure
40
15
(mm Hg)
systemic arch
pressure
40
15
time (sec)

cutanous arch pressures despite a rise in systemic pressure and these results clearly indicate that the conus is closing off the pulmocutaneous outflow. Apparently the normal conduction delay is necessary to allow the ventricle to fully distend the conus before conus contraction and when the delay is eliminated the unfilled conus closes down on the spiral valve and occludes the cavum pulmocutaneu. These findings confirm similar experiments by Morris (1974) although he interpreted the results as evidence that normal conus contraction occludes pulmocutaneous outflow.

Pressures recorded in the conus arteriosis after ligation of the coronary artery for one week indicated a complete loss of conus contractility. Conus pressures fell quickly to diastolic levels following ventricular relaxation and aside from a slightly slower elastic recoil during relaxation pressure followed that within the ventricle (Fig. 1-7). The normal pattern, in which pressures are maintained at arterial levels until late diastole, was lost completely indicating that, while the conus may survive short term coronary occlusion (Jones Shelton, 1965 (b)), coronary vascularization is required for adequate oxygen supply. Although there was a complete loss of conus contraction, pulmocutaneous arch pressure still exhibited a sharp initial rise to systemic pressure clearly indicating that the appearance of this pressure rise in normal animals did

Figure 1-7. A. Pressure recorded in the conus arteriosis of a 'normal' bullfrog. B. Simultaneous pressures recorded in the conus, ventricle and the two arches of a frog following one week of coronary ligation.

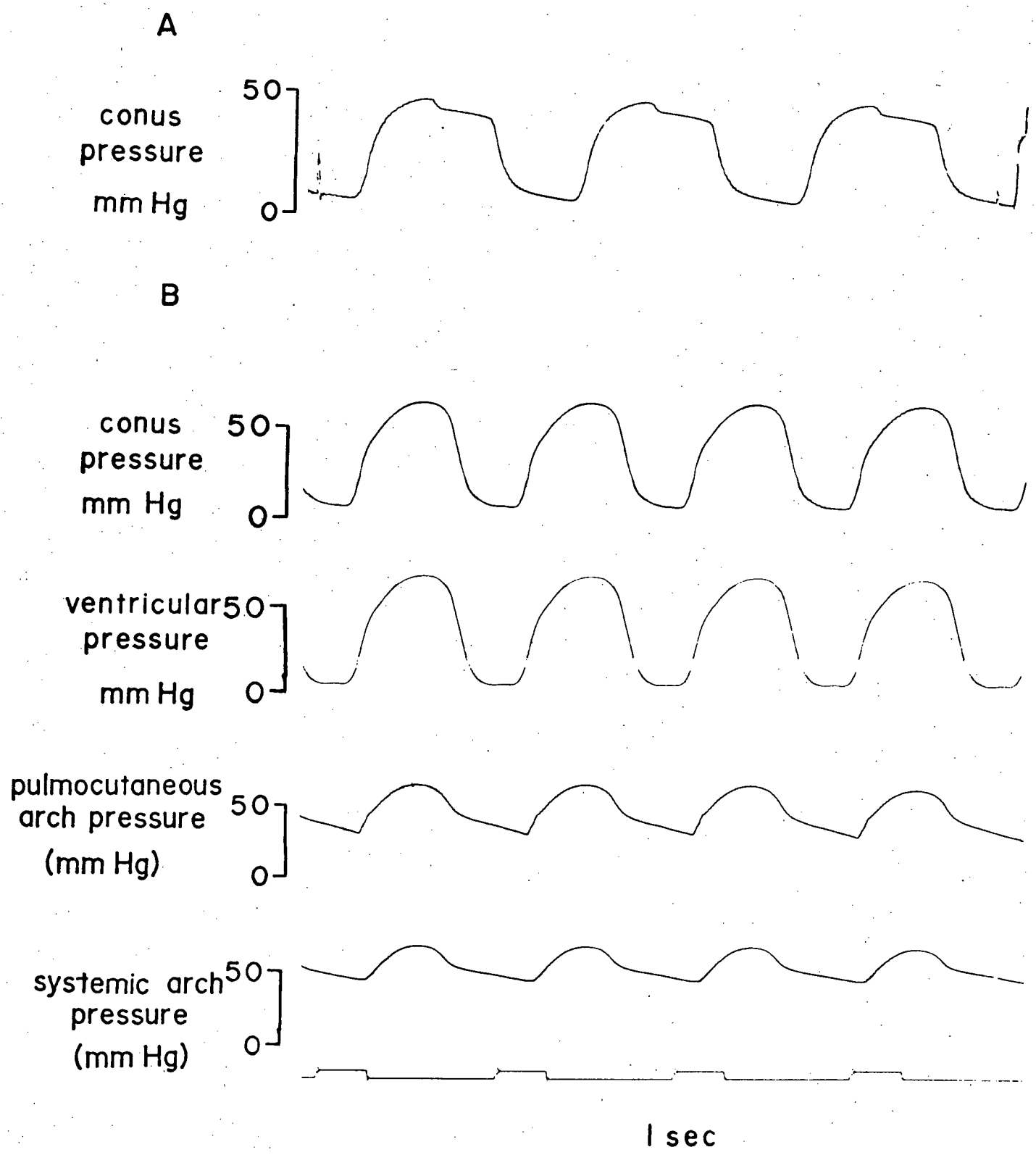
A
conus pressure mm Hg
50
0
B
conus pressure mm Hg
50
0
ventricular pressure mm Hg
50
0
pulmocutaneous arch pressure (mm Hg)
50
0
systemic arch pressure (mm Hg)
50
0
1 sec

not signal the removal of an active conus occlusion of pulmocutaneous outflow.

One final aspect of conus function has been investigated. In the conus of elasmobranch fishes there are three tiers of watch-pocket valves (no spiral valve) and contraction of the conus is required to bring opposing valves in each tier sufficiently close together to permit competency (Satchell and Jones, 1967), a situation permitting smaller valves which require less backflow to close them. In the present experiments the frog conus was examined for a similar function. Frogs were deeply anaesthetized, the sternum opened as described above, and a stout ligature was tied around the sino-atrial junction which stopped the heart beating. Remaining venous return to the atria, and all arterial arches except one systemic arch, were ligated and two pressure reservoirs were then connected via stopcocks and cannulae to the remaining systemic arch and the ventricle. Ventricular pressure was set at 10 mm Hg to fill the cardiac chambers and systemic pressure was raised in steps while recording pressure in the ventricle and conus. Competency of the conus valves consistently broke down, as indicated by a sudden jump in conus and ventricular pressures to resevoir levels, at reservoir pressures of 50 - 80 mm Hg (Fig. 1-8A), i.e. at high physiological pressures. Fig. 1-8B illustrates an experiment in an animal which exhibited persistent atrial

Figure 1-8. A. Pressures recorded in the ventricle and conus in a fresh, post-mortem preparation when pressure to the systemic arch is increased in a step-wise fashion. When a critical pressure is exceeded there is a sudden breakdown in the conus valves and both chambers suddenly fill, as indicated by a sudden jump in pressures (upward arrow). At the downward arrow the systemic arch pressure resevoir is returned to 0 mm Hg.

B. Same experiment as in A except that in this preparation atrial contraction persisted throughout the experiment. Since atrial contractions were immediately superimposed on ventricular and conus pressures it follows that atrio-ventricular valves are not competent in the filled ventricle when it is relaxed.

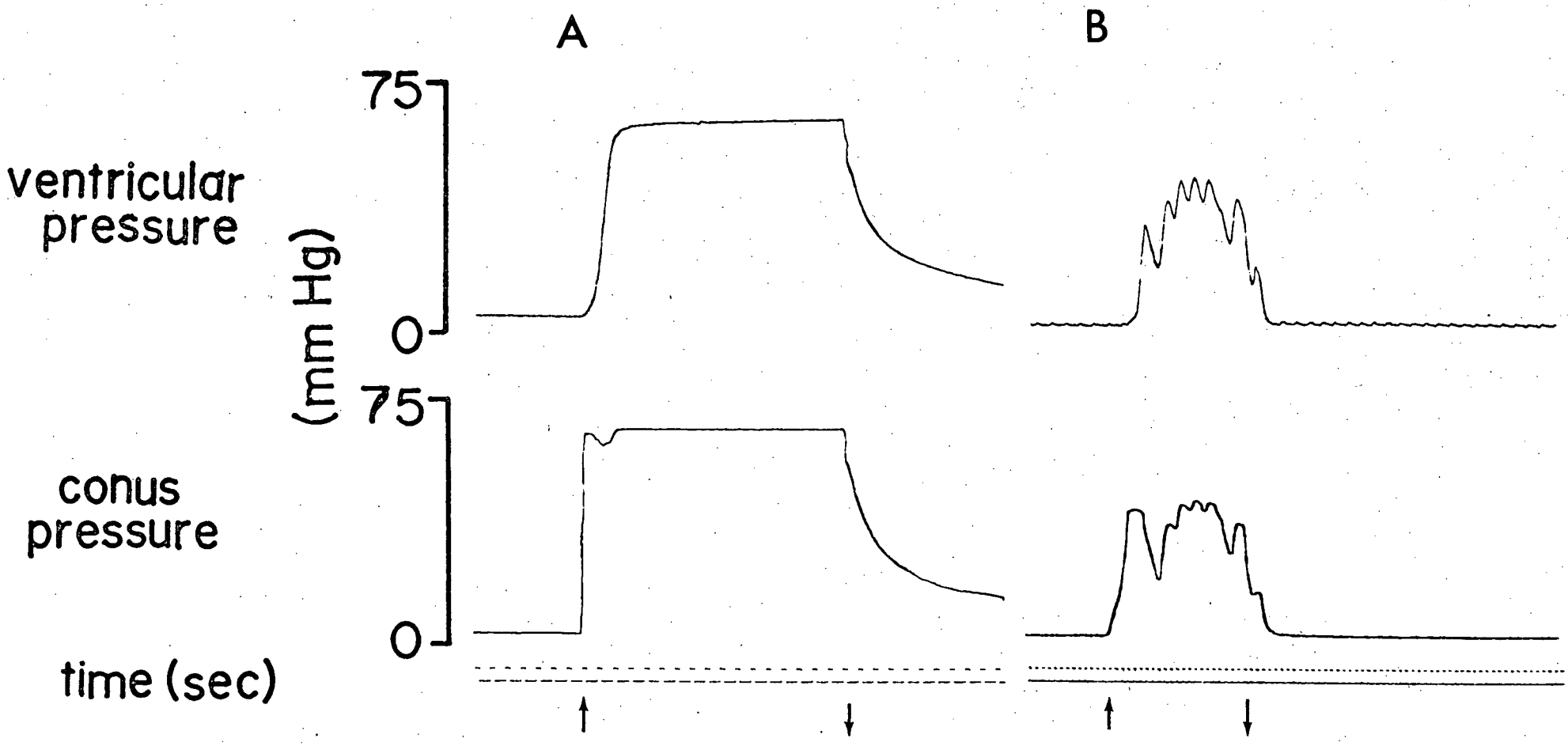
A
B
75
0
ventricular pressure
(mm Hg)
75
0
conus pressure
time (sec)

contractions. Immediately upon breakdown of the conus valves atrial pressure waves were superimposed on conus and ventricular pressures, suggesting that ventricular contraction plays a role in closing the atrio-ventricular valves as well. The survival of frogs with conus dysfunction induced by coronary ligation appeared contrary to the above findings however when these experiments were repeated on such animals no loss in valve function was observed until systemic arch pressure exceeded 100 mm Hg. Apparently a reduced myocardial compliance associated with infarction prevented the normal distension of the conus which draws apart the pocket valves.

Arterial flow and pressure-flow relations

Flows in the arterial arches of the bullfrog resemble those reported for other amphibia (Shelton, 1970, Emilio and Shelton, 1972). The systemic flow pulse is concentrated mainly in ventricular systole (Fig. 1-9) and resembles the flow pulse recorded in the mammalian aorta (McDonald, 1960; O'Rourke, 1967). Ventricular systole is terminated by a reversal of systemic flow which serves to close the pylangial valves and possibly causes the synangial valves between the conus and systemic truncus to close briefly. This backflow is generally followed by a period of positive flow due to conus contraction. The onset of ejection into the pulmocutaneous arches was synchronous with the initiation of the pressure pulse and

Figure 1-9. Pressures and flows recorded in the systemic and pulmocutaneous arches. The vertical line indicates onset of pulmocutaneous outflow.

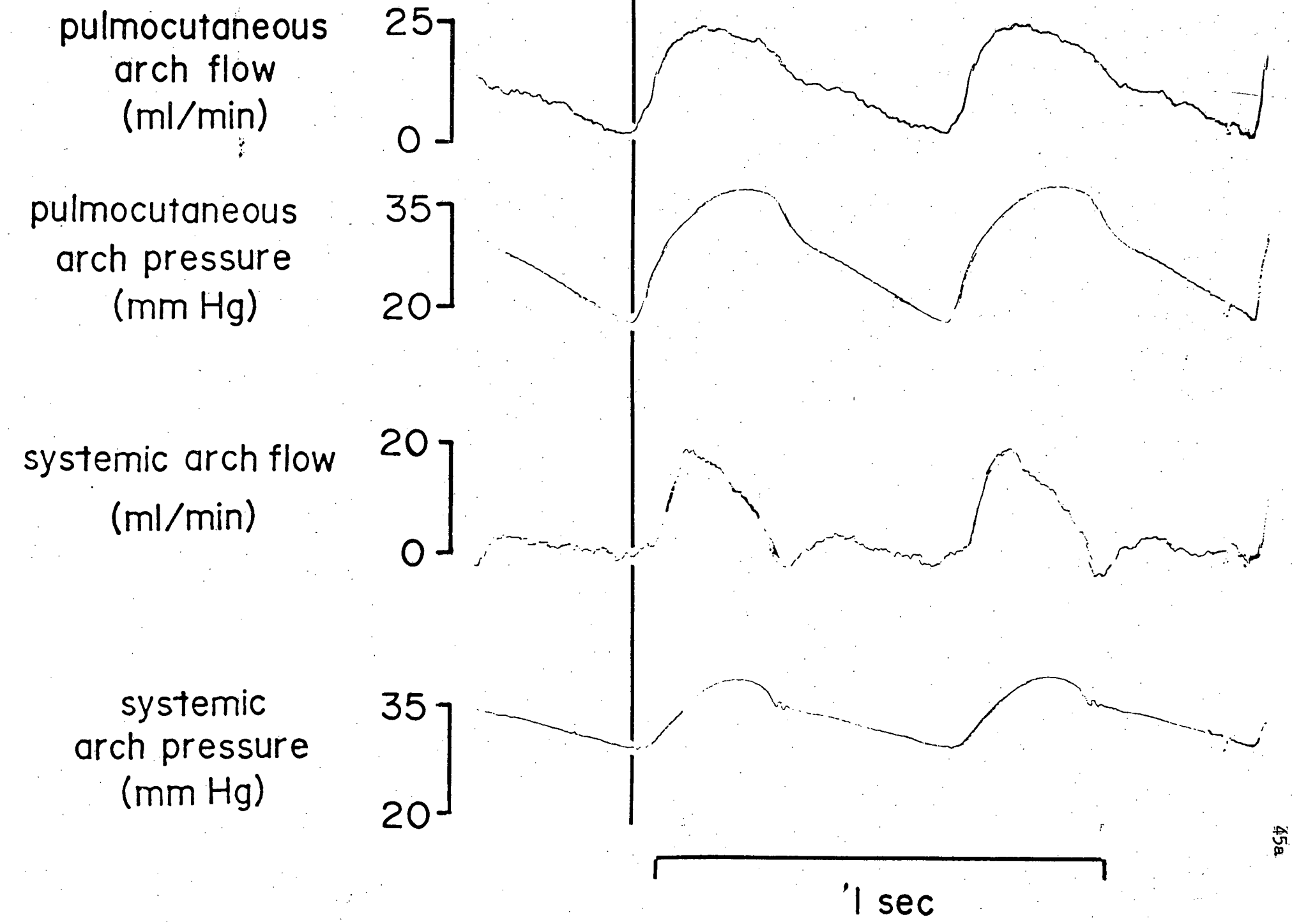
pulmocutaneous arch flow (ml/min)
25
0
pulmocutaneous arch pressure (mm Hg)
35
20
systemic arch flow (ml/min)
20
0
systemic arch pressure (mm Hg)
35
20
1 sec

consequently preceded ejection into the systemic arches. Marked diastolic flows were observed (Fig. 1-9) which typically contributed 35-40% of stroke flow during lung ventilation and up to 50% during apnoea.

At the end of diastole the steady decline in systemic pressure was interrupted at the point when pulmocutaneous outflow started and pressure levelled off or rose slightly before systemic ejection and at the same time a slight positive flow was recorded in the systemic arch (Fig. 1-9). Ventricular pressure was still clearly below systemic pressure at this point. This small disturbance in the systemic system is attributed to deflection of the septum between the systemic and pulmocutaneous channels of the truncus as pulmocutaneous pressure rises and although probably of little functional significance this phenomena again reflects the time difference between ejection into the two circulations.

Fig. 1-10 illustrates the effects of apnoea on pressures and flows in the arterial arches. Apnoea caused a sharp drop in pulmocutaneous flow whereas systemic flow was relatively unaltered in the short term. In ventilated animals pulmocutaneous flow exceeded systemic flow by up to 50% whereas during apnoea pulmocutaneous flow fell to less than half systemic flow despite a rise in mean pulmocutaneous pressure. Although systemic flows were not immediately influenced by lung vent-

Figure 1-10. Arch pressures and flows before (A) and after (B) 10 min apnoea.

47a

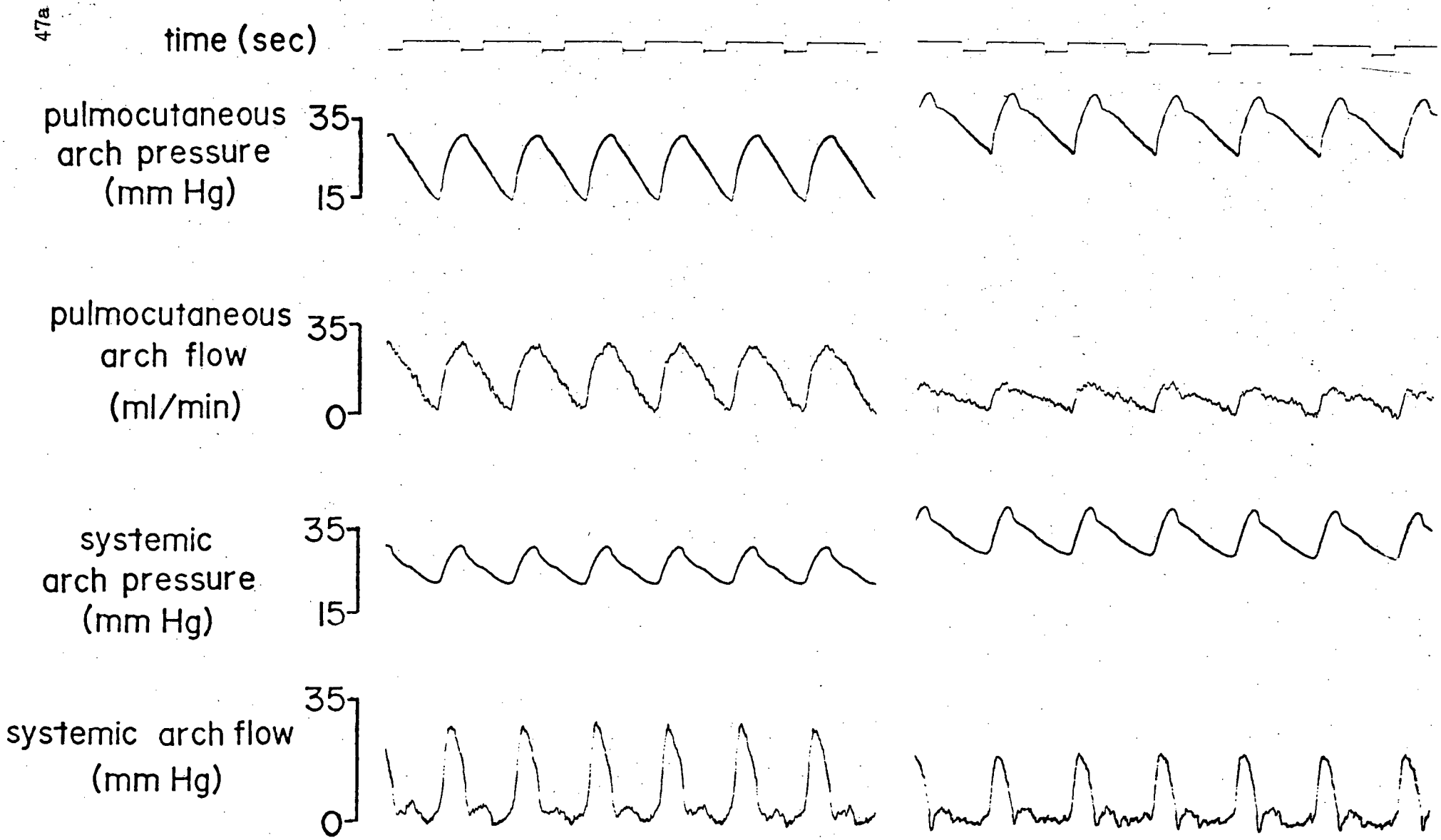
time (sec)
pulmocutaneous arch pressure (mm Hg)
35
15
pulmocutaneous arch flow (ml/min)
35
0
systemic arch pressure (mm Hg)
35
15
systemic arch flow (mm Hg)
35
0

ilation long-term apnoea caused a marked reduction in systemic flow; with flow declining gradually by some 40% over 10 minutes apnoea.

The relationships between arterial pressures and flows are most conveniently expressed in terms of vascular impedance which indicates the relative size and phase relationships between corresponding pressure and flow harmonics. Fig. 1-11 shows systemic impedances calculated for three frogs. Impedance modulus, normalized by dividing by peripheral resistance (zero frequency impedance) to allow comparison of results from different frogs, displayed a sharp initial fall followed by a more gradual but steady decline towards zero at higher frequencies. Impedance phase was between 1 and 1.57 radians (57 and 90°) at all pulsatile harmonics examined. Only three harmonics are used to compute these curves because higher harmonics of pressure were consistently below 1 mm Hg in amplitude and therefore could not be used accurately for impedance determination. The solid curves in Fig. 1-11 are theoretical impedance curves for one frog (triangles) calculated from a windkessel model. Fig. 1-12 illustrates the effects of apnoea on impedance of the pulmocutaneous vascular beds. Apnoea caused an increase in impedance modulus which is most significant at the zero frequency limit and a consistent drop in impedance phase was observed.

Figure 1-11. Input impedance modulus (Z) and phase (Φ) of the systemic circulation in 3 bullfrogs. The solid curves illustrate theoretically predicted (windkessel) impedances for one of the frogs (triangles). Impedance modulus is normalized by dividing by peripheral resistance (R) to allow comparison of different individuals.

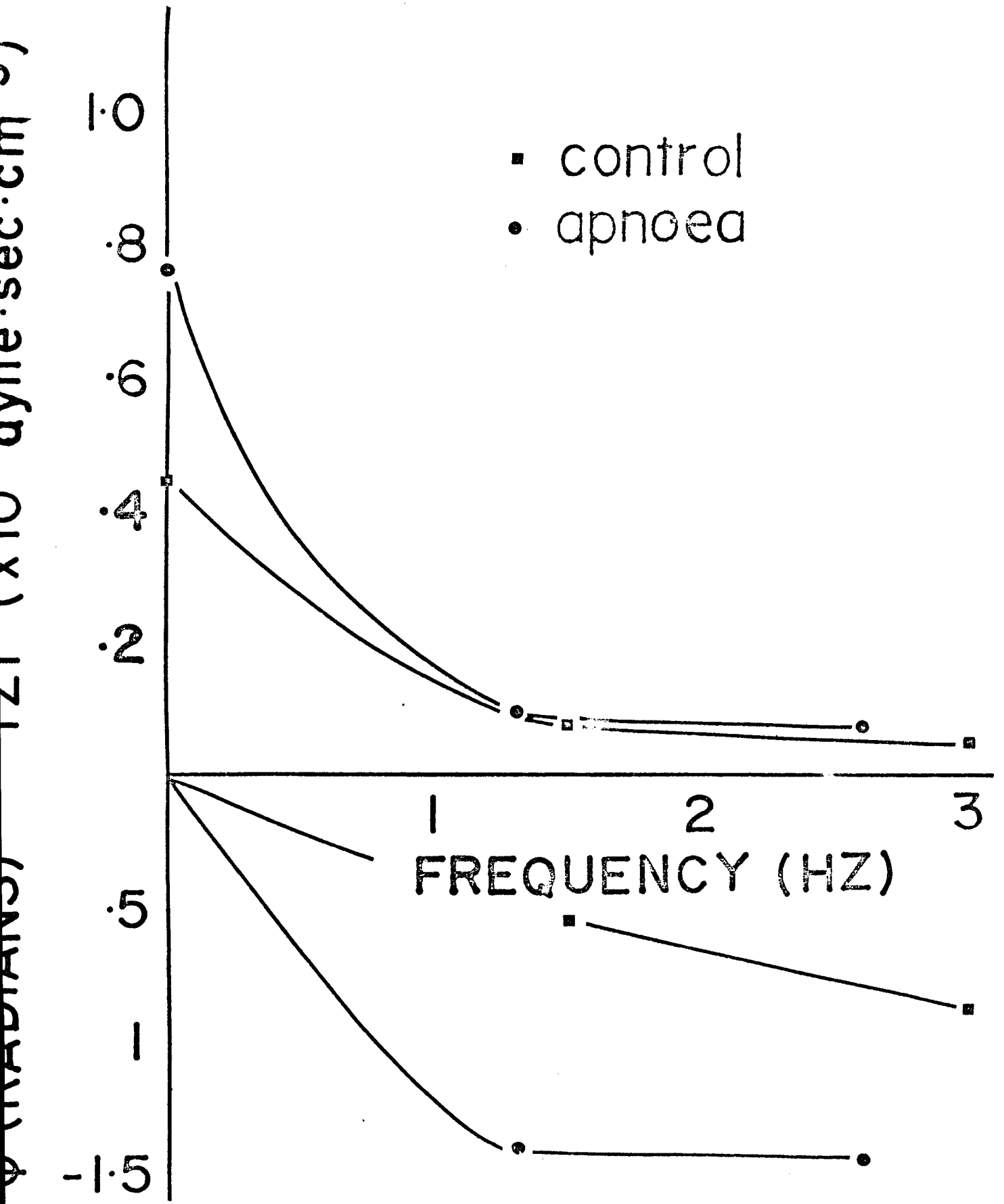
control
apnoea
1·0
·8
·6
·4
·2
·5
1
1·5
1
2
3
FREQUENCY (HZ)

Figure 1-12. Input impedance to the pulmocutaneous circulation during artifical lung ventilation and during apnoea.

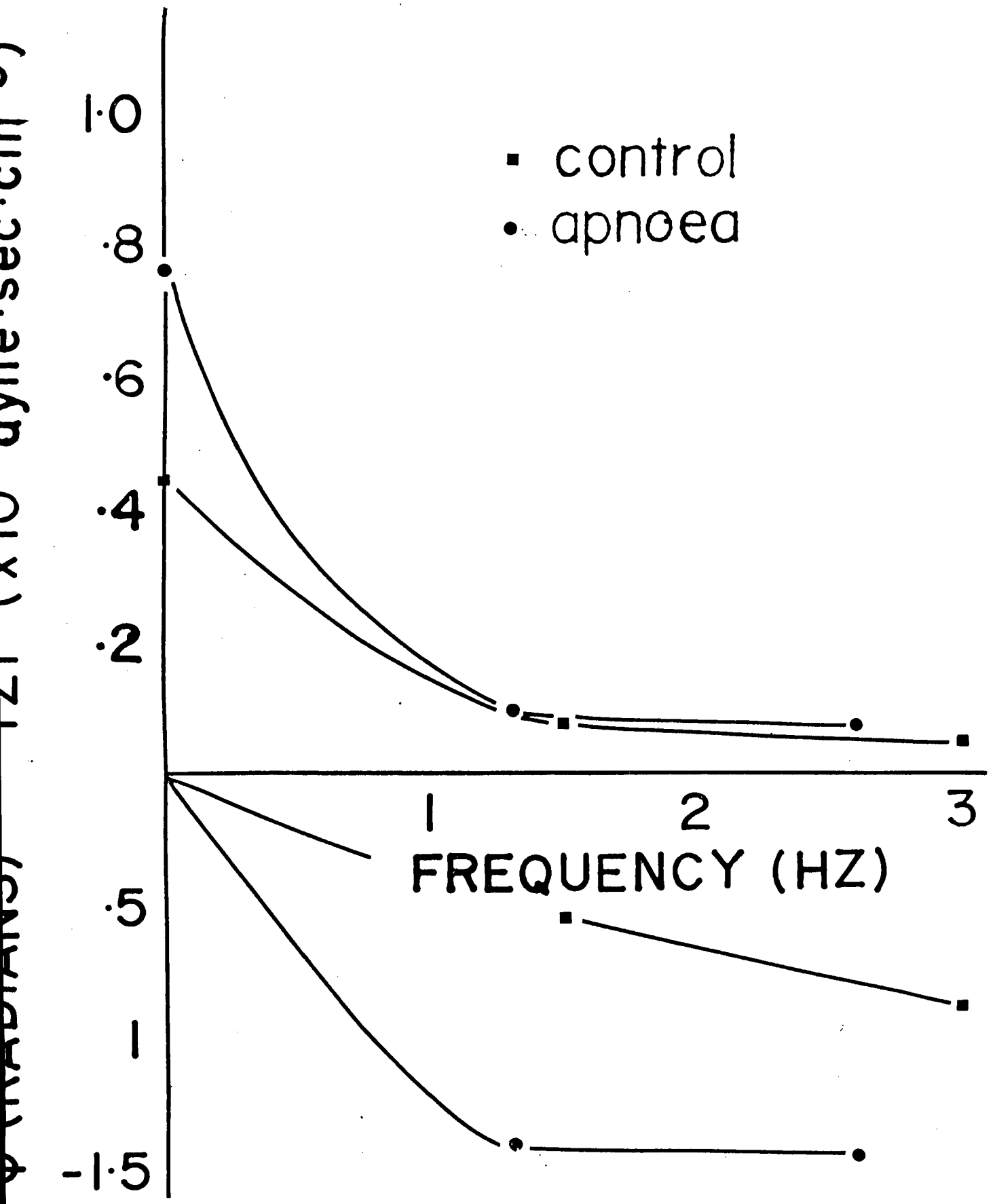
1·0
·8
·6
·4
·2
·5
1
-1·5
control
apnoea
1
2
3
FREQUENCY (HZ)

Pressure wave propagation in the systemic circulation

Fig. 1-13 illustrates systemic arterial pressures recorded in the proximal systemic arch and the sciatic artery 14 cm away. The pressure pulse is unchanged during propagation between the recording sites, aside from slight damping, and, in this individual, arrives at the distal site some 45 msec (3.7% of the cardiac cycle) after it passes the proximal transducer, thus travelling with a mean pulse wave velocity of 3.1 m/sec.

Figure 1-13. Near indentical pressures recorded in the systemic arch (SAP) and sciatic artery (SP) of the bull-frog. Distance between the recording sites is 14 cm (recorded at the level of the heart and midway along the thigh). Mean pressure at the two sites is the same and profiles have been shifted apart for clarity.

SAP

SP

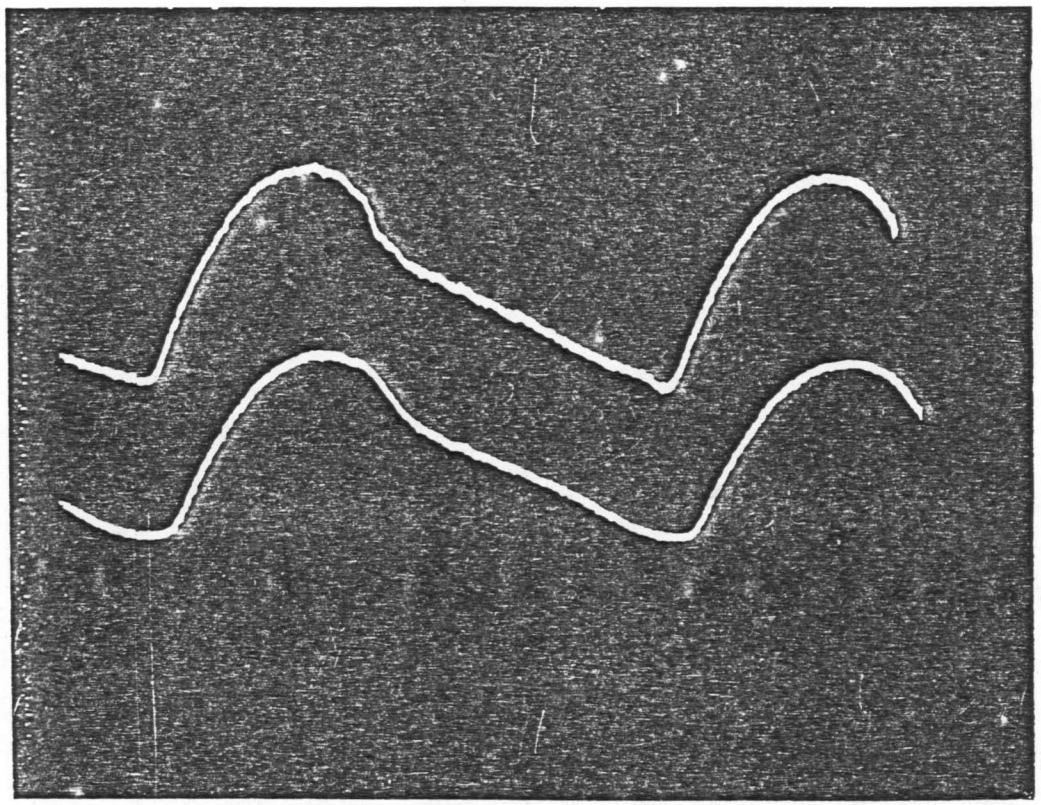

10 mm Hg

1 SEC

Discussion

Function of the conus arteriosis

Results of the present study contradict recent theories on the function of the anuran conus arteriosis since it has been established that no active occlusion of the pulmocutaneous outflow occurs early in diastole in the bullfrog. Among the strongest evidence of this is the marked diastolic flows recorded in the pulmocutaneous arches, for which the only potential sources are diastolic recoil of the truncus arteriosis and/or conus ejection, the latter clearly requiring a patent pulmocutaneous outflow. Shelton and Jones (1965(b)) have measured volume changes in the ventricle, conus arteriosis and truncus arteriosis of Rana pipiens throughout the cardiac cycle and found that truncus volume changes are very small. If similar (percentage) changes apply to Rana catesbeiana then even liberal estimates of truncus volumes indicate that truncus recoil generates a small fraction of pulmocutaneous diastolic flow (20% at most) even if all truncus run-off were directed down the pulmocutaneous circulation. On the other hand the volume of the conus is halved during contraction and the resultant outflows are in the range of pulmocutaneous diastolic flow. The appearance of a conus wave on the pulmocutaneous pressure profile (Fig. 1-4 and 1-5) supports this interpretation.

Previous conclusions to the contrary, i.e. that pulmocutaneous outflow is occluded (Shelton and Jones 1965(a), 1972; Morris, 1974) are based largely on the absence of a detectable time difference between the systolic rise in pressure in the systemic and pulmocutaneous arches. Certainly the rising portion of the pulmocutaneous arch pressure (Fig. 1-5), which exhibits a sharp initial rise followed by a slower rise to peak pressure, is suggestive of the sudden removal of an occlusion, however in the present study a time difference was observed and both arch pressures followed ventricular pressure throughout systole. In addition there is an inflexion in the rising front of ventricular pressure co-incident with that in the pulmocutaneous arch pressure (Fig. 1-5). It appears that this inflexion in pressure rise is due to the sudden release of systemic outflow rather than the removal of a pulmocutaneous occlusion (occasionally ventricular pressure exhibited a similar break co-incident with the start of pulmocutaneous outflow (Fig. 1-4)). It may be that the reason I was able to detect a time difference between rise in the two arches, whereas previous workers were not, is that ventricular pressure rises more slowly in Rana catesbeiana than in other species. The duration of the sharply rising phase of pulmocutaneous pressure is some 50 msec whereas preliminary experiments with Rana pipiens indicate that times of less than 20 msec are more typical. Alternatively it is

possible that the mechanisms of conus function are different in the two species however similarities in the anatomy and physiology of the two systems argue against this conclusion. Finally the persistence of this sharply rising component of pulmocutaneous pressure following coronary ligation verified that it did not result from conus occlusion of pulmocutaneous outflow.

Thus, according to present findings, the conus is pictured as a contractile chamber beating with a time delay with respect to the ventricle, this time delay serving to allow the chambers to work in harmony without disrupting flow to any vascular bed. The pumping action of the conus drives a small fraction of total cardiac stroke volume however during lung ventilation this flow is distributed preferentially to the pulmocutaneous circulation (conus pressure occasionally being insufficient to open systemic outflow valves) and contributes a significant fraction of this flow. In addition contraction of the conus draws opposing synangial (outflow) and pylangial (inflow) valves sufficiently close together to ensure competency and since the conus does not fill before the next ventricular ejection, conus pressure exceeding ventricular pressure throughout diastole, the conus presents undistended valves to both the arterial circulation and the filling ventricle, a situation not possible if this chamber were missing. The initial surge of

flow to the pulmocutaneous circulation may cause minor deflections of the spiral valve to widen the cavum pulmocutaneum and bring the free edge into closer proximity with the conus wall (Sharma, 1957, 1961) however, no major deflections of the spiral valve are envisaged and no valving function appears to be served by this structure.

It is tempting to speculate on the absence of a complete septum within the conus since homologous structures in higher vertebrates, e.g. the foetal bulbus cordis of mammals, are totally divided. It may be that during the course of normal activity when blood is shunted from the lungs to the tissues or vice versa the site of redistribution is within the conus. Simons (1959) observed that dye streams injected into the right atrium would occasionally divide on entering the conus with part of the stream passing into the cavum aorticum. A reverse division could, at times, be seen in dye streams injected into the left atrium. (In this study no control over lung ventilation was exercised.). If shunting does occur within the conus this would allow a variable distribution of blood to the vascular beds without disrupting flow streams along the ventricular outflow tract where no physical separation exists. During prolonged submergence, when flow to the lungs is drastically reduced, such a mechanism might be difficult to maintain, and in any event would convey no advantage since arch PO_2's are the

same in this instance (Toews, 1969; Shelton, unpublished). Flow redistribution within the ventricle might be more likely in this situation. Foxon (1946, 1955, 1964) has suggested that the completely undivided ventricle in the frog is an amphibian specialization associated with the shift from a terrestrial to amphibious environment (and concomitant blood shunting requirements). It is possible that the partial division of the conus is a similar specialization and in this regard amphibia which have returned to a more aquatic environment, the urodeles, commonly exhibit less well developed spiral valves than anura. In any event these considerations serve to stress the importance of firmly establishing stream patterns through the amphibian heart and their relationship to respiration.

Pressure-flow relationships in arteries

It is apparent from the present study that wave transmission phenomena are of little significance in the arterial system of the frog since pressures measured in distal arteries are virtually identical to those measured near the heart and vascular impedance shows no evidence of the oscillations which wave reflections produce in mammals. Undoubtedly the chief reason for this is the brief time taken for the pulse to travel from the heart to peripheral arteries, a result of a short arterial tree and a sufficiently high pulse wave velocity (approximately 3 m/sec). Wave transmission effects, of which

reflection phenomena are most significant, become manifest when pressure (and flow) oscillations are appreciably out of phase at different sites within the arterial tree and in this regard the absence of higher harmonics of the pressure wave contributes to the lack of wave transmission effects since a given time lag between the arrival of pressure waves at two different sites represents a greater phase difference for higher frequencies. Other wave transmission phenomena, dispersion effects for example, are similarly of less significance when transmission time are low. It is widely believed that wave transmission effects contribute to the mechanical efficiency of the mammalian circulation by reducing the energy expended on driving the pulsatile component of arterial blood flow (Milnor et al., 1965; O'Rourke, 1967; Taylor, 1973; McDonald, 1974) although apparently in frogs the costs of higher heart-rates and very low pulse wave velocities outweight these advantages.

The absence of wave transmission effects in the frog circulation implies that simple 'lumped-parameter' models should apply and the findings of this study indicate that the simplest of these models, the two parameter (compliance and resistance) windkessel, yields a good estimate of pressure-flow relationships as measured by arterial impedance. In addition the variations in impedance associated with cessation of lung ventilation can be interpreted in terms of a simple

change in time constant of the system associated with peripheral vasoconstriction (see General Introduction Fig. 3). Consequently the present study has established the viability of a windkessel approach to modelling arterial haemodynamics in small poikilotherms.

SECTION II

The Single Circulation in the Cod, Gadus Morhua

Introduction

In teleost fishes blood is pumped from a single ventricle through a large elastic chamber, the bulbus arteriosis, into the ventral aorta. The bulbus is expanded during ventricular systole and the subsequent passive contraction during diastole generates a significant diastolic flow in the ventral aorta, thus the bulbus performs a depulsating function (Johansen, 1962; Randall, 1968). The ventral aorta divides to form the gill afferent vessels which supply the gill capillary beds. The efferent vessels draining these beds re-unite to form the dorsal aorta which runs the length of the vertebral column posterior to the gills and supplies blood to the systemic circulation. Thus fishes possess a single circulation consisting of two capillary beds joined 'in series' by a major arterial system. The interpolation of the gill capillaries between the heart and systemic circulation must be of fundamental importance to the blood flow dynamics of the arterial system, particularly, since the gill bed typically represents about one-third of the total vascular resistance (Holeton and Randall, 1967). Despite this unique arrangement few workers have investigated haemodynamics in fishes. Primarily blood pressures, heart rates and

flow rates have been recorded in order to gain insight into regulatory mechanisms associated with stress (hypoxia, exercise, etc.) but few attempts have been made to interpret these records in terms of the dynamics of the fish circulation (Holeton and Randall, 1967; Satchell, 1971). The aim of this investigation is to examine present knowledge of haemodynamics in fishes in terms of a simple cardiovascular model in order to see if the model provides physiological insight not apparent from direct inspection of data and to test the viability of the model with respect to more rigorous analysis of cardiovascular dynamics in fishes. A simple windkessel model proposed by Satchell (1971) has been chosen since many fish circulations, like the circulatory systems of frogs, are characterized by low heart rates and short arterial vessels. Although there was no direct test of the validity of a windkessel approach measurements in fish paralleled this study allowing a direct assessment of model predictions.

As described in Section I, Taylor's analysis of windkessel models (1964) indicates that a windkessel has an optimal time constant which represents a compromise between reducing blood flow pulsatility and decreasing the time required to accomplish regulatory changes in pressure. In a simple windkessel the time constant is the product of the total vascular compliance and the peripheral resistance and since peripheral

resistance must be governed by blood supply demands of the tissues one might expect evolutionary trends to establish vessel compliances at the level which produces this optimal time constant. Although the time constant concept is not strictly applicable to two vascular systems connected in series it is apparent that a compromise between the depulsating effect of high vascular compliance and the rapid response characteristics of a stiff system (in which only a small volume of venous blood must be shifted to the arterial system to increase pressure) suggests that there is an optimal total compliance. Satchell (1971) has argued that in fishes the most advantagous arrangement results if as much of this optimal compliance as possible is located proximal to the gills, for if the dorsal aorta were highly compliant each systole would produce large surges in flow through the gills to distend this vessel and thus smooth irrigation of the gills would be compromised. Since the ventral aorta contains the highly elastic bulbus and the dorsal aorta tends to be relatively stiff-walled (Lander, 1964) some weight must be given to Satchell's argument. Thus in the present study pressure and flow patterns recorded in the dorsal and ventral aortae of the cod were examined in light of these concepts in terms of simple hydraulic and electrical models based on the morphology of the system. In vivo recordings from fish cited in this study were recorded by D.R. Jones,

D.J. Randall and G. Shelton.

Methods

Experiments on fish. In vivo

Experiments cited in this study were performed on 18 cod, Gadus morhua, weighing between 2 and 3 kg. The fish were anesthetized in 2% urethane solution, and cannulae and flow probes were inserted with the fish supported, in air, on an operating table. During this time water containing the anesthetic was pumped over the gills.

The ventral aorta was exposed by a 4-cm incision in the ventral midline, just anterior to the pectoral fins, and a flow probe was placed around the ventral aorta. The leads were sutured to the adjacent muscle mass and the incision was closed. The union of the efferent branchial vessels to form the dorsal aorta is extremely variable in fishes. In the cod the efferent branchials on each side join the lateral dorsal aortas, which are linked anteriorly and posteriorly, to form the circulus cephalicus. Part of the right dorsal aorta together with its associated efferent branchials was exposed by an incision in the skin forming the posterior wall of the opercular cavity. The fourth efferent branchial artery was cannulated toward the dorsal aorta with PE-90 tubing to record dorsal aortic pressure. The gill side of the vessel was tied off. A cuff-type flow probe was placed around the right dorsal aorta adjacent to the fourth efferent branchial artery

along with a pneumatic flow occluder. The incision was closed and the cannula and probe leads were sutured to the body wall.

Blood flows were determined by means of a Biotronix 610 electromagnetic flowmeter and pressures with Sanborn 267B pressure transducers. The signals were recorded on a Sanborn 966 six-channel pen recorder writing on rectilinear coordinates. Zero flow in the right dorsal aorta was achieved by inflating the pneumatic cuff and in the ventral aorta by injection of 5-10 g/kg acetylcholine which slowed the heart rate to such an extent that zero flow was well established in late diastole.

After implantation of the cannulas and flow probes, fish were placed, singly, in 50-gal polyethylene tanks containing seawater. Records were obtained from the unrestrained fish in these tanks after recovery from the operation.

Hydraulic Model

The hydraulic model of the fish circulation was constructed as follows: To simulate the heart a constant pressure head was connected to a rotary valve which opened once per cycle for 50% of the total cycle period. The ventral aorta was simulated by using variable lengths of compliant rubber tubing (0.25 in dia.) to which extra compliance could be added by means of a side arm connected to further lengths of blind-ended rubber tubing. The 'ventral aorta' was connected to the 'dorsal aorta' (made of stiff walled vinyl tubing of 0.5 cm. dia.) by a capillary tube

which represented the gill resistance. A side arm from the vinyl tubing connected a blind-ended length of compliant rubber tubing which, in the condition of zero compliance in the 'dorsal aorta', was closed off at the side arm by a pair of haemostats. Removal of the haemostats effected an immediate and marked change in 'dorsal aortic' compliance. The 'dorsal aorta' terminated in a length of capillary tubing which represented the systemic resistance. Cannulating flow probes of 4-5 mm diameter were inserted in both the 'ventral aorta' in a position where 80% of the compliance was upstream and the 'dorsal aorta' immediately after the 'gill resistance', proximal to the introduced compliance. Positioning the ventral aortic flow probe distal to the major portion of "ventral aortic compliance" was intended to mimic, a priori, the recording site of *in vivo* measurements, i.e. immediately distal to the bulbus arteriosis.

Pressures were measured in the "ventral and dorsal aortae" of the model using Hewlett-Packard 267 pressure transducers, connected to 18G hypodermic needles which were forced through the walls of the tubes. Since flow through a pure resistance has the same profile as pressure, dorsal aortic pressure was also used as a measure of flow through the systemic resistance. The hydraulic model was filled with .9% NaCl to allow excitation of the electromagnetic flow probes.

Mathematical analysis of the model was based upon the electrical analogue shown in Fig. 2-4 (after Satchell, 1971). Unlike systems characterized by a single arterial compliance and peripheral resistance this model cannot be completely analyzed in terms of simple time constants because of the interplay between the gill and systemic circulations, thus the approach taken was to examine the effects of varying the physical parameters of the circulation. It was assumed that gill and systemic resistance were determined by gas exchange requirements and consequently the problem was reduced to examining the effects of altering the relative size of ventral and dorsal aortic compliance.

Results

Pressures and flows in the cod

Flows measured just distal to the bulbus arteriosis (ventral aortic blood flow, Fig. 2-1) in the cod confirmed the depulsating role of this chamber. No flow reversal was recorded and flow was significant throughout diastole, in some cases as high as one half peak systolic flow at end-diastole. Flow into the dorsal aorta was even less oscillatory than in the ventral aorta, as on average the amplitude of the oscillations in flow (peak minus minimum flow rate) during each cardiac cycle was 46 $\pm$ 10% of the mean flow in the dorsal aorta (Table 1). The shape of the dorsal aortic flow profile was also markedly different from that in the ventral aorta. The blood velocity in the dorsal aorta increased slowly following ventricular systole and declined even more slowly, resulting in a flow profile that was very rounded in outline (Fig. 2-1 and 2-2).

The pulsatility of the oscillations in dorsal aortic pressure (peak minus minimum pressure during each cardiac cycle expressed as a fraction of mean pressure) was 22 $\pm$ 5% as compared with 46 $\pm$ 10% for the oscillations in flow (Fig. 2-2). In other words the oscillations in flow (as a per cent of mean) in the dorsal aorta were twice as large as the oscillations in pressure.

Table 1. Values for cardiovascular parameters measured in cod.

Heart rate, beats, min	31.5 ± 5.5 (n = 11)
Cardiac output, ml/min	52.0 ± 8.0 (n = 5)
Dorsal aorta	
Systolic pressure, cmH O	43.0 ± 8.0 (n = 7)
Pulse pressure, cmH 0	8.1 ± 4.5 (n = 7)
Pulse: mean pressure	22 ± 5% (n = 6)
Peak blood flow, ml/min	24.4 ± 4.0 (n = 9)
Pulse flow, ml/min	8.3 ± 4.1 (n = 9)
Pulse : mean flow	46 ± 10% (n = 6)

All values are means ± SE. n = number of animals on which observations were made. Pulse pressure and flow refers to the difference between maximum and minimum pressure and flow during each cardiac cycle.

Figure 2-1. Blood flow in the ventral (top trace) and dorsal (middle trace) aortae of the cod.

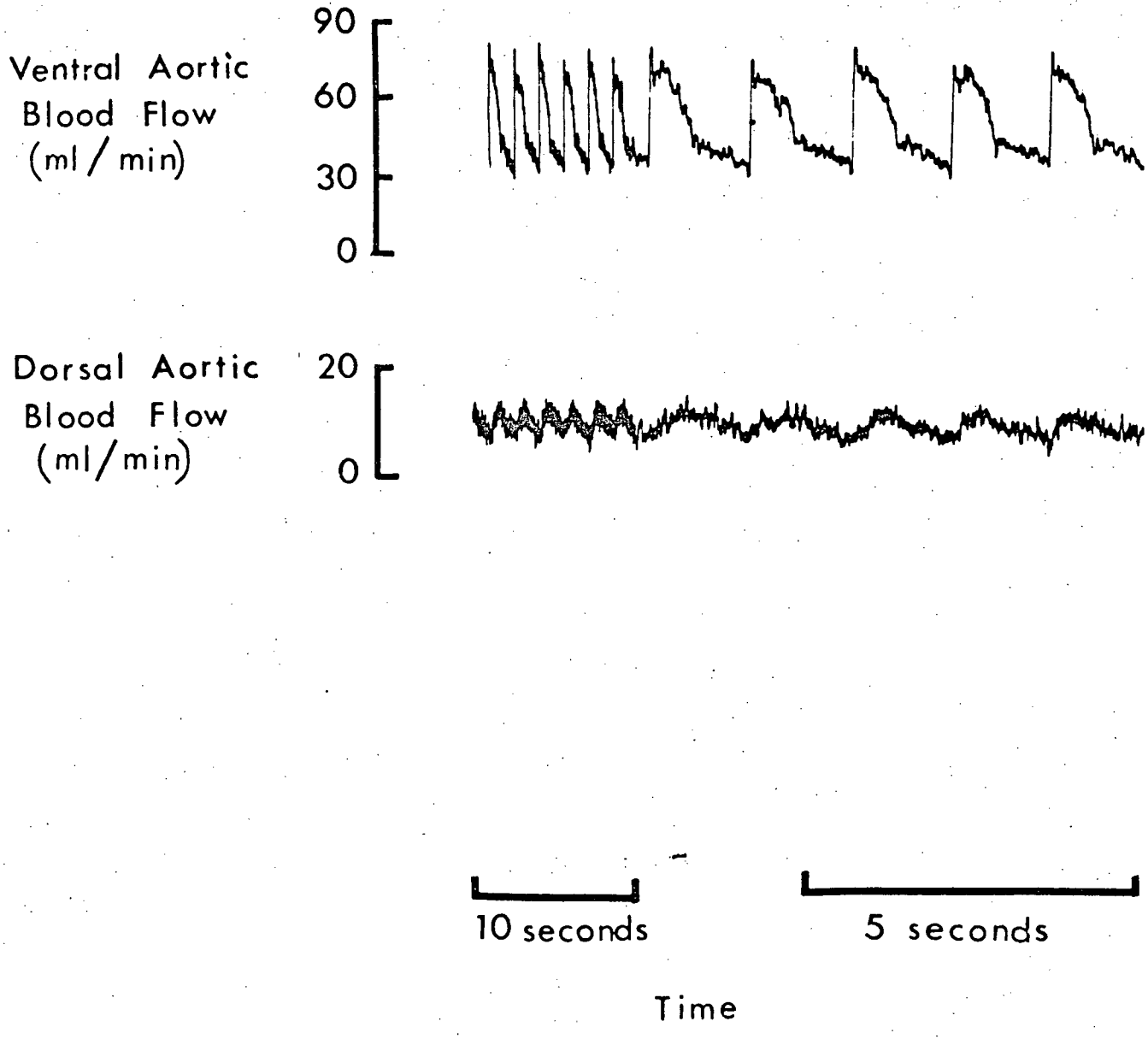
Ventral Aortic
Blood Flow
(ml / min)
90
60
30
0
Dorsal Aortic
Blood Flow
(ml/min)
20
0
10 seconds
5 seconds
Time

Figure 2-2. Dorsal aortic blood pressure (top trace) and flow (bottom trace) in the cod.

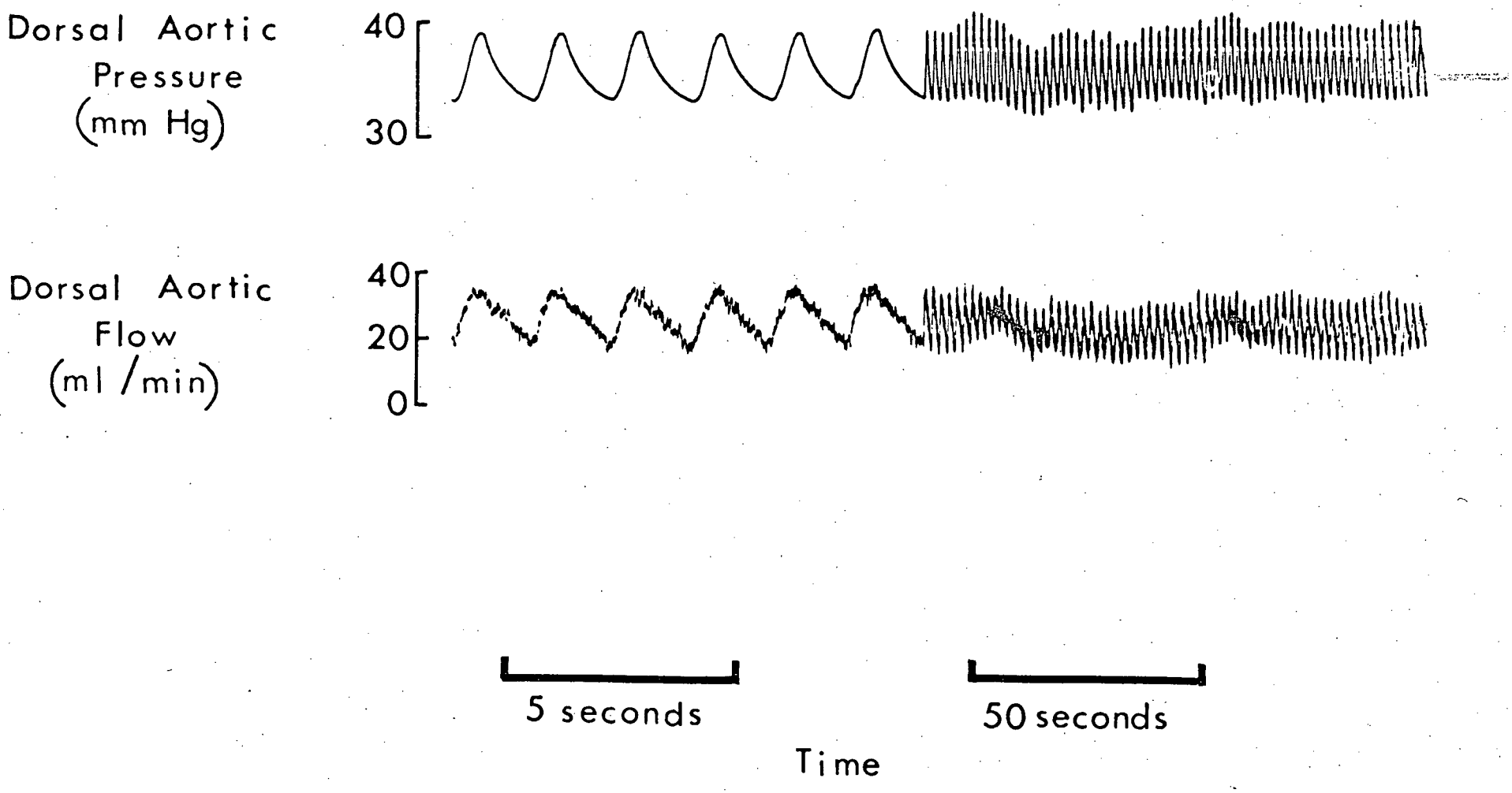
Dorsal Aortic Pressure (mm Hg)
40
30
Dorsal Aortic Flow (ml /min)
40
20
0
5 seconds
50 seconds
Time

Pressure-flow relationships predicted by the model

When all arterial compliance was located proximal to the 'gill resistance', i.e., when the 'dorsal aorta' was rigid, dorsal aortic pressure and flow were of similar wave-form and pulsatility (Fig. 2-3), a situation markedly different from that recorded in the fish (Fig. 2-2). However, when a compliance was introduced into the 'dorsal aorta' flow pulsatility increased whereas pressure pulsatility decreased and pressures and flows more closely resembled those recorded *in vivo*. Since outflow through the systemic resistance vessels is proportional to dorsal aortic pressure, the decrease in pressure pulsatility implies that this outflow is also less pulsatile. This is despite a more pulsatile flow through the gills and therefore, in the compliant system, flow is much less pulsatile at the peripheral end of the 'dorsal aorta' than at the 'gill' end of the same vessel.

Similarly the marked damping of the 'dorsal aortic' pressure profile observed when a compliance is introduced indicates that the flow pulse at the peripheral end of a compliant 'dorsal aorta' also has a much smoother profile than at the input ('gill') end. The origin of the damping effect is most clearly illustrated by a simple mathematical analysis of Satchell's (1971) electrical analogue (Fig. 2-4(A)). The analysis indicates that, with constant input pressure oscilla-

Figure 2-3. Pressures and flows before and after 'gill resistance' in the hydraulic model. Traces (from top to bottom) - first: pressure in the 'ventral aorta' (Pva). Second: flow in the ventral aorta, after 4/5 of the ventral aortic compliance (Qva). Third: flow into the dorsal aorta (Qda). Fourth: pressure in the 'dorsal aorta' (Pda). At the arrow a compliance was introduced into the dorsal aorta.

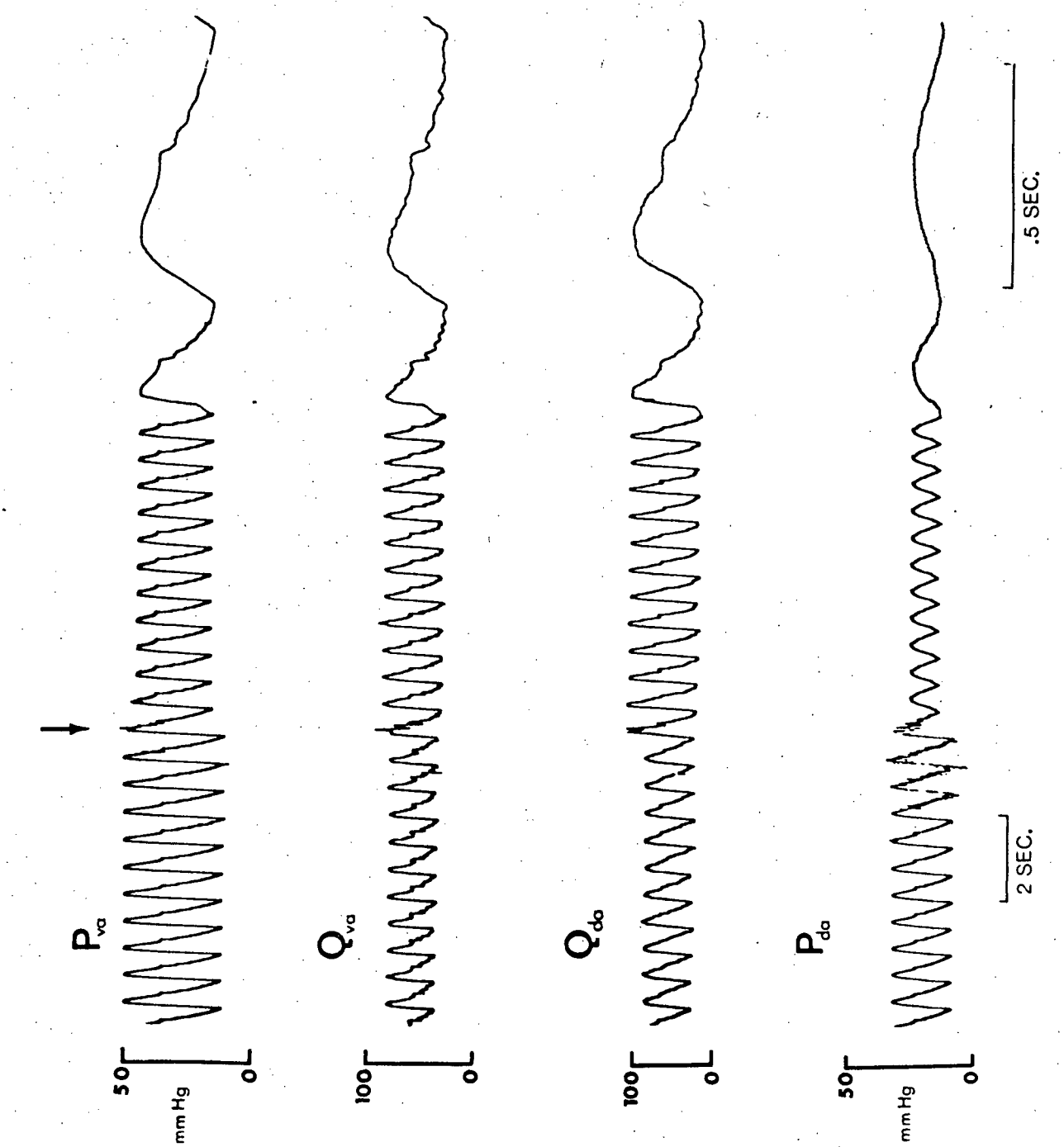
P_{va}
50
mm Hg
0
Q_{va}
100
0
Q_{da}
100
0
P_{da}
50
mm Hg
0
2 SEC.
.5 SEC.

Figure 2-4. An analysis of Satchell's (1971) electrical analogue (A) illustrating the dependence of pulsatility in 'systemic' (B) and 'gill' (C) resistances. In deriving the curves, 'gill' resistance was assumed to be 33% of 'systemic' resistance and 'dorsal aortic' capacitance was taken as the value which best predicted the dorsal aortic pressure and flow patterns seen in the animal.

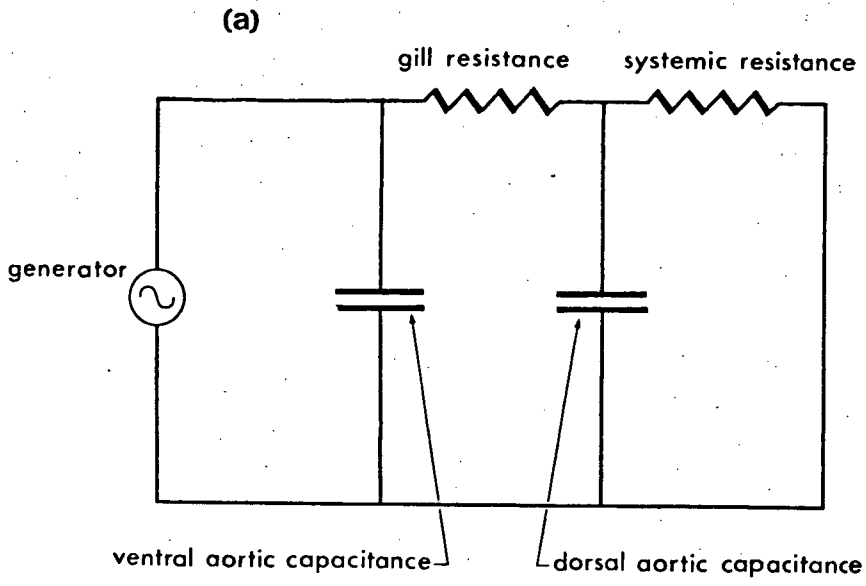
(a)
gill resistance
systemic resistance
generator
ventral aortic capacitance
dorsal aortic capacitance

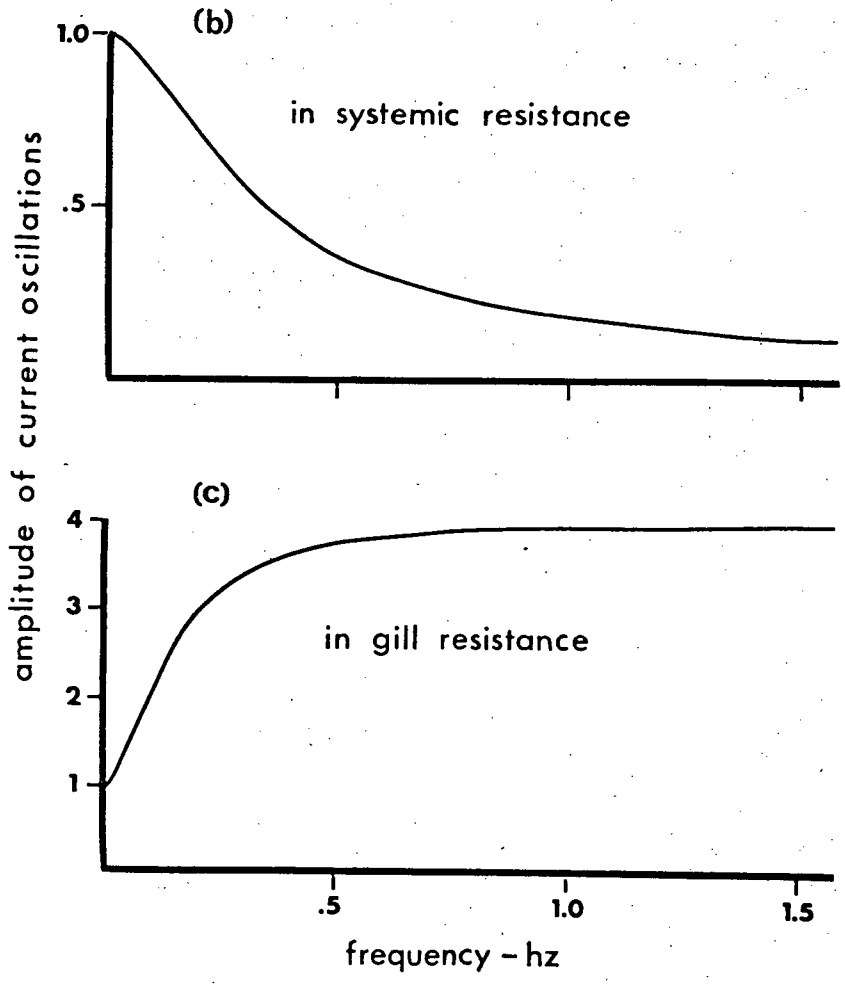
(b)
1.0
.5
in systemic resistance
amplitude of current oscillations
(c)
4
3
2
1
in gill resistance
.5
1.0
1.5
frequency – hz

tions in the ventral aorta, larger current oscillations in the 'gill' resistance (Fig. 2-4(C)) and smaller oscillations in the 'systemic' resistance (Fig. 2-4(B)) are produced as frequency is increased. Consequently the model predicts that the higher harmonics in the complex waveform of flow seen in the dorsal aorta will be relatively much smaller than the corresponding harmonics of ventral aortic flow and therefore the flow profile will appear much smoother. To calculate the curves of Fig. 2-4 the values of resistance and compliance chosen for the analogue are those that best predicted the pressure and flow waveforms observed in the animal, although the general shape of the curves in Fig. 2-4(B) and 2-4(C) are similar over a wide range of such values.

Discussion

Although ventral aortic flow, recorded just distal to the bulbus arteriosis of the cod, was continuous throughout diastole marked depulsation of flow in the ventral aorta also occurs distal to the bulbus (compare the two flow signals in Fig. 2-1). This degree of flow depulsation between the two recording sites was not produced in the model even though 20% of the 'ventral aortic' compliance resided in this region. Obviously, then, the compliance of the ventral aorta is not totally dominated by the bulbus arteriosis, and a significant compliance characterizes the ventral aorta between the bulbus arteriosis and the gills.

The results from the fish also indicate that flow pulsatility in the dorsal aorta was usually double pressure pulsatility. As the present model studies demonstrated, differences between dorsal aortic pressure and flow profiles were diminished as dorsal aortic compliance was reduced and in a rigid system the two profiles were identical in waveform and pulsatility. Since this situation was not observed in the fish measurements a significant systemic compliance must reside distal to the gills. Although there have been no measurements of arterial compliance in teleosts data on the elasticity of the aortae of elasmorbranchs suggests that the wall of the dorsal aorta is some six times as stiff as that of the ventral aorta,

(Lander, 1969). However the dorsal aorta is a much longer vessel and obviously its total compliance is elevated proportionately.

There is some indication that fish may be capable of altering systemic compliance. Occasionally the cod would show a brief rise in blood pressure which was accompanied by an increase in pressure pulsatility and a fall in flow pulsatility. Elevated dorsal aortic pressure may result from either an increase in ventral aortic pressure or a fall in gill resistance. According to model predictions the simultaneous increase in pulse pressure and fall in pulse flow must reflect a drop in dorsal aortic compliance. It is possible that the same agent, norepinephrine for example, could cause both a fall in gill resistance and fall in systemic compliance. Certainly in mammals norepinephrine can induce increases in the moduli of elasticity and viscosity of arterial vessels (Peterson et al., 1960; Bergel, 1964; Gillespie and Rae, 1972) and in teleost fishes norepinephrine is known to cause gill vasodilation (Keys and Bateman, 1932; Ostland and Fange, 1962).

Similarly Stevens and Randall (1967) report that the response of a trout to exercise consisted of a marked increase in ventral aortic pulse pressure and a decrease in dorsal aortic pulse pressure accompanied by a small increase in both mean pressures although the ratio of gill to systemic resistance

changed very little. According to the electrical analogue the amplitude of the harmonics of dorsal aortic pressure (Pda) are related to those of ventral aortic pressure (Pva) by the equation

$$\frac{P_{da}}{P_{va}} = 1 \Big/ \sqrt{\left(1+R_s/R_g\right)^2 + \left(2\Pi R_s C_{da}\right)^2}$$

where Rs and Rg are systemic and gill vascular resistances, f is frequency and Cda is dorsal aortic compliance. Since Rs/Rg and heart rate did not vary and Rs decreases during excercise a marked decrease in Pda/Pva (at least 50%) must reflect an increase in Cda.

The model predicts that any dorsal aortic compliance will result in an amplification of the higher harmonics of gill flow coupled with selective dissipation of these higher harmonics between the gill and capillary circulations. Similarly it must be expected that when higher frequencies are generated by elevated heart rates, for example when the fish is stressed, even more pronounced differences in gill and systemic flow pulsatility will be observed. It has been argued that circulatory systems in general perform optimally in stress situations (Taylor, 1964) and, if this is the case, there seems to be some reason to question the advantages commonly accepted for smooth flow of blood in the gills.

Optimal efficiency of gas exchange requires that minute

volume of water pumped across the gills be in a specific ratio to blood flow through the gills so that the PO_2 of blood closely approaches the PO_2 of the inspired water at a minimal water transport. However, there seems to be little reason to suspect that steady blood flow conveys an advantage over pulsatile flow in this respect. Obviously if the volume of blood exposed to respiratory exchange (gill blood volume) was smaller than cardiac stroke volume then totally pulsatile flow would imply that some blood would be rushed completely through the gills at each cardiac ejection with little opportunity for gas exchange. However the rather limited available data suggests that this situation does not arise. Calculations based on Hughes' (1964) data suggest a gill blood volume of 1.3 ml/kg which is double the stroke volumes (.65 ml/kg) measured in the present experiments. Since direct measurements of gill blood volume in the trout (Salmo trutta) by Stevens (1968) are well above those calculated from Hughes' data on Salmo gairdneri (3.8 ml/kg as opposed to 1 ml/kg) there is reason to suspect that Hughes' data may lead to highly conservative estimates and consequently it seems unlikely, even in exercising cod which may demonstrate marked increases in stroke volume, that stroke volume ever exceeds gill blood volume. Consequently the advantage of smooth blood flow through the gills is suspect and this may indicate why the fish foregoes this adaptation and distrib-

utes the total arterial compliance throughout the arterial system.

SECTION III

Central Cardiovascular Dynamics of Ducks

Introduction

The avian and mammalian stock have been phylogenetically separated for more than 150 million years and one might expect significant differences in cardiovascular function to have arisen during this period of evolution. It is known, for example, that cardiac outputs and systemic blood pressure levels in birds are higher than those of most similarly sized mammals but, unfortunately, extensive studies on avian cardiovascular dynamics which might allow an evaluation of the signficance of such differences are lacking. This is perhaps surprising; avain species are frequently used in studies of cardiovascular disease since they exhibit a propensity for naturally occurring and induced atherosclerosis (Katz and Stamler, 1953; Fox, 1933; Middleton, 1965; Pritchard, 1965) and it might be hoped that birds could be used to study the pronouced haemodynamic effects of arterial degenerative disease observed in humans (O'Rourke et al., 1968). However, sophisticated wave transmission models are required to describe pressure-flow relationships in mammalian arteries (Attinger et al., 1966; Taylor, 1964) whereas it has been suggested that a simple 'windkessel' model might be applied to avian circulations (Taylor, 1964;

O'Rourke et al., 1968). Since the windkessel represents a lumped parameter system in which pressure and flow changes occur simultaneously throughout the system arterial circulations described by this model cannot be used to study characteristics of wave transmission. The physical properties of the avian arterial system, a distensible thoracic aorta distributing blood into stiff-walled peripheral vessels, lend credence to the windkessel model but experimental evidence supporting this approach is apparently limited to single investigation of pressure wave propagation in the turkey aorta (Taylor, 1964). On the other hand the low heart rates and short arterial lengths which made a windkessel approach seem viable in amphibia and smaller fishes are not observed in birds. In the present investigation an attempt has been made to examine the relationships between pressures and flows in the circulation of ducks and to investigate the applicability of different cardiovascular models to this system.

Methods

The Experiments

The experiments were performed on 72 white Pekin ducks (*Anas platyrhynchos*) weighing from 1.75 to 3.40 kg (mean weight 2.2 ± 0.1 kg). The ducks were restrained on their backs and anaesthetized with 25% urethane solution in saline (0.75 ± 1.5 g/kg, I.M.). After cutting through the firculum, a midline thoracotomy was performed to expose the heart and major arteries and an infra-red heat lamp was sited over the duck to assist maintenance of body temperature. The animals breathed normally without assisted ventilation. Blood flows in the aorta (just distal to the branch point with the brachiocephalic arteries), one pulmonary artery and both brachiocephalic arteries were recorded with a Biotronix BL 610 pulsed-logic electromagnetic flowmeter. A wide selection of cuff-type flow probes was on hand and a good probe fit (less than 10% vessel constriction during diastole) was always achieved. When necessary, zero flow was obtained by occluding the vessels distal to the recording site with forceps or pneumatic flow occluders. Often, however, a constant flowmeter output was observed in late diastole and repeated application of the above procedure confirmed that this output represented a reliable measure of zero flow.

Blood pressure was recorded from the aorta, the pulmonary artery and the ventricles using Statham P23 Gb, Hewlett-Packard 267 BC, Bio-tec BT-70 and size 3F and 4F Bio-tec catheter tip manometers. Aortic pressure was recorded by cannulating the left brachiocephalic artery and advancing the cannula to the point where this artery joined the aorta (about 3 cm from the heart). The brachiocephalic artery was not permanently occluded by this procedure. In a few cases the aorta was cannulated just distal to the aortic flow probe. Pulmonary arterial pressure was recorded by inserting a cannula into the proximal pulmonary artery and advancing the cannula until the tip was so some 4-6 cm from the heart. Theoretically pressures recorded with the cannula directed downstream differ from true lateral pressures by a kinetic energy component, $1/2\ pv^2$, where p is the blood density and v is the blood velocity. For pulmonary arterial pressures this difference could amount to 10% during systole. (The kinetic energy component was estimated by assuming a flat velocity profile and taking v as the volume flow rate recorded by the flowmeter divided by the cross-sectional area of the flowmeter probe lumen. A blood density of 1.08 g/cm^3 was assumed (McDonald, 1960)). Consequently, the tips of the fluid-filled arterial cannulae were trimmed to a very long bevel so that recorded pressure would closely follow true lateral pressure. This precaution was also taken when

recording aortic pressure although kinetic energy effects in this vessel alter recorded blood pressures by at most 1%. Hepp et al., (1973) were in fact unable to detect a difference between downstream and lateral pressures either in models or in vivo. They suggest that turbulence around the catheter tip transmits true lateral pressure to the transducer.

Ventricular pressures were recorded by direct ventricular puncture using cannulae tipped with short lengths of 18G hypodermic needles. Alternatively a catheter tip transducer was inserted half way through a hypodermic needle which was subsequently forced through the ventricular wall. Implanting the pressure probes rarely resulted in detectable changes in the blood flows recorded during the cannulation.

In four ducks the four pressures and four flows were recorded simultaneously whereas in seven other only flow in one brachiocephalic artery was not monitored. In twelve ducks single pairs of pressure and flow were recorded from the same vessel for detailed pressure-flow analysis. In thirteen ducks aortic pressure was measured at several sites by advancing a cannula well down the aorta then withdrawing it, in 3 cm steps, to the normal recording site. In five ducks pressures and rate of change of pressures (dP/dt) (computed by Biotronix Bl620 and BL622 analogue computers) were recorded simultaneously in the aortic arch and at varying known positions in the aorta.

Fig. 3-1 illustrates a typical recording. Pulse wave velocity, as a function of position in the aorta, was determined by comparing the difference in transit time of peak dP/dt between the recording sites, marked as ΔT in Fig. 3-1, with the difference in position between the recording sites (usually 3 cm). This technique was found superior to the standard approach to measuring the transit time of the ascending limb of the pressure pulse between recording sites (McDonald, 1968) since changes in the pressure profile during propagation resulted in difficulty in identifying corresponding points on the two profiles whereas peak dP/dt was always well determined. In the remaining thirty-one animals different combinations of at least 3 pressures and/or flows were recorded.

Recording systems and data analysis

Some of the pressure and flow data were recorded directly on a Techni-Rite Tr 888 pen recorder writing on rectilinear co-ordinates. The pen recorder was tested using a sine wave generator and had a maximum frequency response of 120 Hz when the pen deflection was 5 mm peak to peak. At a pen deflection of 40 mm peak to peak the frequency response fell to 35 Hz. For this reason the pen recorder traces were only used to establish the temporal relationships between pressure and flow pulses whereas pressure and flow traces which were subjected to more rigorous analysis were converted to frequency modulated

Figure 3-1. Demonstration of the technique used to measure pulse wave velocity. The top two traces are pressures (P) recorded at two sites, separated by 3 cm, in the duck aorta. The bottom two traces are the corresponding rates of change of pressure, dP/dt. Traces, from top to bottom; pressure recorded proximal to the heart; pressure recorded distal to the heart; rate of change of pressure recorded proximal to the heart; rate of change of pressure recorded distal to the heart.

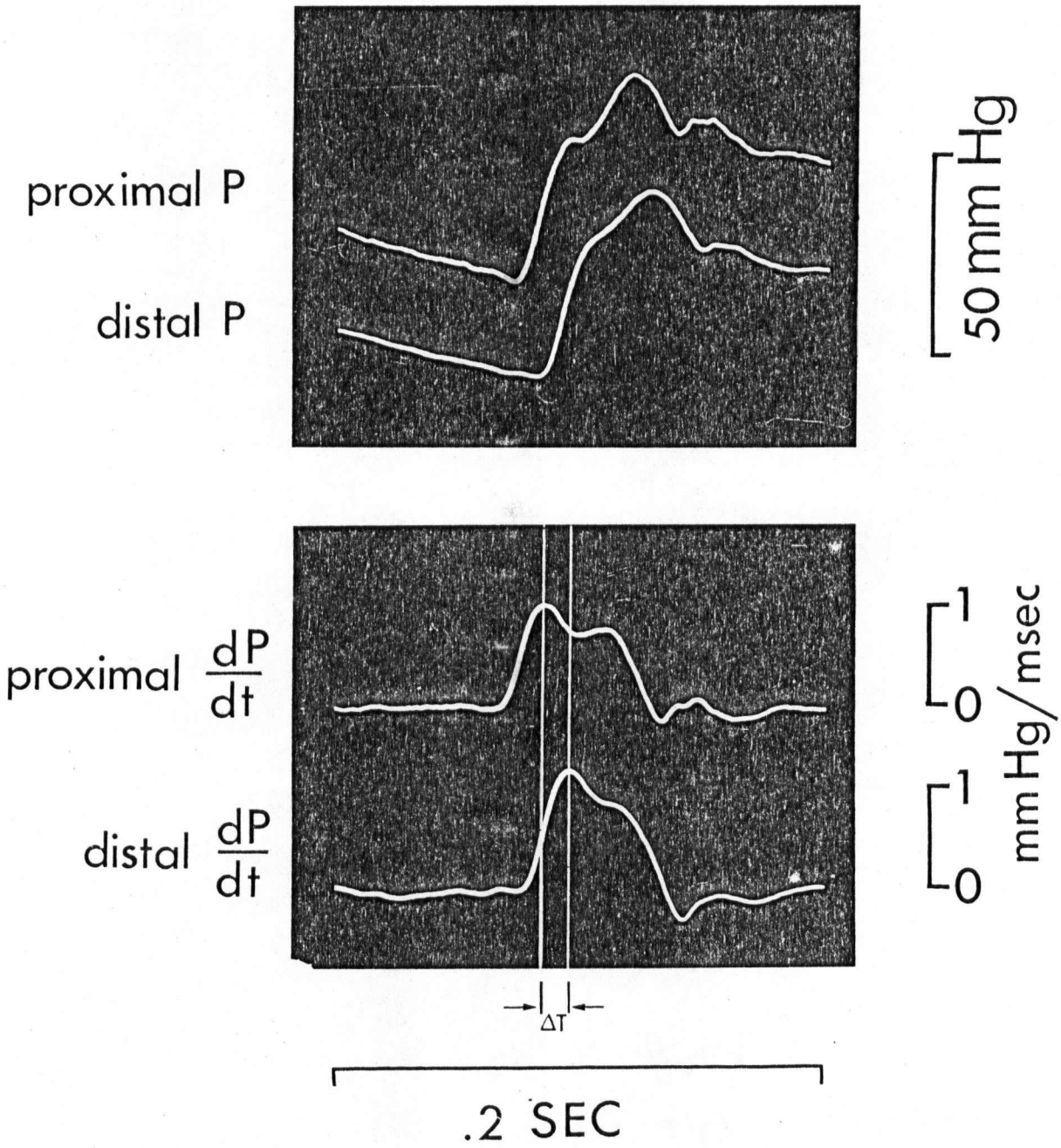
proximal P
distal P
50 mm Hg
proximal dP/dt
distal dP/dt
1
0
1
0
mm Hg/msec
ΔT
.2 SEC

signals by an FM adaptor (A.R. Vetter & Co., Pa., U.S.A.) and stored on magnetic tape on an Akai 2800 DSS four channel tape recorder. These signals were simultaneously displayed on a Hewlett-Packard 1201 A storage oscilloscope. The FM adaptor demodulated the taped signal when the recorder was in the playback mode. The tape-recorder adaptor system was tested with an audio frequency generator and was found to produce less than 1% amplitude distortion in the range 0-100 Hz and a linear phase lag (0.25 /Hz) that was identical on all recorder channels, therefore no correction for recorder distortion was required. These pairs of arterial pressures and flows were digitized and the resulting data subjected to Fourier analysis using a "fast Fourier transform" program (Cooley and Tukey, 1965) on an IBM 360 computer. The impedances (modulus and phase) of the aortic circulation and the vascular bed supplied by one pulmonary artery were calculated from these computed pressure and flow components and appropriate corrections were made for flowmeter phase lag.

Mean blood pressures and flows were calculated by measuring areas under the respective pulses, either with a planimeter or by comparing the weight of the paper defining the area to be determined with the weight of a known area of the same paper and dividing by the cycle length. Cardiac output was calculated as the sum of the flows in the two brachiocephalic arteries plus

the aortic flow. Biotronix BL 620 and BL 622 analog computers were used to compute time derivatives of aortic pressure for the determination of aortic pulse wave velocity.

Because of the high frequency content of signals generally recorded in homeotherms rigorous static and dynamic calibration of manometric and flowmeter systems is essential if sophisticated methods of analysis are to be applied to data obtained using these systems. This constraint is particularly important when attempting to record pressures from such sites as the left ventricle where the higher harmonics make significant contributions to the total signal. These higher harmonics often cause manometer resonance resulting in overshoot artefacts which in some cases have been attributed to a physiological origin (Spencer & Greiss, 1962). For such reasons the static and dynamic calibrations of the recording systems used in this series of experiments will be discussed in detail. All manometric systems, except the catheter tip manometers, were filled with de-aerated avian saline containing 40 i.u./ml of heparin, after first flushing the system with CO_2 gas. These manometers were connected to two saline-filled reservoirs (the surface of the saline was covered with paraffin oil) which could be moved independently to give the zero level (which, in the recording situation was at the opening of the catheter) and a known pressure head. Static calibration of the catheter tip manometers

was achieved by submerging the manometer to known depths in a vertical column of water which was maintained at 38-40°C. Short polythene or vinyl cannulae of various diameters were used to make connection between the saline-filled manometers and the blood vessels. Dynamic calibration of all manometers was performed before or after each experiment by applying a sudden pressure change to the tip of the catheters (Hansen 'pop-test') and recording the free vibrations of the manometric system on the recording system used in the experiment. The frequency responses of the manometric systems which could be consistently obtained were as follows: Hewlett-Packard 267 BC - 70 Hz at 0.1 relative damping; Statham P23 Gb - 90 Hz at 0.15 relative damping; Bio-tec BT-70 - 200 Hz at 0.1 relative damping and the Bio-tec catheter tip manometers - 380 Hz at 0.05 relative damping. Although all these manometers were capable of accurately reproducing arterial pressures this was not the case with ventricular pressures. With the lower frequency manometers a pronounced 'overshoot' occurred early in systole, the size of which was progressively reduced as the frequency response of the manometer used increased.

Static calibration of the Biotronix BL 610 pulsed-logic electromagnetic flowmeter was perfomed at the end of an experiment. At this time a portion of the artery was excised and, with the transducer in place, saline or blood was passed through

the vessel from a reservoir. The fluid passing through the transducer was collected in a graduated cylinder and the period for collection of 100 ml was timed by stopwatch. Saline and blood gave identical calibrations when a single probe was tested with both. Other investigatiors have found that saline calibrations differ from blood calibrations by 2% or less when the blood haematocrit is normal (Pierce et al., 1964; Greenfield et al., 1966). Flowmeter outputs were linear throughout the range tested (0-1000 ml/min).

Dynamic calibration of the flowmeter and recording systems (Techni-Rite TR 888 or Akai recorder and Hewlett-Packard 1201 A oscilloscope) was performed using a pump similar to that described by Taylor (1959) or by applying a known a.c. signal to the input side of the flow transducer cable. The pump allowed assessment of the transducer phase lag and amplitude distortion up to frequencies of 10 Hz whereas the electronic calibration could be applied over an unlimited range. When a step voltage was applied to the input connectors of the flowmeter the output response was identical to that seen when a constant flow through the flow probe was suddenly occluded by a solenoid valve, thus verifying the validity of the electronic calibration, i.e. confirming that virtually all distortion was produced in the input amplifier of the flowmeter rather than in the flow probe. Other investigators have previously established

the validity of this type of electronic calibration (Gessner and Bergel, 1964; Case et al., 1966). With both the pen recorder and the oscilloscope systems amplitude distortion was negligible over the frequency range 0-20 Hz, (3db point was 50 Hz) however, phase lag was 1.8 /Hz when recording on the oscilloscope and 3.2 to 3.7 /Hz when using the pen-recorder. The larger and more variable phase lag with the pen recorder was related to the characteristics of the pen galvanometer rather than the input amplifiers of the system.

Results

Pressures and flows in the Central circulation

Pressure and flow pulses recorded from the aorta, both brachiocephalic arteries, pulmonary artery and both ventricles are shown in Fig. 3-2. The eight traces shown in Fig. 3-2A were recorded simultaneously so that temporal relationships between events of the cardiac cycle could be established. The oscilloscope traces in Fig. 3-2B were recorded in pairs so that particular attention could be paid to the fidelity of each recorded signal to assure an exact representation of all waveforms. For presentation purposes typical pulses are superimposed in Fig. 3-3. The onset of contraction occurred synchronously in the two ventricles and the aortic and pulmonic valves opened simultaneously. Left ventricular systole lasted approximately 0.12 sec and varied little with changes in heart rate. At the mean heart rate of 219 $\pm$ 4 beats/min left ventricular systole occupied 44% of the cardiac cycle but the duration of right ventricular systole exceeded left by up to 30% (Fig. 3-2B and 303). The central aortic pressure pulse was characterized by a sharp initial rise which was usually terminated in a distinct anachrotic shoulder, followed by a slower rise to peak pressure (Fig. 3-1, 3-2 and 3-3). At peak pressure there was no detectable pressure difference between the left ventricle (mean value 165 $\pm$ 1.2 mm Hg) and the aorta (mean value

Figure 3-2 A. Pressures (mm Hg) and flows (L/min.) recorded simultaneously in the central arterial system of the duck. Traces, from top to bottom; flow in the right brachiocephalic artery, RBAF; flow in the left brachiocephalic artery LBAF; pulmonary arterial flow, PAF; pulmonary arterial pressure PAP; aortic flow, AF; aortic pressure, AP; right ventricular pressure, RVP; left ventricular pressure, LVP.

B. Oscilloscope records of central pressures and flows recorded in pairs. Traces match those in Fig. 2A, but were recorded, each pair, from a different animal.

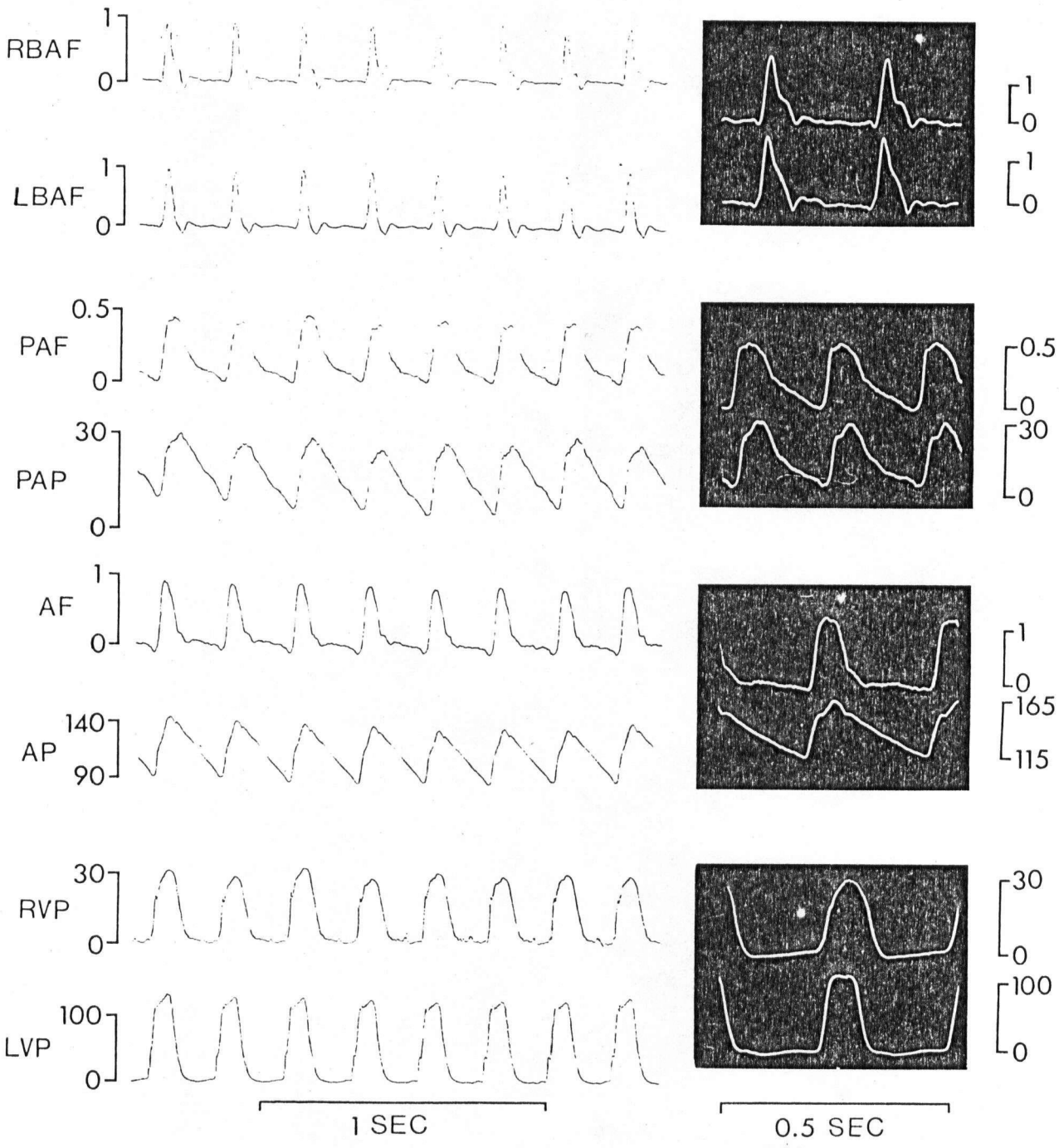
RBAF
1
0
LBAF
1
0
PAF
0.5
0
PAP
30
0
AF
1
0
AP
140
90
RVP
30
0
LVP
100
0
1 SEC
0.5 SEC
1
0
1
0
0.5
0
30
0
1
0
165
115
30
0
100
0

Figure 3-3. Overlap drawing of pressure (——) and flow (----) pulses in the systemic (A) and pulmonary (B) circulations of the duck. The vertical lines are separated by time intervals of 0.025 sec. LVP, left ventricular pressure; AP, aortic pressure; AF, aortic flow; RVP, right ventricular pressure; PAP, pulmonary arterial flow; PAF, pulmonary arterial flow.

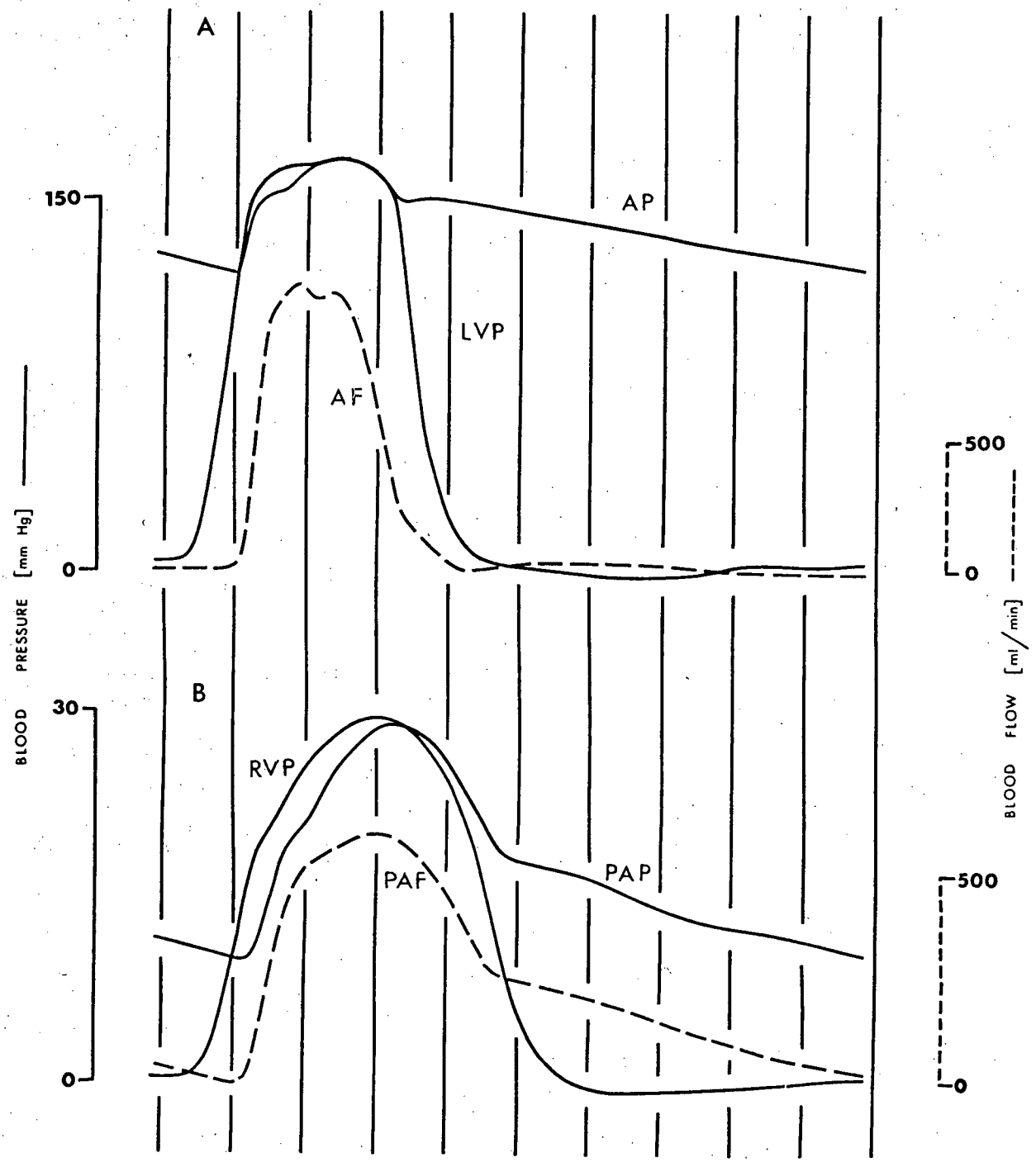
A
150
0
AP
LVP
AF
BLOOD PRESSURE [mm Hg]
500
0
BLOOD FLOW [ml/min]
B
30
0
RVP
PAF
PAP
500
0

165 ± 1.6 mm Hg). An incisura marked closure of the aortic valves and the diastolic decline of aortic pressure rarely displayed a dichrotic wave. During diastole central aortic pressure declined to a mean value of 121 ± 2 mm Hg. However, during transmission along the aorta the pressure pulse changed in both pulse amplitude and contour with pulse pressure increasing by an average of 29.1 ± 3.1%. This increase in pulse pressure (peaking of the pressure wave) resulted from a marked increase in the amplitude of the systolic portion of the pressure pulse with little change in the diastolic portion (Fig. 3-4). Ducks which displayed only slight increases in pulse pressure also exhibited little change in pulse contour. The pulse wave velocity also increased along the aorta rising from 4.4 ± 0.8 m/sec in the aortic arch to 11.7 ± 1.2 m/sec in the adbominal aorta. In the majority of animals the increase in pulse wave velocity was effected in the thoracic aorta. The total transit time for the pulse to reach the distal end of the aorta, at a mean blood pressure of 143 ± 2 mm Hg obtaining in these experiments, was approximately 20 m.sec, or 5-10% of the cardiac cycle.

Aortic blood flow rose sharply after opening of the aortic valve and peak flow preceded peak pressure by about 25 msec. (Fig. 3-2B and 3-3). Aortic flow rate fell sharply at the end of systole but little or no backflow was recorded (Fig. 3-2).

Figure 3-4. Pressure waves recorded in the abdominal aorta (left trace) and the aortic arch of the duck. Marked changes in the amplitude and profile of the wave are seen during propagation along the aorta.

mm Hg
100
150
1 SEC
1SEC

Frequently aortic flow displayed a double maximum. Flow traces were nearly identical in the two brachiocephalic arteries (Fig. 3-2B; a narrow peak flow rate was observed whereas the falling limb of the flow profile was interrupted by a levelling off in late systole. This phase was consistently followed by a brief period of backflow and later return to zero flow for the remainder of diastole. Three-quarters of the total cardiac output (482 $\pm$ 7 ml/ min) was distributed equally between the brachiocephalic arteries which supply the wing, flight muscles, and head.

The pulmonary arterial pressure wave was similar to that seen in the aorta but pressure was more pulsatile, with the average diastolic pressure of 9 $\pm$ 0.2 mm Hg being less than one-half the average peak systolic pressure of 26 $\pm$ 0.5 mm Hg (Fig. 3-3). The peak systolic pressure in the pulmonary artery was, on average, some 2 mm Hg below the peak right ventricular pressure although this difference was not significant. Blood flow in the pulmonary artery was consistently maintained during diastole and at normal heart rates flow fell to zero only immediately before the onset of the next cardiac ejection (Fig. 3-2 and 3-3). In this regard the flow profile closely resembled that recorded in the pulmocutaneous arches of amphibia (Section I; Fig.1-9; Shelton, 1972). However, the application of adrenalin (20 ug/ml) to the external wall of the pulmonary artery resulted

in a marked change in flow profile (Fig. 3-5). Forward diastolic flow was completely eliminated and a distinct period of backflow following systole was observed.

Pressure flow relationships

Impedance versus frequency curves from individual ducks are presented because averaging procedures cannot be applied to impedance data from animals with uncontrolled heart rates since each animal supplies impedance information at a different distribution of frequencies. In any event when such data can be combined, for example when the heart is artificially paced, the averaging procedure tends to obscure details of impedance relationships (O'Rourke and Taylor, 1966). The impedance curves presented are typical of all experiments and although the high heart rates encountered necessitate considerable interpolation of impedances at anharmonic frequencies, impedance curves from other ducks displayed no consistent features not illustrated by the curves presented here. Fig. 3-6 illustrates typical impedance modulus and phase graphs determined at the input of the aortic circulation (Fig. 3-6A) and the circulation of the left pulmonary artery (Fig. 3-6B). Aortic impedance modulus fell sharply from its maximum at zero frequency (resistance to steady flow) to a minimum at 9-12 Hz before rising again. At higher frequencies the impedance modulus was less than one-thirtieth the d.c. resistance. Aortic impedance phase fell to -1 radian

Figure 3-5. Pulmonary arterial flow recorded before (a) and after (b) application of adrenaline (20 µg/ml) to the external wall of the pulmonary artery. Positive diastolic flow in the control situation (a) is replaced by a period of backflow followed by a return to zero flow after application of adrenaline (b).

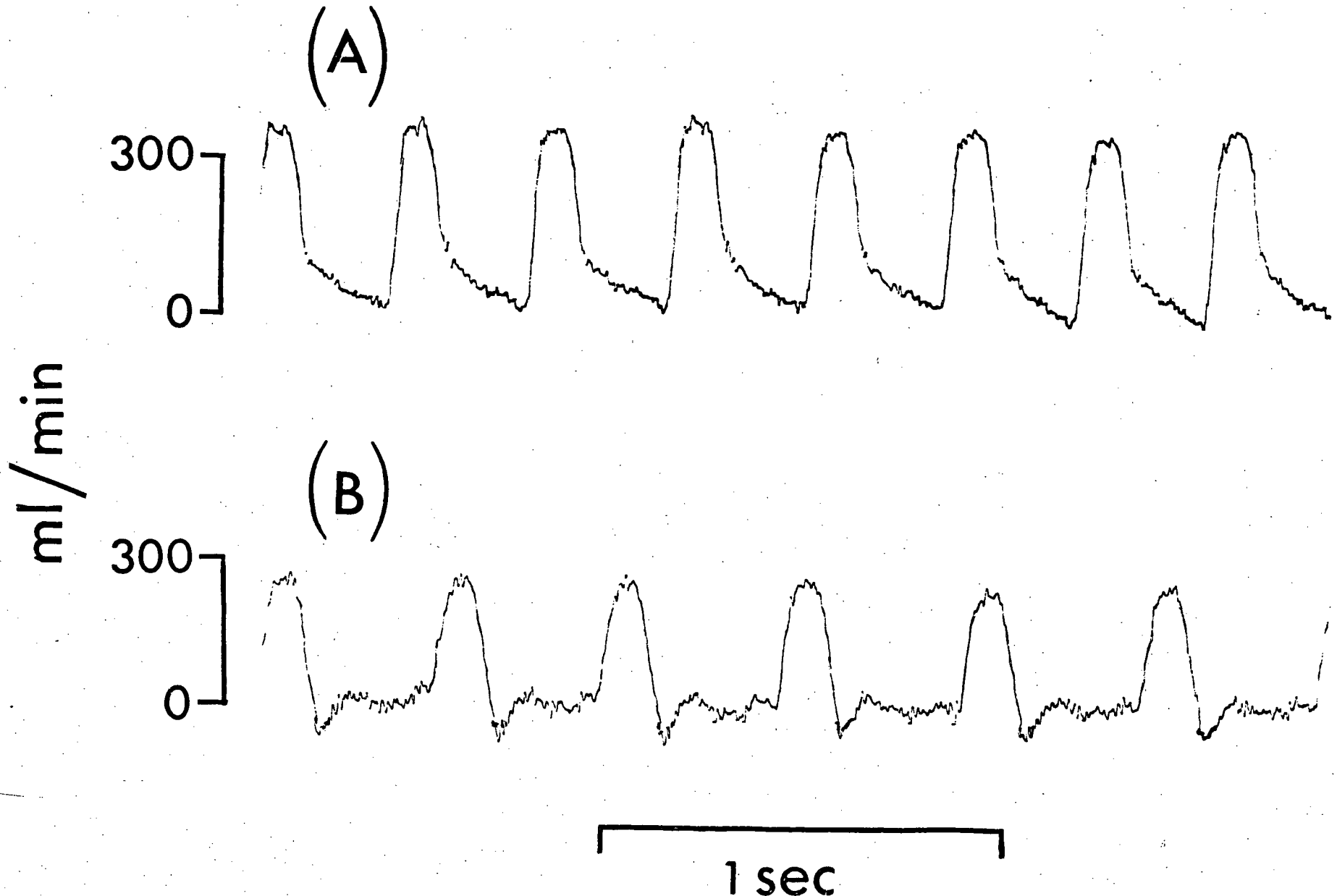
(A)
300
0
ml/min
(B)
300
0
1 sec

Figure 3-6. Input impedance modulus and phase versus frequency graphs for the aortic (A) and pulmonary (B) circulations of the duck. Impedance data from 6 ducks is supplied, one pair of modulus and phase curves from each animal. Also shown is the harmonic content of the pressure and flow waves in the aorta and pulmonary artery.

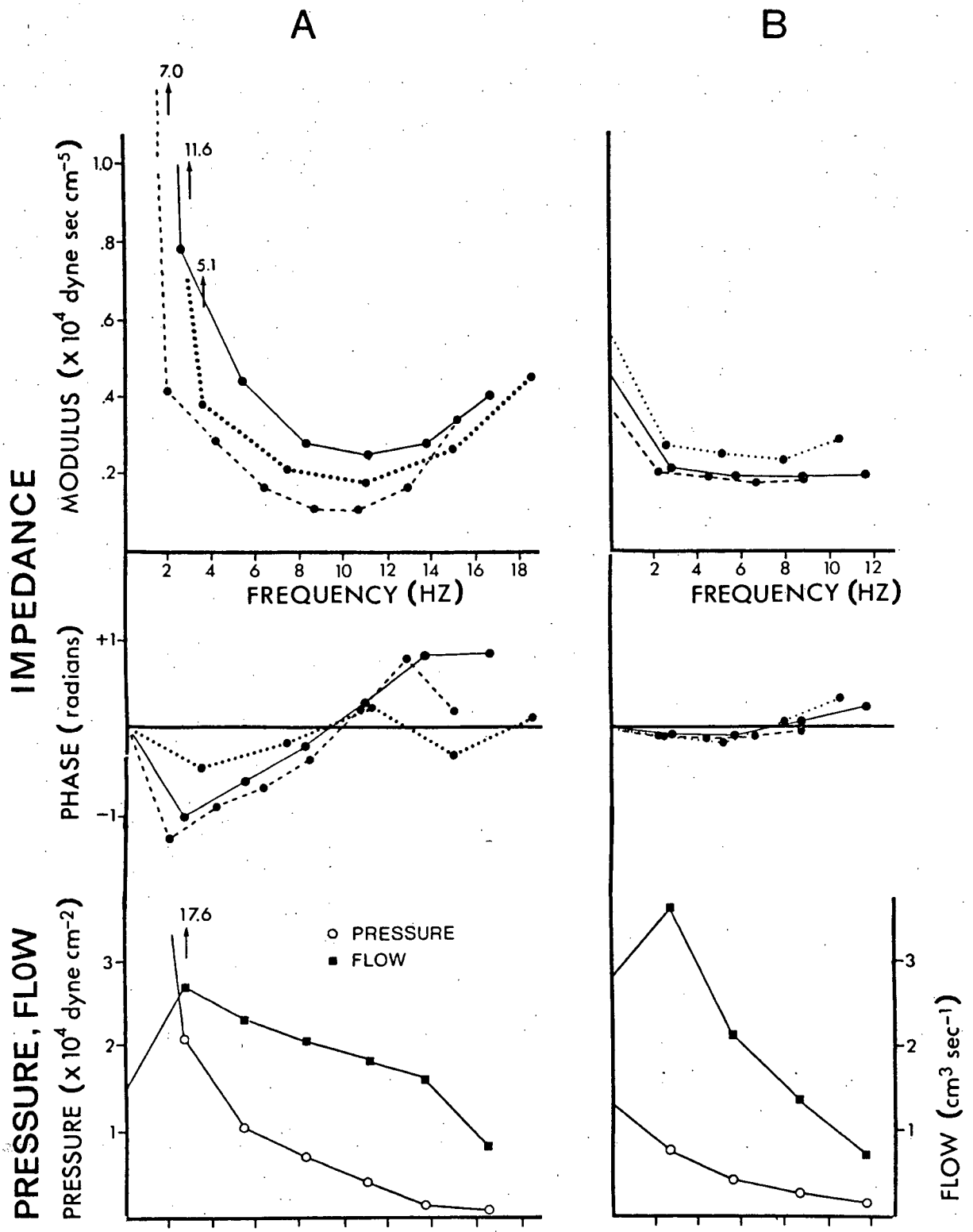
A
B
IMPEDANCE
MODULUS (x 10⁴ dyne sec cm⁻⁵)
7.0
11.6
5.1
1.0
.8
.6
.4
.2
2 4 6 8 10 12 14 16 18
FREQUENCY (HZ)
2 4 6 8 10 12
FREQUENCY (HZ)
PHASE (radians)
+1
−1
PRESSURE, FLOW
PRESSURE (x 10⁴ dyne cm⁻²)
17.6
PRESSURE
FLOW
3
2
1
FLOW (cm³ sec⁻¹)

at low frequencies then rose sharply to about +1 radian. Zero phase occurred at the frequency of the minimum in impedance modulus. Impedance of the pulmonary arterial bed showed much less dependence on frequency than aortic impedance (Fig. 3-6). Impedance modulus fell to slightly less than half its d.c. value then remained independent of frequency while impedance phase was close to zero throughout the frequency range tested. This relative independence of impedance on frequency implies that corresponding pressure and flow harmonics were proportionately related and in phase, hence the similar profiles of pulmonary arterial pressure and flow (Fig. 3-3). Fig. 3-6 also illustrates the harmonic content of the pressure and flow waves from one duck. Although the sixth harmonic of flow is still highly significant in the systemic circulation the same harmonic of pressure is very small and higher harmonics make no measureable contribution to the pressure wave.

Discussion

High systemic blood pressures reported for other birds (Sturkie and Vogel, 1957; Speckmann and Ringer, 1963) have been confirmed in the present experiments. This high blood pressure is a reflection of an elevated output of the cardiac pump rather than a high flow resistance since total peripheral resistance (mean arterial pressure divided by cardiac output) for the systemic circulation is below that reported for mammals of similar size (e.g. cats, Spector, 1956). Cardiac output in the present acute preparations was lower than those determined in ducks by the dye dilution technique (Sturkie, 1966; Folkow et al., 1967; Jones and Holeton, 1972a), but was in the same range as those recorded chronically with electromagnetic flow-meters (Jones and Holeton, 1972b). It now appears obvious that a major discrepancy exists between these techniques which is unrelated to whether the experiments were performed on open or closed chest animals. Mean pulmonary arterial pressures (17 $\pm$ 0.3 mm Hg), unlike the mean systemic arterial pressures, were within the mammalian range (Patel et al., 1963; Bergel and Milnor, 1965). Evidently the vascular arrangement in the avian lung accommodates high pulmonary flow without elevated pressures; in other words, the resistance of the pulmonary vascular bed is extremely low.

Dynamically the avian circulation shares many properties with that of the mammal. The increase in amplitude and velocity of the pressure pulse during transmission through the aorta resembles the situation observed in mammals (McDonald, 1968; O'Rourke et al., 1968). On the other hand, the aortic pulse rarely displayed dichrotic waves which are frequently seen in mammals (McDonald, 1960; Remington, 1960). The shape of the pressure and flow waves in the central circulation were similar to those observed in mammals (Bergel and Milnor, 1965; O'Rourke, 1967; Oboler et al., 1973), with the marked exception of pulmonary arterial flow. The appreciable pulmonary arterial flow during diastole may be attributed, in part, to siting the flow probe further from the heart than in typical experiments on dogs (in birds the root of the pulmonary artery is not easily accessible). Nevertheless this marked diastolic flow must indicate a high distensibility of the proximal portion of the pulmonary artery. A highly distensible pulmonary artery may be necessary to depulsate pulmonary pressure and flow since the volume of the avian puomonary circulation is small (Burton and Smith , 1968), and, as flow resistance is low, stiff supply vessels would be unable to store sufficient blood during systole to maintain diastolic pressure and flow. The extended duration of right ventricular systole compared with left, which decreases the diastolic interval over which pressure and flow rate decline,

also contributes to the maintenance of flow throughout the cardiac cycle (Taylor, 1964), this feature of the avian circulation not being shared by mammals (Franklin et al., 1962; Oboler et al., 1973). The distinct alteration in the flow profile following external application of adrenalin to the arterial wall indicates a decrease in the time constant of the pulmonary vascular bed. Such an effect can only be the result of a fall in pulmonary compliance or resistance and, as pulmonary resistance rose following adrenalin application, this decreased time constant is interpreted as indicating a marked stiffening of the arterial wall. The flow profile resulting after adrenalin application closely resembled that normally recorded in the pulmonary artery of mammals (Bergel and Milnor, 1965; Pace, Cox, Alvarez-Vara and Karreman, 1972). Undoubtedly, the adrenalin was absorbed systemically and caused generalised circulatory changes in that heart rate and stroke volume fell but those effects cannot provide an explanation for the observed changes in the flow profile.

The need for sophisticated cardiovascular models to describe pressure-flow relationships in mammalian arteries can be attributed, for the most part, to the finite velocity of the pulse wave generated by the heart. Pressure (and flow) oscillations at different sites in mammalian arterial systems are significantly out of phase and pressure and flow waves may be

markedly altered by reflection and dissipation effects and by spatial variation of arterial wall properties, factors which can only be described in terms of wave transmission models. Reflection effects, for example, are maximal when the transit time of a pressure wave between the heart and reflecting sites (the arteriolar beds) is 1/4 of a cycle and can be neglected only for much lower transit times. Since at least the first five harmonics make significant contributions to typical pressure waves (Patel et al., 1963) transit times must be below 5% of the total cardiac cycle if reflection effects are to be ignored, a situation not encountered in mammals commonly studied. Certainly measurements of aortic pulse wave velocities in ducks give no indication that a windkessel model can be used to characterize the avian systemic circulation. Pulse wave velocities are not significantly above those reported for the dog (McDonald, 1968) and the transmission time of the pulse wave along the aorta is 5-10% of the cardiac cycle and consequently not even the first harmonics of the pressure and flow waves will be free from wave transmission phenomena.

In addition, the impedance curves of the aortic circulation displayed features commonly observed in studies of mammalian circulations (Patel et al., 1963; O'Rourke and Taylor 1967) except that in the latter the minimum in impedance modulus occurs at a lower frequency (2-6 Hz) and large positive

phase angles are not always observed. A minimum in impedance modulus and the corresponding pattern of impedance phase are not predictable from a windkessel model and are normally attributed to the effects of wave reflection. Further evidence that wave transmission effects are significant in the aortic circulation was observed when pressures were recorded at different sites in the aorta. Pronounced 'peaking' or amplification of the pressure pulse was observed with pulse pressure increasing by approximately 30% between the aortic arch and the abdominal aorta. This degree of amplification is similar to that reported in humans. O'Rourke et al (1968) found that the pressure pulse increased in amplitude by an average of 35% (calculated from their graphical data) during transmission along the aorta of patients who displayed no evidence of vascular lesions (20 patients, aged 6-70 years). The change in shape of the pressure pulse during propagation was also quite similar to that reported by O'Rourke et al., (1968). Peaking of the pressure pulse has been attributed to both reflection effects (McDonald, 1960) and the progressive stiffening of the arterial wall at sites more distal to the heart (Taylor, 1964). In any event peaking is a manifestation of wave transmission and cannot be predicted from a windkessel model. On the other hand, although the major characteristics of pulmonary arterial impedance, a moderate decline in modulus and near-zero phase, are similar to those

reported for the mammal (Caro and McDonald, 1961; Bergel and Milnor, 1965; Reuben et al., 1971; Pace et al., 1972) no oscillations in pulmonary impedance modulus and phase were observed in the duck. It may be that wave transmission effects are not of major importance in the avian pulmonary circulation or that terminations in the low -resistance pulmonary bed are well-matched with the characteristic impedance of the supply vessels, in which case reflection effects would be minimized. However, since pulse wave velocities were not determined in pulmonary vessels this question cannot be settled at the moment.

SECTION IV

The Effects of 'Elastic Taper' and Reflections on Wave Propagation in Mammalian Arteries

Introduction

Theories describing the dynamic aspects of blood flow in arterial systems have developed almost exclusively from studies on mammals, most notably the dog, cat and rabbit, and consequently far more is known about haemodynamics in these species than in any others. Nonetheless a complete, quantitative analysis of pressure-flow relationships throughout a mammalian arterial system is still not possible and undoubtedly this is related to the myriad of factors which influence these relationships. Rapid gains in this direction were made in the 1950's following the realization that lumped parameter models of mammalian arterial systems, such as the windkessel, had to be abandoned in favour of a wave transmission approach. Most notably the theories of Womersley (1958) appeared capable of incorporating most factors which influence pressure-flow relations in uniform segments of arteries and certainly his approach was highly successful in predicting local flow patterns from the pressure gradient along short lengths of vessel (McDonald, 1955, 1974). The hope was expressed that by dividing the arterial system into a multitude of such vessel segments and integrating the effects of wave

transmission over these many segments that transmission through the complete arterial tree could be synthesized. Unfortunately the most cursory attempts in this direction were unsuccessful and it soon became apparent that such an approach could not account for such factors as the continuous, gradual changes in vessel properties, e.g. the progressive stiffening of the arterial tree at sites more distal to the heart, for reflection of waves from discontinuities such as branch sites or for the flow distrubances which these discontinuites produce.

Perhaps the greatest obstacle to progress in this direction, certainly the most extensively investigated, lies in assessing the phenomenon of wave reflection. Although it is now widely accepted that reflections occur their importance to arterial dynamics is still a point of dispute (McDonald, 1974). There are a number of reasons for this controversy. Firstly wave reflections in a system of elastic tubes may occur wherever there is a discontinuity in the system and in the highly arborized arterial tree the near infinite number of bends and branch points at many different distances from the heart will send back numerous small reflections which summate in a highly complex fashion. The approaches of treating the summed reflected wave as if it originated from an 'average' reflection site (McDonald, 1974) or lumping together all reflections from specific regions (O'Rourke, 1967) are useful but clearly limited.

It is also not clear which sites makes the greatest contribution to wave reflections. Originally it was felt that major branch points such as the aortic trifurcation generated the greatest reflections (see Remington and O'Brian, 1970) whereas it is now argued that the many smaller discontinuities in the arteriolar beds are of greater signifigance. The reason for the shift in opinion is that impedance curves are said to show more evidence of reflections when peripheral beds are vasoconstricted and less during vasodilation (O'Rourke and Taylor, 1966; Westerhof et al., 1973) although these differences in impedance pattern appear, to this worker, equivocal at best.

In recent years a further difficulty in assessing reflection phenomena has been elucidated. Taylor (1964, 1965) has developed a theory based upon an electrical transmission line analogue which predicts that the progressive stiffening of arterial vessels at sites more distal to the heart, the so-called "elastic tapering" of arteries, may produce effects which mimic those of reflections. Both amplification of the pressure wave and oscillations in impedance curve, the two most striking effects of reflections, may be generated and thus distinquishing reflection effects from those of elastic taper is difficult. Although this theory has prompted a number of related studies in the last decade (e.g. Barnard et al., 1966; Fich et al., 1966; Fich and Welkowitz, 1967; Attinger et al., 1968) there

has been no experimental verification that this transmission line theory is meaningful in a fluid mechanical system. Certainly, such tests would be difficult to perform in _in vivo_ studies since so many factors affect the nature of pulse wave propagation. In the present investigation the effects of elastic taper are studied in a model 'artery', an elastic tube which has been chemically treated to produce a continuously varying wall stiffness. The propagation characteristics of pressure waves of varying frequency are examined by a new approach which may have widespread applications in other areas of cardiovascular research. The possibility of treating elastic taper effects as reflection phenomena is discussed. Further _in vivo_ experiments are aimed at investigating the effects of drug-induced vasomotion on wave reflections by examining pressure wave propagation characteristics as opposed to studying the effects of such interventions on impedance curves.

Methods

Hydraulic model of an artery with elastic taper

The model was prepared by filling a polyvinyl tube (radius 0.8 cm, wall thickness 0.2 cm) with a softening chemical (cyclohexanone) and draining the chemical at controlled rate so that certain regions of the tube were exposed for longer periods than others. In order to determine an appropriate drainage rate lengths of similar tubing were first treated with the chemical for different time periods in order to establish an exposure time versus tube stiffness relationship. "Stiffness" (Youngs modulus, E, times wall thickness, h) was determined by stretching samples of the tubes in the apparatus shown in Fig 4-1. The extension, read off the micrometer scale, was compared with the force recorded by the strain gauge and stiffness was calculated according to the equation

$$Eh = L_o \Delta F \Big/ 2\pi R \cdot \Delta L$$

where ΔF is the force applied, ΔL is the resulting extension, L_o the resting length and R the tube radius. Drainage rate of the actual model was then regulated to produce a tube which was softened to the maximal extent possible for the first 30 cm of the inflow region with stiffness then increasing linearly to a maximum at 150 cm from the origin. Tube stiffness was then

Figure 4-1. Apparatus for measuring elasticity of cyclohexanone-treated polyvinyl tube. Tube sample is clamped to two plugs one of which is attached to a strain gauge and the other is mounted on a moveable stage which can be displaced known distances with a micrometer

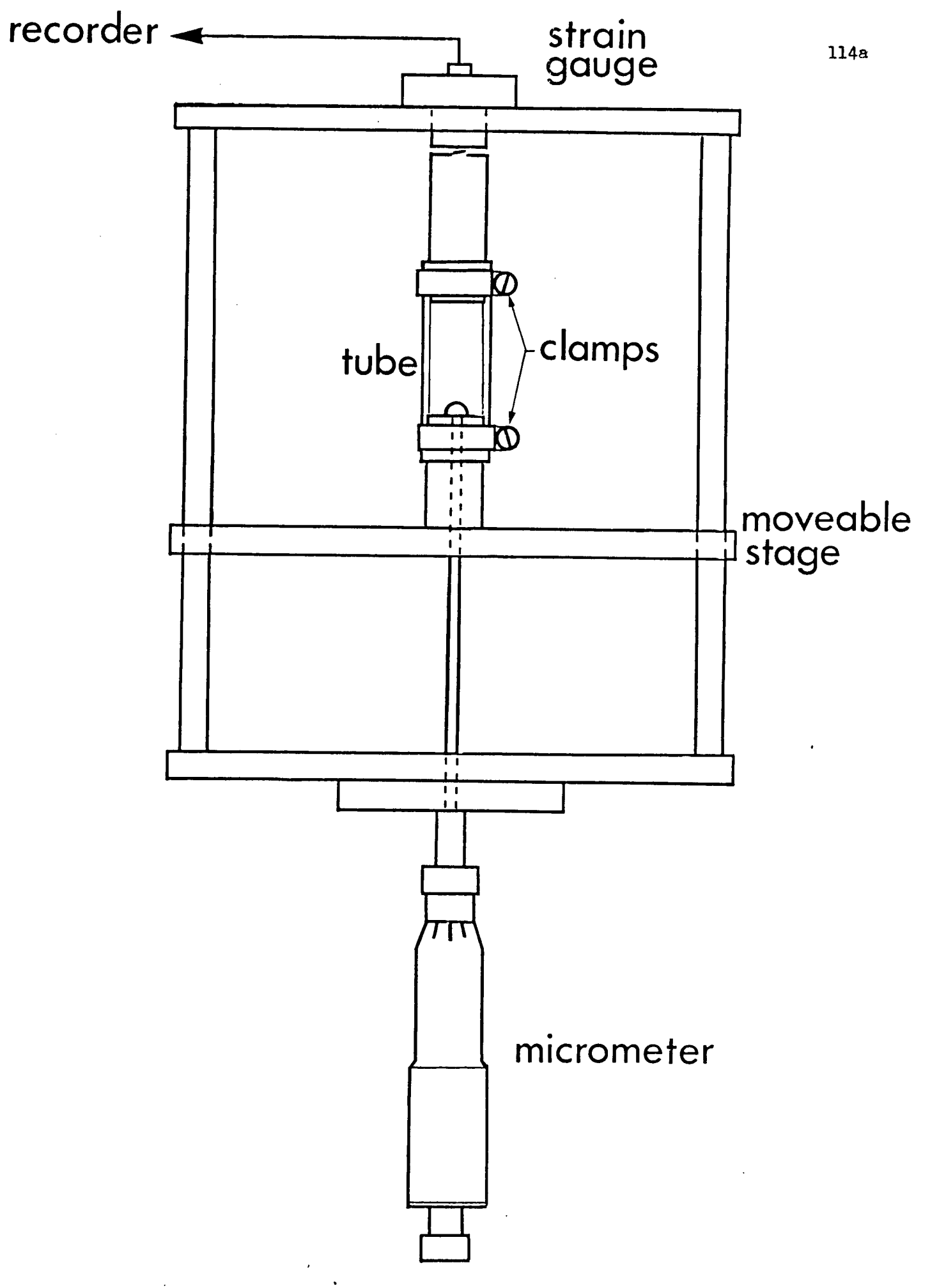
recorder
strain gauge
tube
clamps
moveable stage
micrometer

constant at this maximum level throughout the rest of its length which was 7 m. At the end of experiments tube stiffness as a function of position was determined directly by cutting the model into short lengths and measuring the stiffness of each segment. In preparing the model it was necessary to pretreat the entire tube with cyclohexanone for 15 min. since shorter exposure times produced erratic results. In addition treatment times were limited to a maximum of 4 hours since longer exposures caused a complete breakdown of the tubing material as indicated by a liquifying and 'running' of the inner wall.

The experimental set-up consisted of connecting the tube to inflow and outlfow resevoirs, the inflow resevoir being completely filled and closed so that resting pressure in the tube was determined by the water level in the outflow resevoir. This level was set to 100 cm H_2O, a pressure sufficient to ensure that the cross-section of the tube, which was slightly elliptical when unloaded, was circular. Transient pulse waves were driven through the model by rapidly infusing 1 ml H_2O into the inflow resevoir and the resultant pressure pulses were recorded at a reference site, the distal end of the tapered section using two Bio-tec BT-70 pressure transducers which were coupled to the tube lumen with 24 gauge hypodermic needles forced through the tube wall (experiments repeated for each test site). The test manometer was then moved distally in 20 cm

steps and the procedure was repeated for each test position. Data was stored on magnetic tape (Akai 280D-SS recorder) using the FM conversion system described in Section III and these pressure signals were later digitized at a rate of 200 samples/sec with an A-D converter (Digital Equipment Corp.). The resultant data were fed into a Lab 8/E computer (Digital Equipment Corp.) which computed the Fourier transforms of the transient pressure pulses by standard techniques. 'Aliasing' errors (see appendix) were avoided by electronically filtering out all signals above 100 Hz. The Fourier transform of a transient signal expresses the amplitude distribution of the frequencies which make up the signal (Tsien, 1959) and thus by comparing the transforms of pressures recorded at the reference and the various test sites the response of the system to a distribution of input frequencies can be determined. This Fourier transform approach and a sample application are discussed in the appendix.

The response of the model tube to oscillatory inputs was expressed as pressure amplification, A(f), vs. frequency and was calculated according to the equation

$$A(f) = \frac{P_r(f)/P_o(f)}{P_r(f)/P_i(f)} \qquad (1)$$

where $P_r(f)$ is the reference pressure at a frequency, f,

and $P_o(f)$ is amplitude of pressure at the origin of the tapered

section of tube and $P_t(f)$ is pressure amplitude at the test site. The advantages of this 'transient analysis' approach over that of applying sinusoidal inputs of varying frequencies are that required data acquistion is greatly reduced since one test run supplies information on a distribution of frequencies and, since transient pressures are applied to the system, reflections from the tube outflow resevoir are distinctly separated in time from the incident pressure wave and can thus be easily eliminated from data analysis. Normally such terminal reflections greatly complicate this type of analysis. In the present study the frequencies investigated were those which exhibited wave length to taper length ratios varying from 0.1 to 1 which correspond to those observed *in vivo* (McDonald, 1974) since for these frequencies the model was hydrodynamically similar to the physiological situation.

Results of the above experiments were compared with the theoretical predictions of Taylor's (1964, 1965) electrical transmission line analogue. According to this theory the equation describing pulse wave propagation in elastic tubes are (Noordergraaf,1971)

2 $$\frac{\partial Q}{\partial z} = -\frac{\Pi R^3}{2Eh}\frac{\partial P}{\partial t}$$

3 $$\frac{\partial P}{\partial z} = -\frac{\rho}{\Pi R^2(1+\eta F_{10})}\frac{\partial Q}{\partial t}$$

where P = pressure, Q = volume flow rate, R = internal radius of the tube, E = Young's modulus of the vessel wall (a measure of the elasticity of the wall material), h = wall thickness, ρ = fluid density, $\frac{\partial}{\partial Z}$ = differentiation with respect to Z, the distance along the tube axis, $\frac{\partial}{\partial t}$ = differentiation with respect to time and $1 + \eta F_{10}$ is, in general, a frequency dependent parameter but for tubes of the dimensions studies here is equal to 1 for all frequencies examined. In analogy with an electrical transmission line (pressure analogous to voltage, flow to current) equations (2) and (3) can be written as

$$\frac{\partial Q}{\partial z} = - C \frac{\partial P}{\partial t} \tag{4}$$

$$\frac{\partial P}{\partial z} = - L \frac{\partial Q}{\partial t} \tag{5}$$

where the capacitance, $C = \Pi R^3 / 2Eh$ is a measure of tube compliance and the inductance $L = \rho / \Pi R^2$ is a measure of fluid inertia. For sinusoidal inputs expressed in complex form ($P = P(z)e^{i\omega t}, Q = Q(z)e^{i\omega t}$) equations (4) and (5) become

$$\frac{\partial Q}{\partial z} = - i\omega C P \tag{6}$$

$$\frac{\partial P}{\partial z} = - i\omega L Q \tag{7}$$

where $\omega = 2 \Pi X$ frequency and $i = \sqrt{-1}$. When tube compliance is dependent on position, i.e. $C = C(z)$, equation (6) and (7) can

can be integrated numerically by a simple iterative procedure (Carson, 1921; Taylor, 1965) to predict pressure and flow amplitude at all sites along the tube provided pressure and flow at a single site are known. Briefly, for a tube which is elastically tapered between positions a and b it follows from (6) and (7) that

$$8 \qquad Q(z) = Q(a) - \int_a^z i\omega C(z')P(z')dz'$$

$$9 \qquad P(z) = P(a) - \int_a^z i\omega L Q(z')dz'$$

where Z is any position between a and b. If Q(a), P(a) are known then, as a first approximation, P(Z') is set equal to P(a), Q(Z') to Q(a) and (8) and (9) integrated to obtain a second approximation for P and Q. This second approximation is again substituted in equations (8) and (9) for P(Z') and Q(Z') and the integration repeated and thus successive approximations can be refined until accurate assessments of P(Z) and Q(Z) are obtained. In practice the procedure is halted when successive iterations produce no significant change in approximations of P(Z) and Q(Z). Since, in the present study, the elastically tapered tube was terminated in a long, uniform section of tubing for which $P = \sqrt{\frac{L}{C}} \cdot Q$ (Taylor, 1966) a single pressure recording at the junction between tapered and uniform sections (reference pressure) provided necessary boundary conditions, P(a) and Q(a).

Equations (8) and (9) were integrated for the case when C varied as in the present model on the LAB 8/E computer and a check for programming errors was performed by analyzing the wave propagation characterictics of electric transmission lines which have been previously investigated (Taylor, 1965).

The above theoretical computations take no account of the dissipative losses which may occur in the actual tube. Such losses dut to fluid viscosity should be small for tubes of the diameter of the model but losses due to viscoelastic properties of the wall are more difficult to predict. In order to correct theoretical predictions for such effects a number of tubes, softened uniformly to varying degrees, were placed in the experimental set-up and pressure was recorded at two sites (1 m apart) to assess damping effects as a function of wall stiffness.

Animal Experiments

Young rabbits weighing from 2.0 to 3.6 kg were anaesthetized, thoracotomized and artificially ventilated as described in Section V. Blood pressure was recorded in the aortic arch through a catheter attached to a Bio-tec BT-70 pressure transducer. The catheter was either inserted directly through the wall of the aorta or was introduced into a carotid artery and fed down to the junction of the innominate artery and the aorta. A 2 in incision was then made in the lower abdomen and the aortic trifurcation was exposed. A baloon cuff occluder was

secured around the aorta just proximal to the trifurcation and a catheter connected to a second BT-70 pressure transducer was inserted into the aorta just proximal to the vessel occluder. The net alteration of the pressure wave propagated along the aorta was assessed by comparing the Fourier components of the two pressure signals recorded at the output (trifurcation) and input (arch) of the vessel, i.e. a 'transfer function' of pressure wave propagation (output/input as a function of frequency) was determined. The effects of vasoconstriction on the transfer function were assessed by rapid intra-venous injection of epinephrine (5ml, 4μg) whereas acetylcholine (ACh) infusion (.5ml, 50μg) was used to examine the effects of vasodilation. Inflation of the balloon cuff occluder at the trifurcation was employed to introduce a discrete reflecting site into the system. McDonald's (1974) investigations indicate that the effects of distributed reflections are best approximated by a single reflecting site if that site is located in the pelvic region and therefore it was hoped that occlusion of the trifurcation would, in some sense, simulate increases in reflections of a physiological origin.

Pressure recordings were stored on an Akai 280D SS tape recorder interfaced with a two channel FM adaptor (Vetter Instruments) and the two pressures were later digitized simultaneously by an A-D converter (Digital equipment). A Fourier

analysis of the digitized signals was performed by a LAB 8/E computer utilizing a convential Fourier analysis program and the results were printed out as a transfer function. The same rigorous controls of manometer system frequency response characteristics described in Section III were exercised in this study.

Results

Model Studies

Fig. 4-2 illustrates the variation in elastic modulus of the model artery as determined at the end of experiments. The linear dependence on position predicted by preliminary studies was not strictly observed although wall stiffness did vary in a smooth, steadily increasing fashion. The elastic modulus more than doubled along the tapered region, a variation corresponding to an increase of 50% in pulse wave velocity. Although well below the 3 to 5 fold increase in pulse wave velocity reported in mammals (McDonald, 1968) it is sufficiently large to produce significant amplification of the pressure pulse according to transmission line theory . In Fig. 4-3 experimentally observed pressure wave amplification along the tapered section of the model for frequencies of 1-10 Hz are compared with theoretically predicted results. Transmission line theory (no allowance for damping) predicted that low frequency pressure waves would steadily increase in amplitude during propagation along the tube whereas higher frequency waves would exhibit oscillations in amplitude superimposed on a general amplification. Similar findings characterised earlier theoretical investigations of asigmoidal variation in wall stiffness, although oscillations at higher frequencies were not so pronounced (Taylor, 1965), and it would appear that these general features of pressure

Figure 4-2. Elastic modulus of the model 'artery' as a function of distance from the tube inflow.

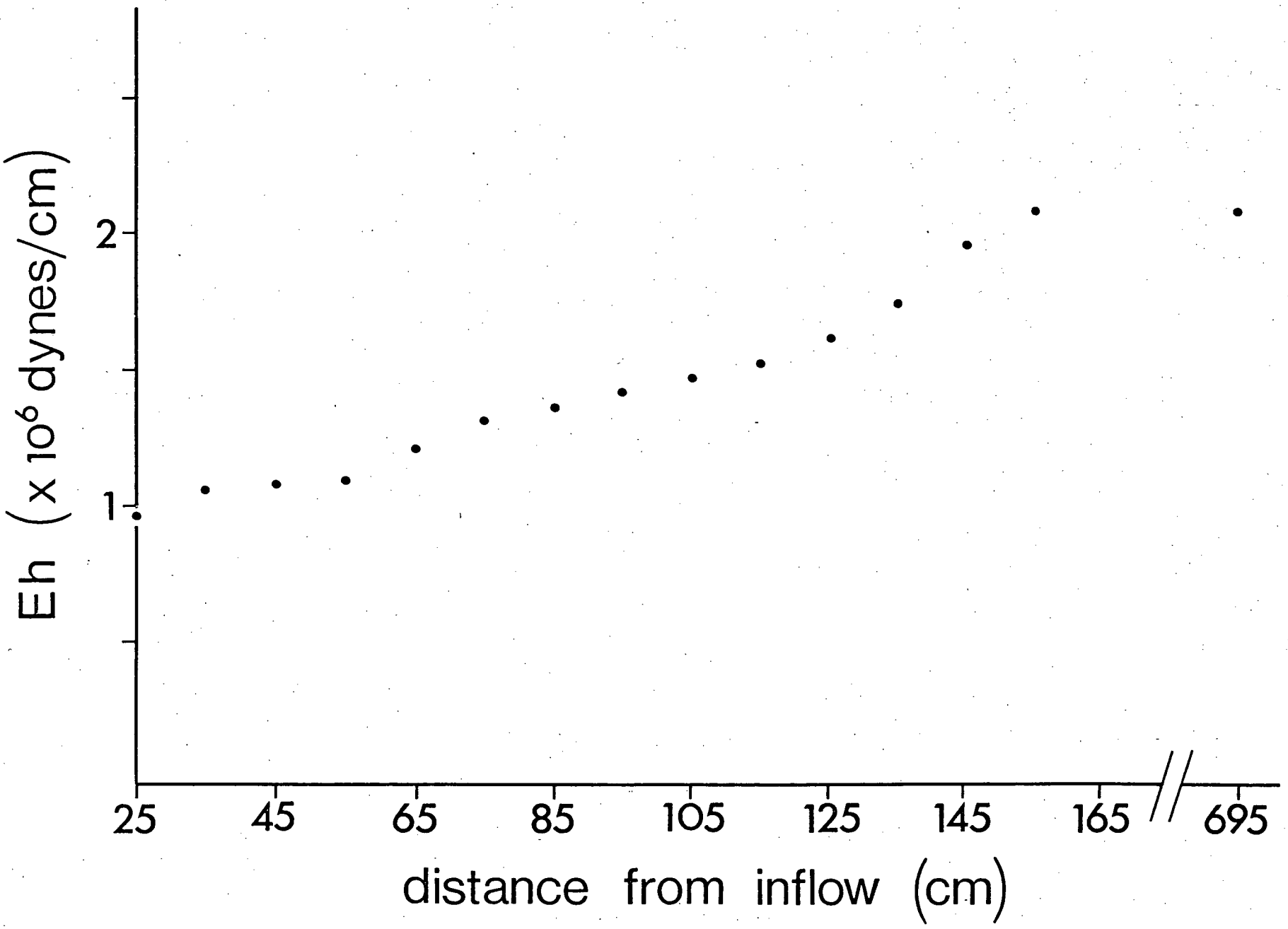
Eh (x 10⁶ dynes/cm)
2
1
25
45
65
85
105
125
145
165
695
distance from inflow (cm)

Figure 4-3. Theoretically predicted and experimentally observed pressure wave amplification for frequencies of (A) 1 and 2 Hz (B) 3 and 4 Hz (C) 6 Hz (D) 8 Hz (E) 10 Hz. Solid curves are theoretical predictions with no allowance for damping whereas dashed curves (6,8,10 Hz) include a damping correction.

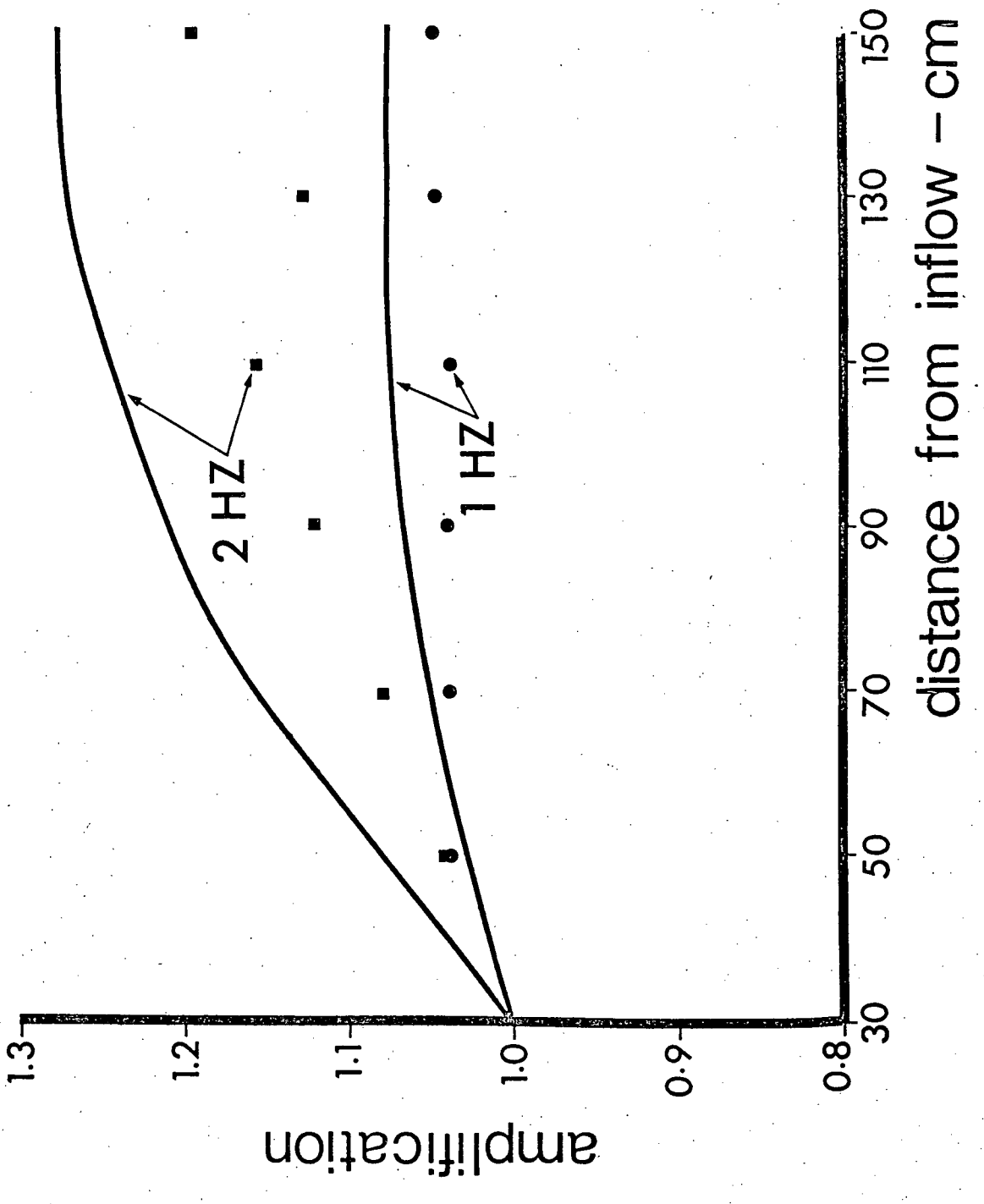
A
amplification
1.3
1.2
1.1
1.0
0.9
0.8
30
50
70
90
110
130
150
distance from inflow – cm
2 HZ
1 HZ

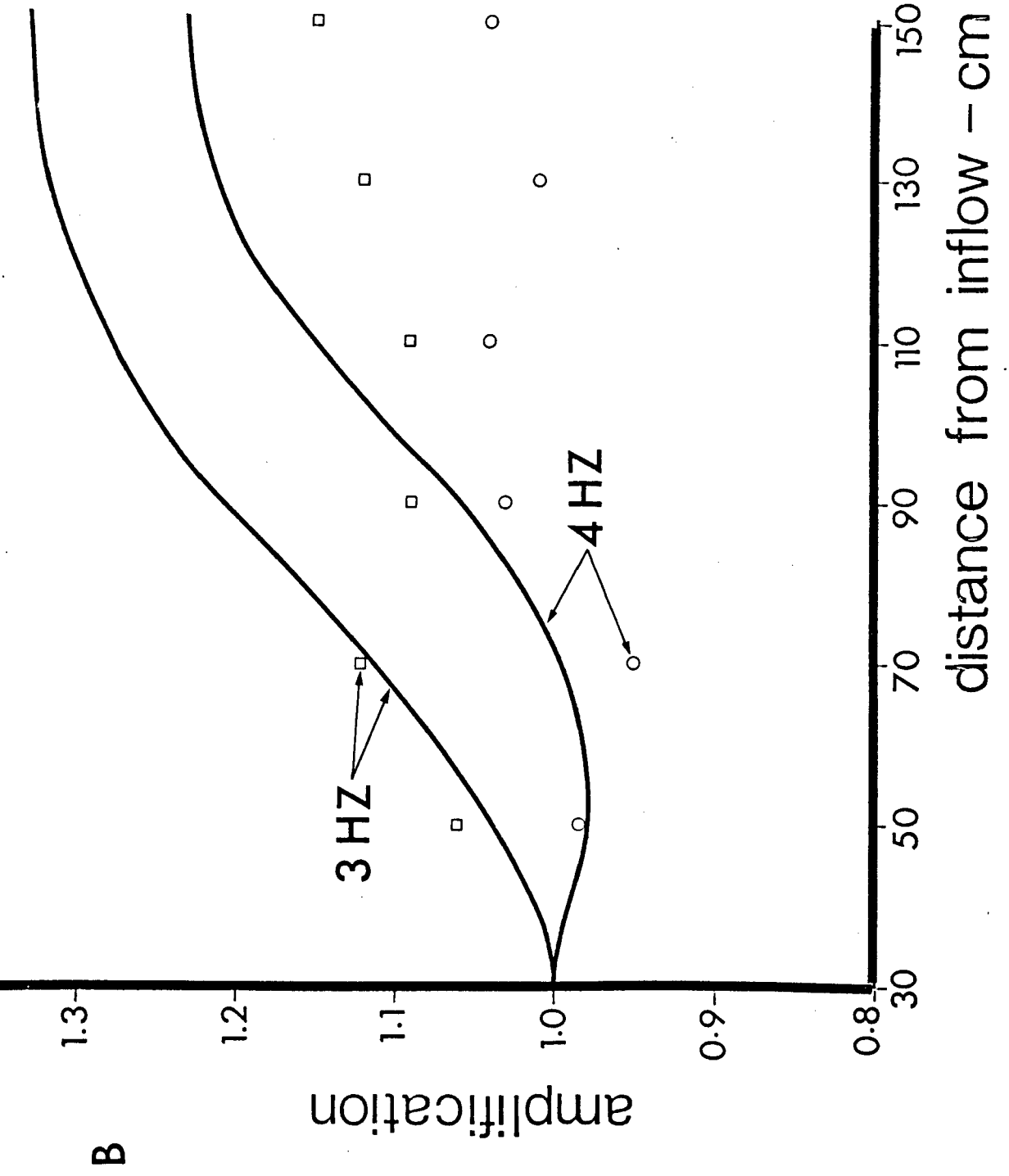
B
amplification
1.3
1.2
1.1
1.0
0.9
0.8
30
50
70
90
110
130
150
distance from inflow – cm
3 HZ
4 HZ

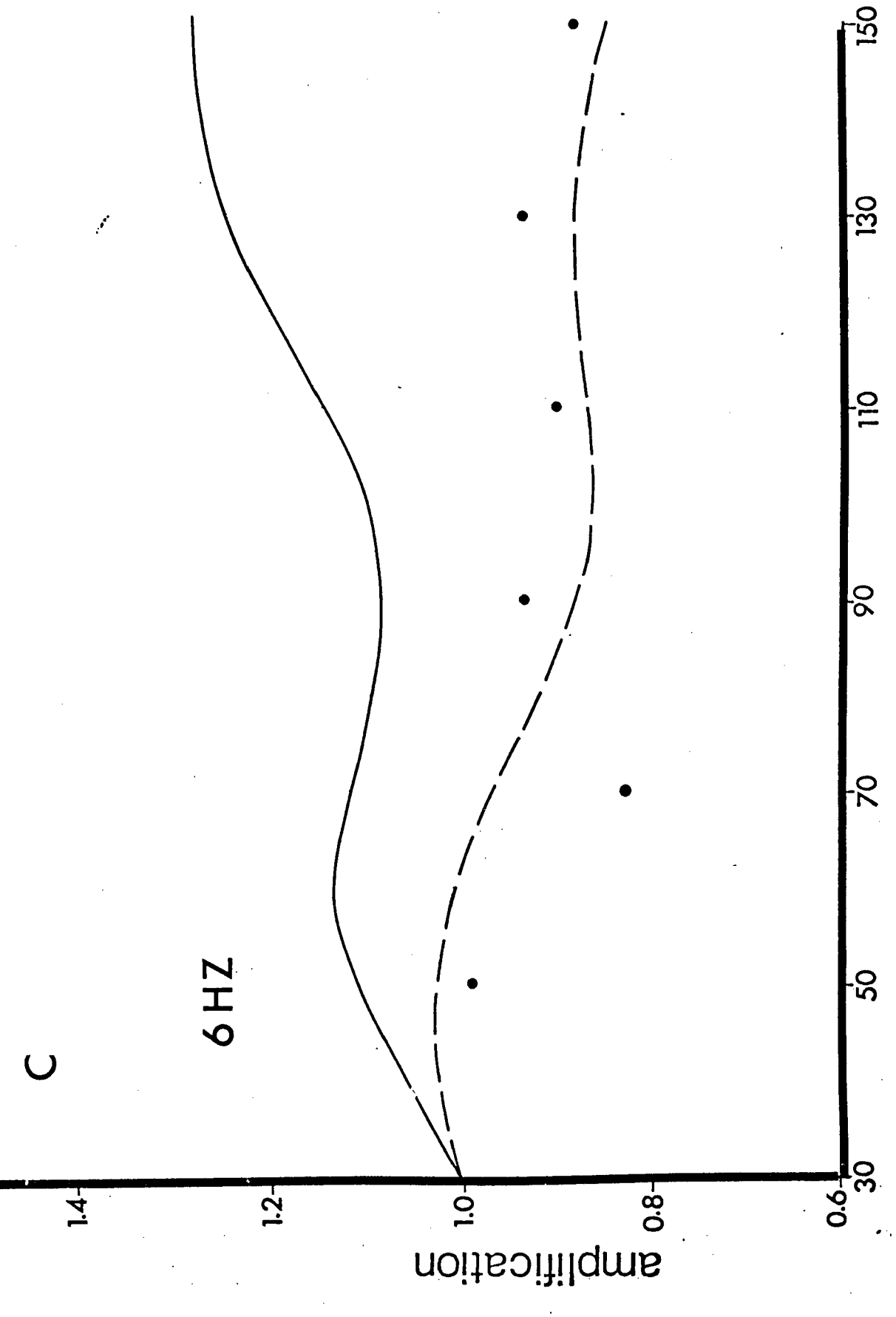
C
6 HZ
amplification
1.4
1.2
1.0
0.8
0.6
30
50
70
90
110
130
150
distance from inflow – cm

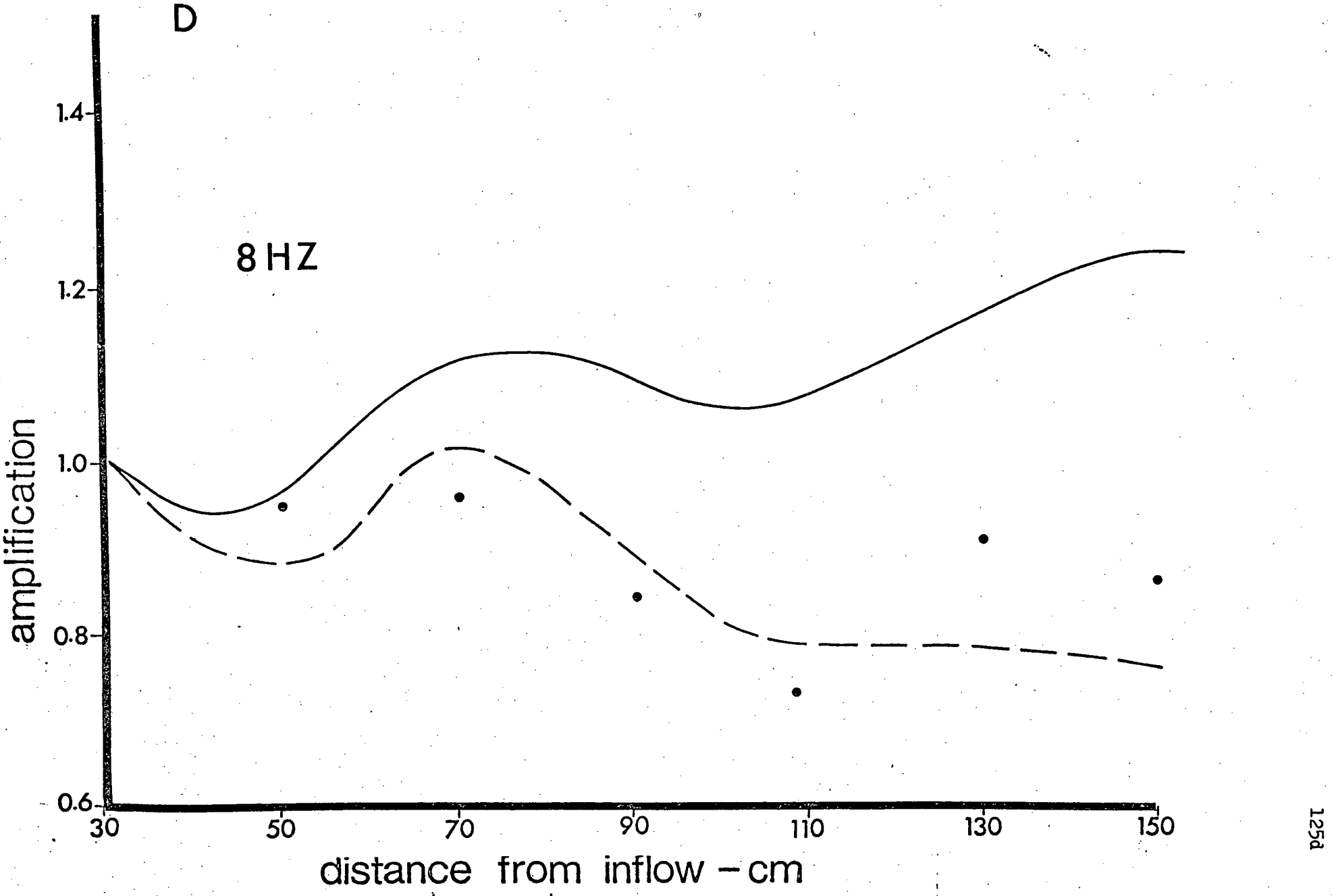
D
8 HZ
1.4
1.2
1.0
0.8
0.6
amplification
30
50
70
90
110
130
150
distance from inflow – cm

E

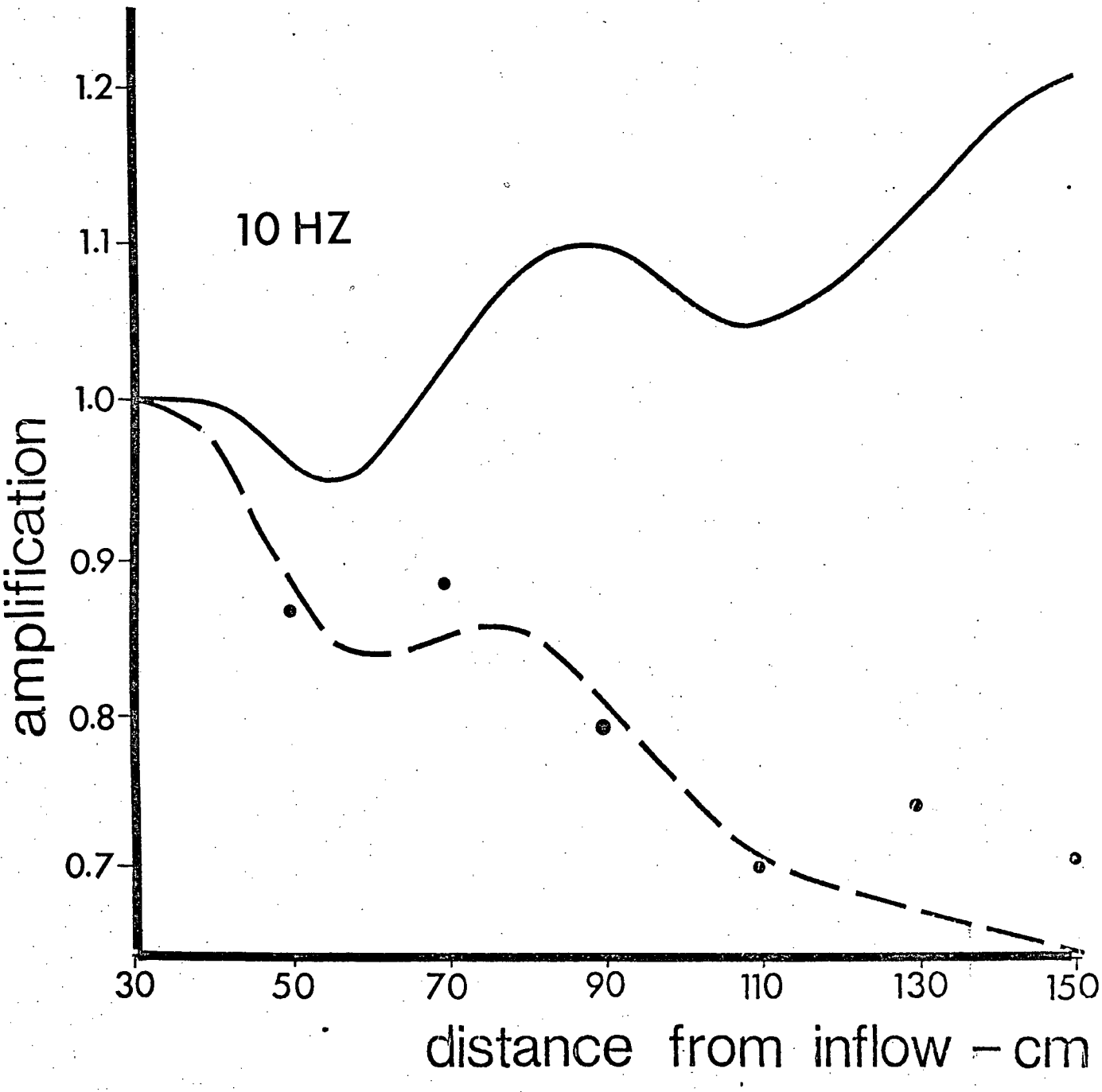
10 HZ
amplification
1.2
1.1
1.0
0.9
0.8
0.7
30
50
70
90
110
130
150
distance from inflow – cm

wave propagation would be predicted for any smoothly increasing elastic taper. Pressure wave amplification was experimentally observed at lower frequencies but to a lesser extent than predicted and this deviation between theory and observation increased with increasing frequency with attenuation being observed at all frequencies above 4 Hz. These results are suggestive of dissipative effects and indeed when correction was made for such losses the large deviations at higher frequencies were accounted for. Fig. 4-4 illustrates the transfer function (total amplification vs. frequency) for pressure wave propagation along the tube model. In a lossless tube transfer function rises with frequency then oscillates around an equilibrium value at higher frequencies whereas experimental results clearly exhibit the distortion of the predicted pattern which results from a selective damping of higher frequencies.

Pressure wave propagation in the aorta

Mean arterial blood pressure in the rabbits used in these experiments (83.5 $\pm$ 1.8 mm Hg) was below typical values for other mammals. These low pressures were apparently not related to experimental protocol since similar blood pressures were recorded when pressure manometers were implanted in the femoral artery under local anaesthesia. In previous studies blood pressures recorded in adult rabbits (Dawes et al., 1957;

Figure 4-4. Transfer function (total pressure wave amplification along tube) vs. frequency as observed and as predicted (no damping correction)

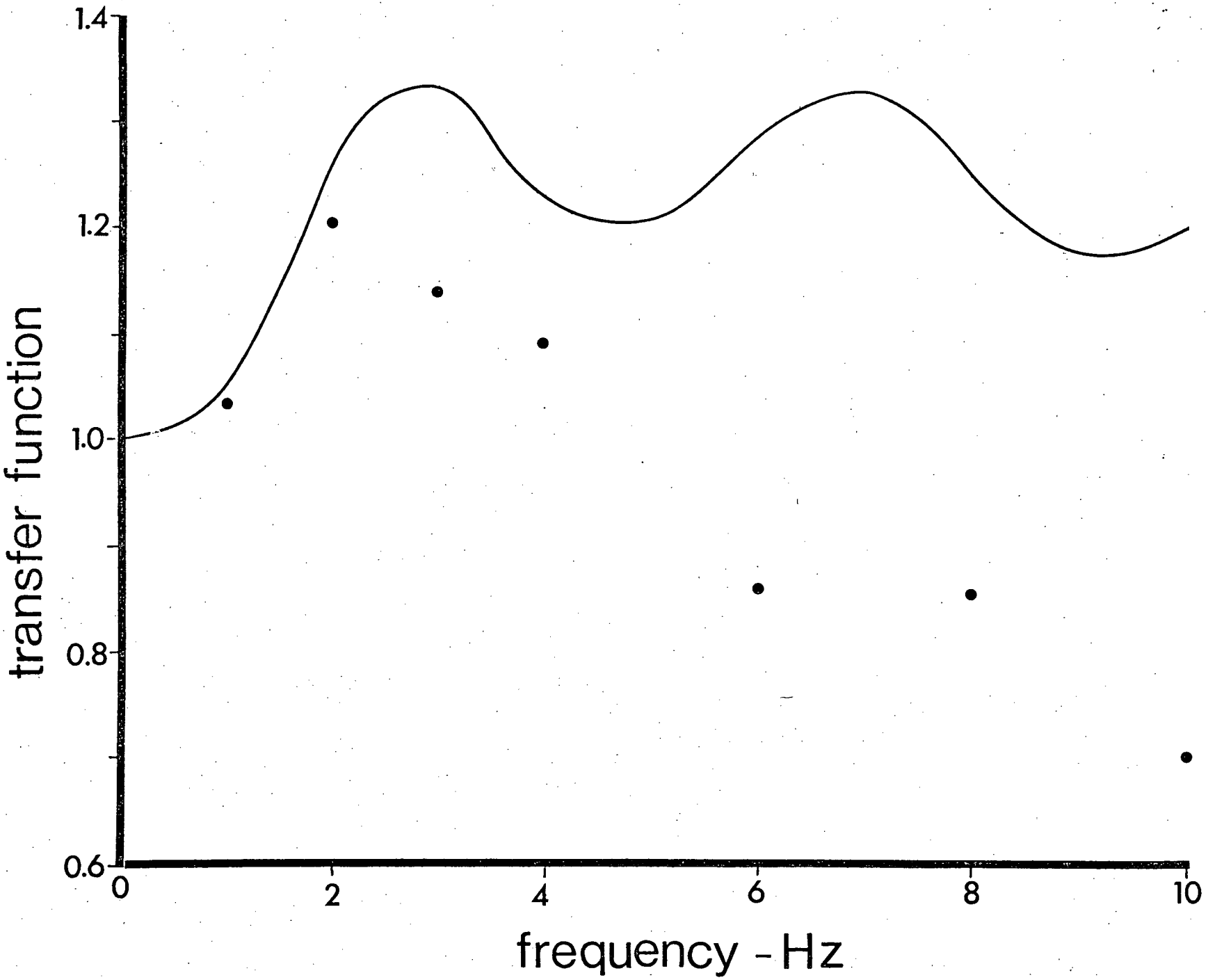
1.4
1.2
1.0
0.8
0.6
transfer function
0
2
4
6
8
10
frequency - Hz

McCloskey and Cleary, 1974) were similar to those found in the dog (Patel et al., 1963) however young rabbits such as those used in present experiments (3-6 mo.) yield lower values (Bauer, 1938; Dawes et al., 1957; McCloskey and Cleary, 1974). Despite these differences in mean blood pressure the shapes of central and peripheral profiles are virtually identical to those found in dogs (McDonald, 1974) and humans (O'Rourke, 1968). Central pulse pressures are characterized by a dome-shaped systolic wave terminated by an incisura as the aortic valves close and diastolic pressures are convex and exhibit a second maximum (Fig. 4-5). In peripheral arteries the pulse pressure is much larger than that recorded near the heart and the systolic wave is much more peaked in form. An incisura is no longer observed and diastolic pressures exhibit a secondary oscillation, the dichrotic wave. Introducing a discrete peripheral reflecting site by occluding the distal abdominal aorta tended to accentuate the difference between central and peripheral pressure waves. The difference in pulse pressure at the two sites increased significantly, largely as a result of increased pulse pressure at the periphery although central pulse pressure fell slightly, and the diastolic hump of central pressures and the dichrotic wave recorded at the periphery became more pronounced. The effects of adrenalin induced vasoconstriction were very similar to those of the

Figure 4-5. Top row. Pressures recorded in the aortic arch (earlier rising profile) and in the distal abdominal aorta in the control situation (normal), during occlusion of the trifurcation and following adrenalin infusion.

Bottom row. Pressures recorded in the same sites in the control situation, during ACh infusion and while the aortic trifurcation is occluded during the response to ACh infusion.

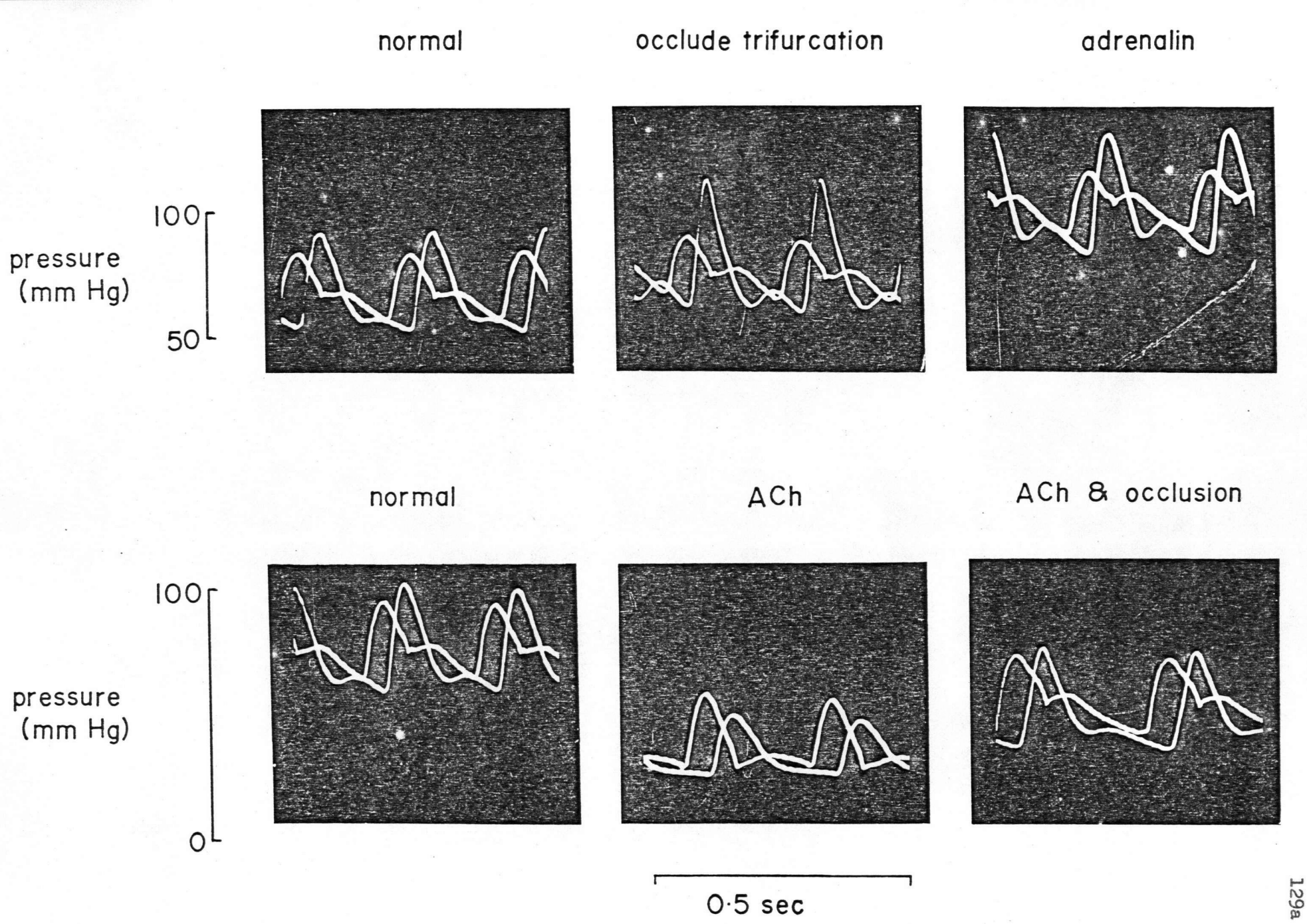
normal
occlude trifurcation
adrenalin
100
pressure
(mm Hg)
50
normal
ACh
ACh & occlusion
100
pressure
(mm Hg)
0
0·5 sec

occlusion experiments although some differences can be observed. The systolic wave of the central pulse took on a more complex shape exhibiting an earlier maximum, diastolic waves at both sites occurred earlier and the transit time of the pulse between the recording sites decreased.

Vasodilation induced by ACh infusion had a marked effect on both central and peripheral pressure waves. The central pulse exhibited a more peaked systolic wave and a reduced diastolic hump. The peripheral pressure displayed a dramatic decrease in amplitude to below that of the central pressure, the dichrotic wave was lost and the peripheral pressure pulse appeared very much like a damped version of the central pulse. Occlusion of the trifurcation during this response caused an immediate return to profiles resembling those of the control situation.

A more quantitative assessment of aortic pressure wave propagation is achieved by comparing the harmonic content of the two pressures. Fig 4-6 illustrates the ratio of peripheral pressure to central pressure (the transfer function) for the first 5 harmonics of the pressure wave in the control situation, during vasoconstriction and during occlusion of the distal end of the aorta. The rabbits showed little scatter in heart rate (mean control H.R. = 4.39 $\pm$ .19 Hz) and consequently data was grouped at the mean heart rates to allow averaging of data.

Figure 4-6. Alterations in transfer function for pressure wave propagation along the rabbit aorta caused by adrenalin induced vasoconstriction (squares), ACh induced vasodilation (open circles) and occlusion of the aortic trifurcation (closed circles). Data from the first 5 harmonics of pressure waves has been averaged and presented at the mean heart rates for each case except ACh infusion for which H.R. exhibited too large a standard error. In this case only a representative sample is displayed although all animals (4) subjected to this procedure exhibited similar transfer function curve.

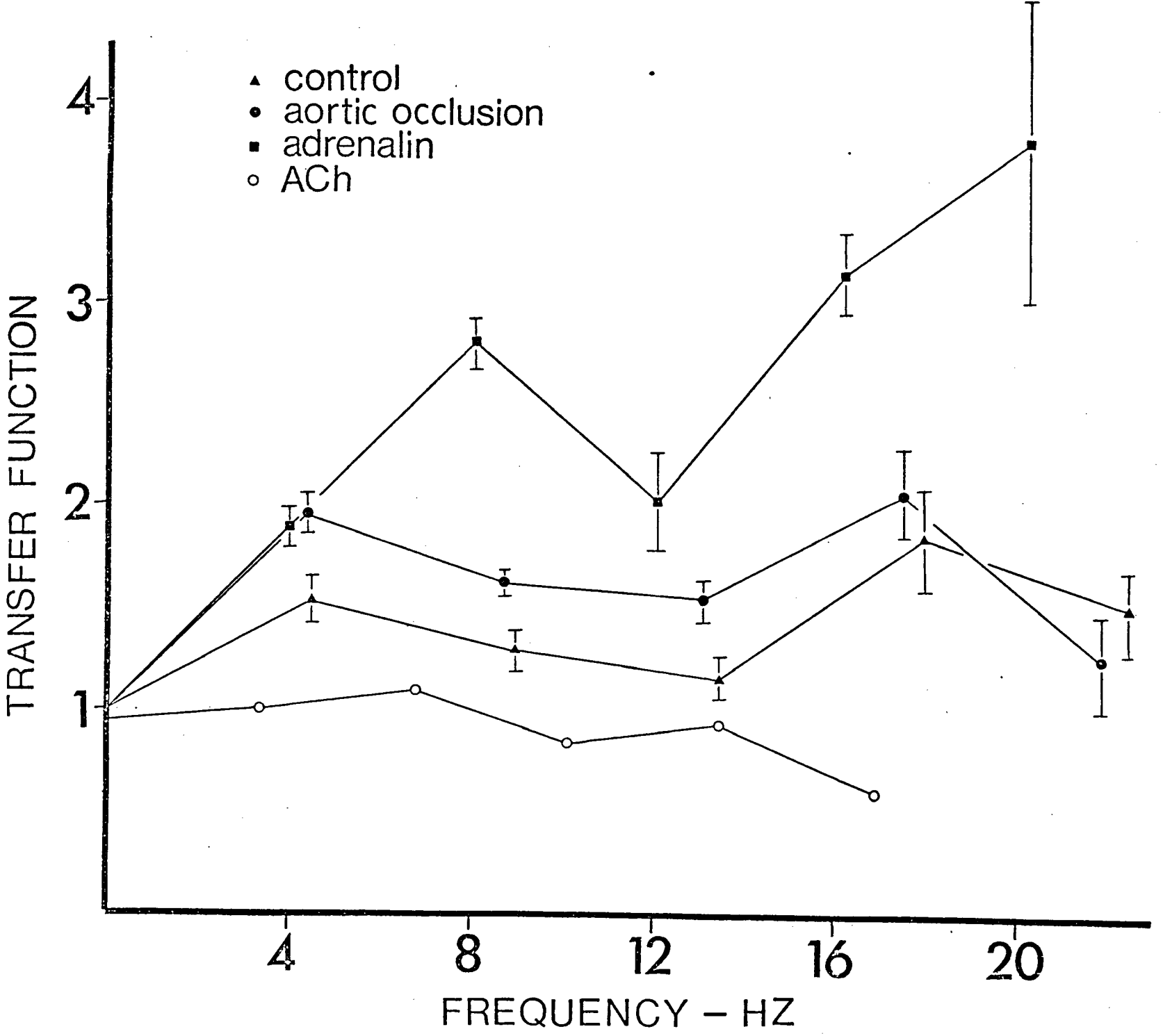
control
aortic occlusion
adrenalin
ACh
TRANSFER FUNCTION
1
2
3
4
4
8
12
16
20
FREQUENCY – HZ

Under control conditions the pressure wave was amplified during propagation along the aorta (transfer Function > 1) at all frequencies although marked oscillations in transfer function were observed (the pattern of maximum, minimum, maximum in transfer function was seen in all rabbits). Occlusion of the aortic trifurcation caused in increase in wave amplification at all but the highest frequencies and the pattern of oscillation in transfer function was maintained. Adrenalin infusion caused an increase in transfer function at most frequencies and the pattern of oscillation in transfer function was spread out over wider ranges in frequency. Spreading out of these oscillations can be interpreted as resulting from the increase in pulse wave velocity which accompanied the increase in blood pressure during vaso-constriction.

Discussion

Investigations of the hydraulic model of an artery exhibiting elastic taper support theoretical predictions of the effects of taper when appropriate corrections are made for dissipative losses. The effects of elastic taper on pressure wave propagation have been discussed previously (Taylor, 1964; 1965) however some further remarks are in order. The oscillations in transfer function and in pressure amplification with position along the tube are difficult to interpret intuitively when one considers the very steady increase in wall stiffness of the model. Similar oscillations are generated in uniform tubes with reflecting sites although in this case such patterns are easily described in terms of the varying phase relations between outgoing and reflected waves as position and frequency varies, a maximum in amplification occurring at sites where the two waves are in phase and a minimum where they are 180 out of phase. Taylor (1965a,b) has also found that impedance curves for a system of randomly distributed reflecting sites (Taylor 1965(b)) are remarkably similar to those of tapered vessels (Taylor 1965 (a)). It is difficult to accept that these similarities between elastically tapered and reflecting systems are purely co-incidental and since it is well known that an abrupt change in vessel compliance acts as a site of reflections (Womersley, 1958) it is tempting to

interpret the effects of elastic taper as resulting from a summation of infinitessimal reflections from each increment in wall stiffness. Indeed such an interpretation stands up to rigorous inspection. Given a tube of length, a, with a continuously varying compliance, C(Z), where Z is distance along the tube then, for sinusoidal inputs, flow rates and pressure within the tube are given by equations (8) and (9). i.e.

10 $$Q(z) = Q(o) - \int_o^z i\omega C(z') P(z') dz'$$

11 $$P(z) = P(o) - \int_o^z i\omega L Q(z') dz'$$

If a second tube of the same length contains a number, n, of equally spaced abrupt changes in compliance such that the compliance of the jth segment is given by $Cj = C(ja/n)$ then the effects of reflections from these sites on pressure and flow waves propagated over a number, k, of these vessel segments are determined by integrating equations (5) and (6), i.e.

12 $$Q(z=ka/n) = Q(o) - \left[\int_o^{\frac{a}{n}} i\omega C_1 P(z') dz' + \int_{\frac{a}{n}}^{\frac{2a}{n}} i\omega C_2 P(z') dz' + \cdots + \int_{\frac{(k-1)a}{n}}^{\frac{ka}{n}} i\omega C_k P(z') dz'\right]$$

13 $$P(z=ka/n) = P(o) - \int_o^{\frac{ka}{n}} i\omega L Q(z') dz'$$

Equation (12) can be rewritten

$$14 \qquad Q(z) = Q(o) - \sum_{j=1}^{k} \int_{\frac{(j-1)a}{n}}^{\frac{ja}{n}} i\omega C_j P(z')\,dz'$$

However, if the number of segments into which the tube is divided increases indefinitely ($n \to \infty$) and the size of each increment in compliance correspondingly drops so that total change in compliance along the tube is unchanged then

$$\int_{\frac{(j-1)a}{n}}^{\frac{ja}{n}} i\omega C_j P(z')dz' = i\omega C_j P(ja/n)\cdot a/n$$

and equation (14) becomes

$$Q(z) = Q(o) - \lim_{n \to \infty} \sum_{j=1}^{k} i\omega C_j P(ja/n)\cdot a/n$$

However by definition of the integral

$$\lim_{n \to \infty} \sum_{j=1}^{n} i\omega C_j P(ja/n)\cdot a/n = \int_{o}^{\frac{ka}{n}} i\omega C(z')dz'$$

so that the summed effect of these infinite number of small reflections on pressures and flows within the system are described by

$$Q(z) = Q(o) - \int_{o}^{z} i\omega C(z')P(z')dz'$$

$$P(z) = P(o) - \int_{o}^{z} i\omega L Q(z')dz'$$

which are identical with equations (10) and (11) describing pressures and flows in an elastically tapered tube. Since

C(Z) was an arbitrary continuous function it follows that any continuous elastic taper of arteries can be treated simply as an additional source of reflections within the major vessels of the arterial tree.

The present in vivo experiments demonstrate that the nature of pressure wave propagation in the aorta is highly sensitive to wave reflections from both externally applied (cuff occluder experiments) and naturally occurring reflecting sites. Results of these experiments support earlier contentions that the major source of reflections in the mammalian arterial system are located in the arteriolar beds since reflection phenomena, which were greatly augmented by drug-induced vasoconstriction, almost disappeared during vasodilation. Certainly some of these changes in wave propagation characteristics may be due to non-vasomotor effects of adrenalin and ACh however, since the effects of introducing a discrete peripheral reflecting site by occluding the aortic trifurcation were capable of both closely mimicking those of vasoconstriction or eliminating those of vasodilation, it must be concluded that reflection phenomena are predominant. It is conceivable that alterations in pulse wave velocity, as blood pressure changes, occur preferentially in certain regions of the arterial tree so that variations in elastic taper could contribute to the drug induced alterations of reflection phenomena. However Learoyd

and Taylor (1966) have found that taper is reduced rather than increased when blood pressure rises so that resultant reflections from this source should be reduced during adrenalin infusion and augmented during ACh infusion.

Since peripheral vasodilation almost totally elimates the effects of reflections on pressure wave propagation it must be concluded that reflections from sites within the major arteries, both from discrete discontinuities and from elastic taper of major vessels, make a minor contribution to the total reflected wave. This finding seems at odds with the marked elastic taper found in the aorta of mammals including both young and adult rabbits (Saxton, 1942; Cleary and McCloskey, 1962; Cleary, 1963; McCloskey and Cleary, 1974), which exhibit aortic wall properties similar to those of the dog (Harkness et al., 1957) and the human (Cleary, 1961). However quantitation of elastic taper is generally performed by measuring pulse wave velocity which, in mammals, increases some 4-5 times (McDonald, 1968) and there is some indication that this approach may considerably overestimate real changes in wall stiffness. Pulse wave velocity is measure either by recording the time delay between the rising fronts of the pressure wave at two sites a known distance apart (McDonald, 1968) or by measuring a similar time difference between peak rates of change of pressure (present study) and both of these approaches measure

the velocity of the higher harmonics of the pressure wave. However Learoyd and Taylor (1965) have directly measured the frequency dependence of aortic elasticity and found that while wall stiffness increases some 5-7 times at high physiological frequencies (4-10 Hz) increases less than 3-fold are found at lower frequencies (less than 2 Hz). Thus at these lower frequencies, which make the largest contribution to the pressure wave (McDonald, 1974), elastic taper approaches the range observed in the present model studies. Since pressure wave amplification was limited to at most 30% in these studies, even if viscous damping does not occur, earlier conclusions on the major effects of elastic taper on pressure wave propagation seem questionable, particularly when the counter-effects of large dissipative attenuation in arteries (McDonald and Gessner, 1968; Bergel, 1961) are considered.

It may be that elastic taper is an adaptation to reflection effects rather than a major source of reflections. Were distal arteries as compliant as proximal vessels then the large pressure swings that reflections produce in these arteries would cause equally large strains in the arterial wall. It is now a popular theory that dynamic stresses on arterial walls are damaging and ultimately result in arterial degenerative disease (for a review see Gessner, 1973) and consequently it is tempting to view the greater stiffness of peripheral vessels

as a protection against such damage. However much more information on the effects of mechanical stress on arteries is needed before such conjecture can be examined closely.

SECTION V

Mechanical Interaction Between the Ventricles of the Mammalian Heart

Introduction

In amphibia the systemic and gas exchanger circulations are supplied by the same ventricle and consequently the nature of ejection to either bed is affected by the hydraulic load presented to the heart by the opposite circulation. On the other hand in aves and mammals the intraventricular septum is complete and the two sides of the heart are, in reality, two separate pumps. However the degree to which two ventricles function independently is controversial. The volume outflow of both ventricles must, in the long term, be equal if volume loading of one circuit is to be avoided; this balanced output being a result of the Starling mechanism (Starling, 1915) whereby the strength of contraction of either ventricle increases or decreases with the venous return from the opposite circulation, or more exactly, with the diastolic distension of the ventricle produced by this return.

It seems likely that some direct mechanical interaction should also occur between the two ventricles as a result of their structural coupling since the free wall of the right ventricle is continuous with the left ventricular epicardium

and a single wall, the intraventricular septum, divides the cavities. Indeed a number of recent studies (Taylor et al., 1967; Laks et al., 1967; Bemis et al, 1974) have established that the diastolic filling pressure of either ventricle can inhibit the filling rate and alter the geometry of the opposite ventricle and that this interaction is augmented by constraints resulting from the presence of the pericardium (Elzinga et al., 1974). However, the physiological importance of interactions between the ventricles during systole is controversial. On the one hand it has been argued from experiments involving destruction of the right ventricular free wall (Starr et al., 1943; Bakos, 1950; Kagen, 1953) or by observing changes in right ventricular pressure (RVP) promoted by instantaneous changes in left ventricular pressure (LVP) (Oboler et al.; 1973), that right ventricular pumping is aided by left ventricular contraction. On the other hand increases in preload to one ventricle augment the performance of that ventricle and inhibit the performance of the opposite ventricle when steady state is achieved (Elzinga et al., 1974) and Moulopoulos et al. (1965) report that left ventricular function was impaired by by-pass or distension of the right ventricle. Consequently in order to extend present views on mechanical interaction between the mammalian ventricles, instantaneous alterations in function of either ventricle

concurrent with induced changes in function of the opposite ventricle have been examined.

Methods

Preparations

The experiments were performed on 32 young (3-9 months) New Zealand White rabbits weighing from 1.9 to 4.3 kg. All animals were anaesthetised with sodium pentobarbital (30 mg/kg, i.v.), restrained on their backs, and the heart was exposed by a median sternotomy. Following sternotomy the animals were artificially respirated with a Harvard 670 positive pressure respirator. In three animals experiments were performed following β blockade with propranolol (Inderal, I.C.I. Ltd., U.K.) and mid-cervical vagotomy in order to assess the role of cardiac reflexes in ventricular interaction. Abolition of the inotropic and chronotropic responses to rapid i.v. infusion of 2 µg isoprenaline was taken to indicate complete β blockade (peak left ventricular dP/dt was used as a measure of inotropic state). In all other animals the nerve supply to the heart was intact.

Recording methods

Blood pressures in the two ventricles were recorded by direct ventricular puncture using Bio-Tec BT-70 pressure transducers equipped with short, wide-bore vinyl cannulae tipped with 2 cm trocars cut from 18 G hypodermic needles. To optimize the dynamic performance of the manometers they were filled with heparinized de-aerated Tyrode solution (50 I.U./ml)

after first flushing the manometers and their connections with CO_2 gas. The manometers were connected via stopcocks to two oil-covered reservoirs of Tyrode solution which allowed for static calibration. Dynamic calibration was performed before and after each recording session by applying a step change in pressure to the tip of the manometer cannula (Hansen'pop-test') and recording the free vibrations of the manometer and associated recording system. The manometers consistently yielded frequency responses of 125 Hz or better with relative damping of less than 0.1.

The output from the transducers was converted to a frequency modulated signal by an F.M. adaptor (A.R. Vetter, Co., Pa., U.S.A.) and stored on magnetic tape (Akai 280 DSS). The unmodulated signal was simultaneously displayed on a Hewlett Packard 1201 A storage oscilloscope. The FM adaptor demodulated the taped signal when the recorder was in the playback mode. The first derivative of ventricular pressure, dP/dt, was recorded using Biotronix BL 620 or BL 622 analogue computers set to a corner frequency of 160 Hz. For presentation purposes the taped data was played onto a Techni-rite Tr 888 chart recorder writing on rectilinear co-ordinates.

Experimental Procedures

Abrupt increase in the afterload presented to either ventricle was accomplished by diastolic occlusion of the aortic

or pulmonary outflow either with a balloon cuff or snare occluder. To alter left ventricular preload a 15 G hypodermic needle connected to an infusion pump (Cole Parmer, Chicago, U.S.A) was inserted into the left ventricle. Switching the pump on resulted in an infusion of warmed saline (36-39°C) into the ventricle which produced an immediate sharp increase in left ventricular pressure. Right ventricular preload was altered by inflating a balloon implanted in the right atrium since in preliminary trials I found the infusion pump to be incapable of raising RVP rapidly enough, an effect attributed to the greater compliance of the right ventricle. In some experiments a perturbation of LVP during diastole or systole was produced by connecting a cannula from a 60 Hz pump to the left ventricle. High frequency oscillatory flow (60 Hz, 0.05-0.1 ml/stroke) was applied to the ventricle when the pump was switched on.

The hearts of ten rabbits, killed by overdose of sodium pentobarbital (50-90 mg/kg), were excised in a state of rigor and transferred to a bath of warm (37-39°C) Tyrode solution. The pulmonary outflow as ligated and a balloon was inflated in the aorta at the valves and tied in place. The latter served to occlude both the aorta and coronary arteries. Pressure and infusion cannulae were implanted in both ventricles via the atria. The infusion cannulae were connected via stopcocks

to syringes so that pressure alterations in either ventricle could be produced by saline infusion. All tests were made 1-2 hours after excision of the heart, a period during which mammalian cardiac muscle exhibits constant maximal rigor when held at physiological temperatures (Kolder et al, 1963). It has been reported that rigor mortis reduces left ventricular compliance by some 5-10 times (Laks et al., 1967; Kolder et al, 1963) which appears to be of the order of the change in compliance between diastole and systole in normal hearts (Templeton et al., 1970). This was confirmed in the present experiments by applying oscillations from the 60 Hz pump to the left ventricle in rigor and comparing the induced pressure oscillation with the systolic oscillation produced by the pump in the same heart in vivo. For this test the ventricle was inflated to a pressure of 75 mm Hg, the mean peak systolic level recorded in vivo.

Results

Changes induced in RVP generation by alternations in left ventricular function

At the mean peak systolic LVP and RVP (74.3 ± 2.7 mm Hg and 27.1 ± 0.8 mm Hg respectively) pertaining in these experiments suddenly and drastically increasing the afterload presented to left ventricular contraction by occluding aortic outflow caused an increase in peak LVP or 54.9 ± 4.7% (mean increase ± S.E.M.) and co-incident with this change in LVP was an instantaneous increase in peak RVP, which occasionally reached values some 30% above those pertaining before aortic occlusion (Fig. 5-1). However the average increase in peak RVP was 11.4 ± 1.8% (mean ± S.E.M.). No preparation demonstrated a fall in ventricular pressure following occlusion of the opposite outflow tract although a small number of occlusions gave no change in pressure. Peak left ventricular dP/dt was not increased in the first contraction following aortic occlusion whereas right ventricular dP/dt increased by approximately the same fraction as peak RVP (Fig. 5-1).

The dotted profiles in Fig. 5-1 illustrate the increments in ventricular pressures resulting from aortic occlusions (the difference between the last pressure pulse before occlusion and the first pulse after occlusion). The pressure difference

Figure 5-1. Response of left and right ventricular pressures and rates of change of pressures to aortic occlusion (arrow marks the time of occlusion). The dotted profiles illustrate the change in systolic pressures following occlusion (see text). Traces (from top to bottom) - first: time markers separated by .5 sec. Second: left ventricular pressure (LVP). Third: rate of change of left ventricular pressure (LV dP/dt). Fourth: right ventricular pressure RVP). Fifth: rate of change of right ventricular pressure (RV dP/dt).

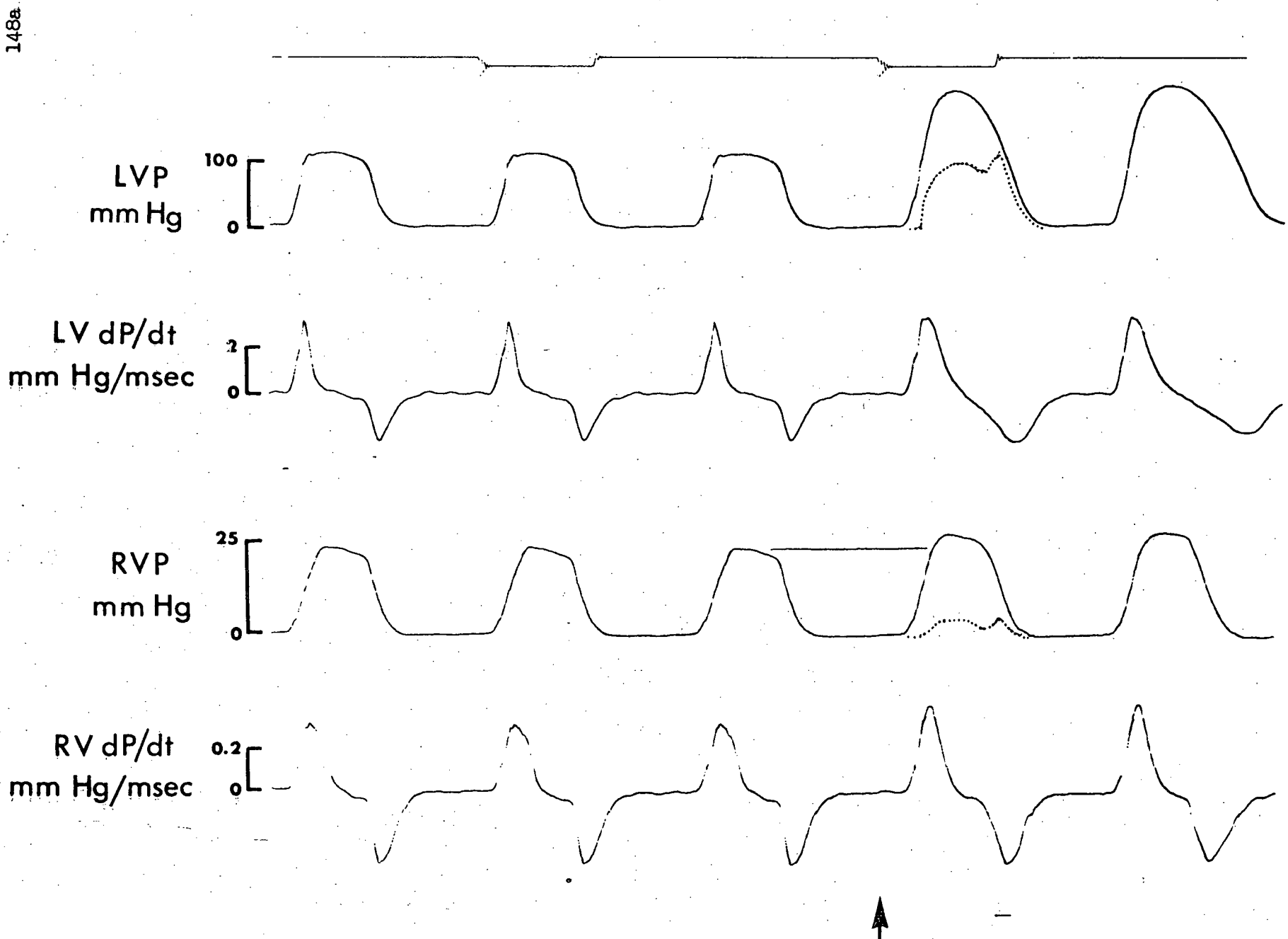
LVP
mm Hg
100
0
LV dP/dt
mm Hg/msec
2
0
RVP
mm Hg
25
0
RV dP/dt
mm Hg/msec
0.2
0

for the two ventricles are similar in shape and both exhibit a mid-systolic drop, resulting from a narrower pressure peak following occlusion, followed by a second brief rise reflecting an extended duration of systole. Instantaneous changes in LVP and RVP caused by aortic occlusion were identical in intact and denervated preparations. Although changing left ventricular afterload affected generation of RVP this was not the case when left ventricular preload was altered. Rapid infusion of saline into the left ventricle produced an immediate, marked increase in peak LVP of 35% after one systole and 75% at the third heart beat while RVP was unchanged until the effects of volume loading the circulation altered right ventricular preload.

Mechanical transference of pressure oscillations from the left to right ventricles was observed during oscillatory infusion of Tyrode solution into the left ventricle (Fig 5-2). The 60 Hz oscillations in LVP produced co-incident oscillations in RVP which were about 1/4 the magnitude of those in the left ventricle. This interaction is considerably greater than that seen during aortic occlusion where RVP increase was 1/14 as large as LVP increase (Fig. 5-1). No pressure oscillations were observed during diastole confirming that the infusion method caused no vibration artefacts.

Figure 5-2. Left and right ventricular pressures during sinusoidal infusion of saline into the left ventricle. Top trace is left ventricular pressure (LVP) and bottom trace is right ventricular pressure (RVP).

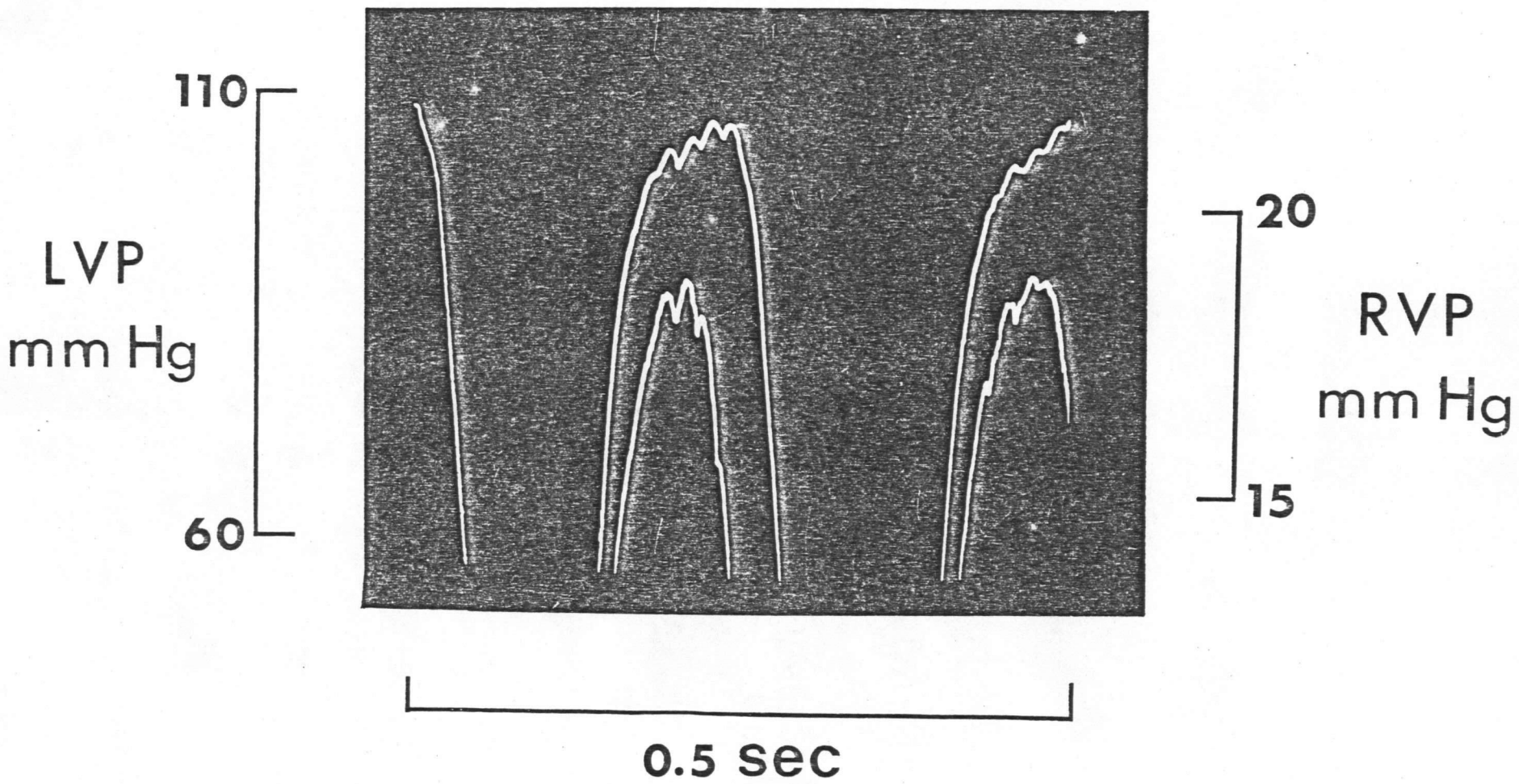
110
LVP
mm Hg
60
20
RVP
mm Hg
15
0.5 sec

Changes induced in LVP generation by alteration in right ventricular function

Occlusion of the pulmonary outflow caused an instantaneous increase in systolic RVP and a co-incident rise in peak LVP (Fig. 5-3). However, the magnitude of the rise was extremely variable, the major cause of this variation being the level of systemic blood pressure (Fig. 5-3A and B). At normal LVP the induced pressure rise caused by occlusion of the pulmonary arteries was negligible (Fig. 5-3A) whereas during systemic hypotension (produced in this case by controlled haemorrhage) the affect of increased RVP, was a prominent increase in LVP (Fig. 5-3B). Nevertheless this marked change in LVP was not accompanied by a change in peak left ventricular dP/dt. Unlike the case noted above, in which changes in left ventricular preload has no effect on RVP, a decrease in right ventricular preload (accomplished by inflating a balloon in the right atrium to diminish diastolic filling) caused an instantaneous drop in pressure in both ventricles. The instantaneous changes in LVP induced by changes in right ventricular preload or afterload were the same in animals with intact cardiac innervation and in denervated animals.

The right to left ventricular interaction was further investigated in excised hearts in rigor mortis. LVP was raised by injection of saline and monitored while it fell due to stress

Figure 5-3. The effects of pulmonary outflow occlusion (at arrows) on ventricular pressures and rates of change of pressure before (A) and after (B) induced systemic hypotension (see text). Abbreviations as in Fig. 5-2.

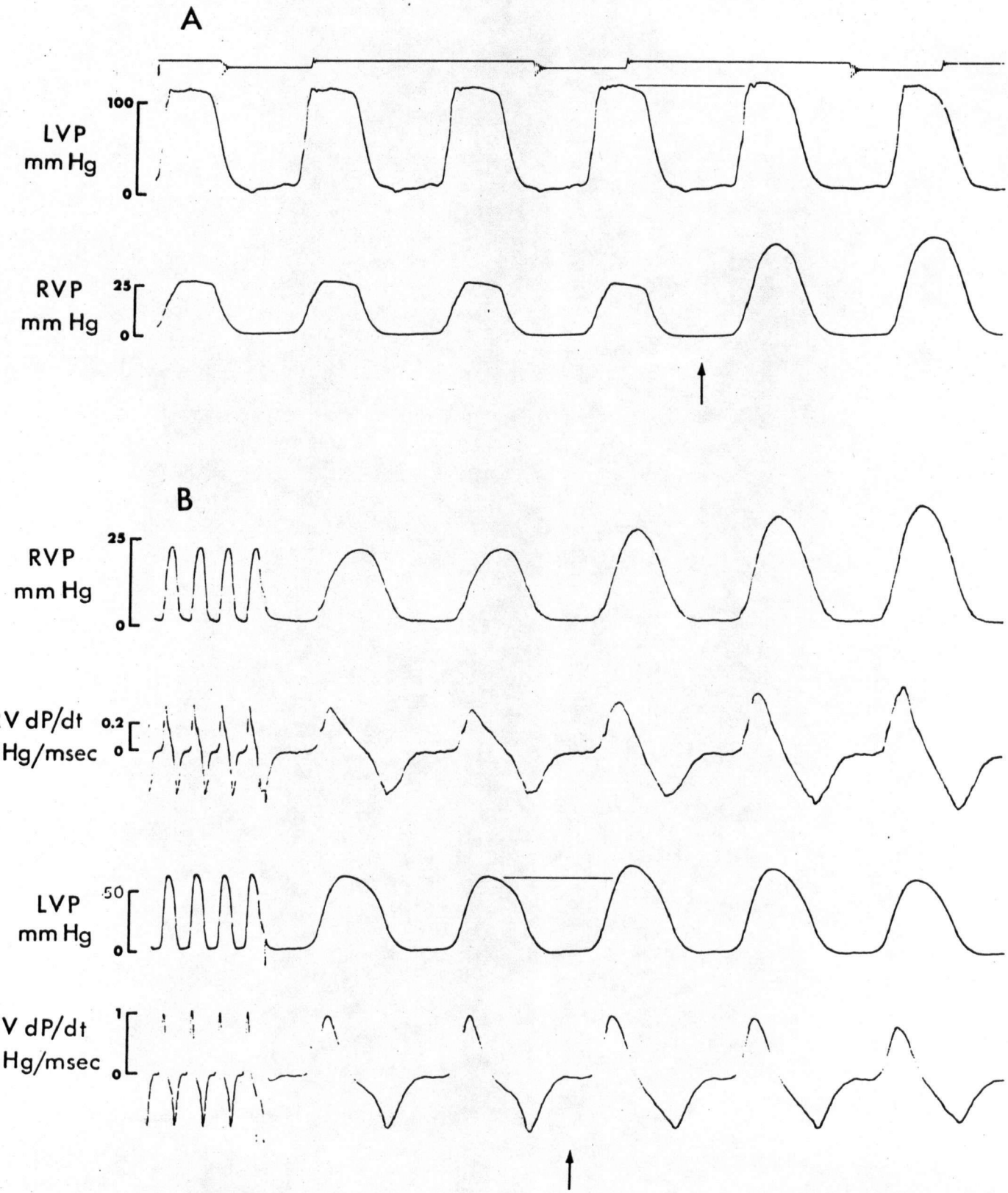
A
LVP
mm Hg
100
0
RVP
mm Hg
25
0
B
RVP
mm Hg
25
0
RV dP/dt
mm Hg/msec
0.2
0
LVP
mm Hg
50
0
LV dP/dt
mm Hg/msec
1
0

relaxation. When LVP has fallen to a predetermined level (e.g. 130, 100, 75 or 55 mm Hg in the heart used in Fig. 5-4A and B) the effect of sudden increased in RVP, caused by saline injection, on LVP was monitored. Suddenly increasing RVP caused a concomitant increase in LVP which later declined due to stress relaxation. Consequently it was possible to study the effect on LVP of step changes in RVP at the same mean level of LVP (see insert, Figure 5-4). In all hearts a range of mean LVP levels was applied, in random order, spanning from about 50 to 150 mm Hg and the same results were repeatedly obtained with a single heart. The change in LVP was compared to the step change in RVP which provoked the change in LVP and the ratio LVP: RVP was expressed as a % to indicate the degree of pressure transfer from the right to the left ventricle (Fig. f-4A). Figure 5-4A shows that at a given LVP the interaction from the right ventricle becomes more significant as the latter is distended and furthermore the degree of pressure transfer decreases as mean LVP increases at any given value of mean RVP. This finding suggests that pressure transfer from the right to left ventricle is determined by the relative distension of the right compared with that of the left and this was confirmed by replotting the data of Fig. 5-4A with RVP expressed as a fraction of LVP (Fig. 5-4B). When this experiment was reversed, i.e. when right ventricular volume was

Figure 5-4. Pressure transference from right to left ventricle in the excised heart in rigor mortis as a function of right ventricular pressure at a series of maintained left ventricular pressures. In 'A' RVP is indicated in absolute units whereas in 'B' RVP is expressed as a per cent of LVP. Pressure transference is expressed as a per cent of applied increments in RVP.

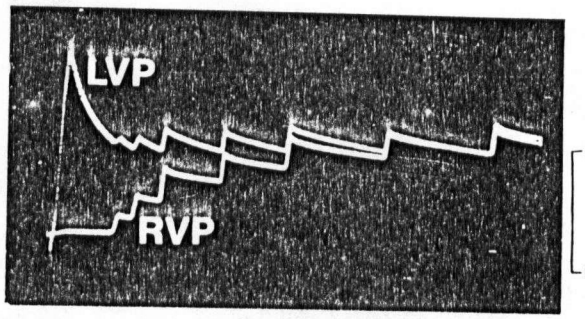
LVP
RVP
50
mm Hg
0

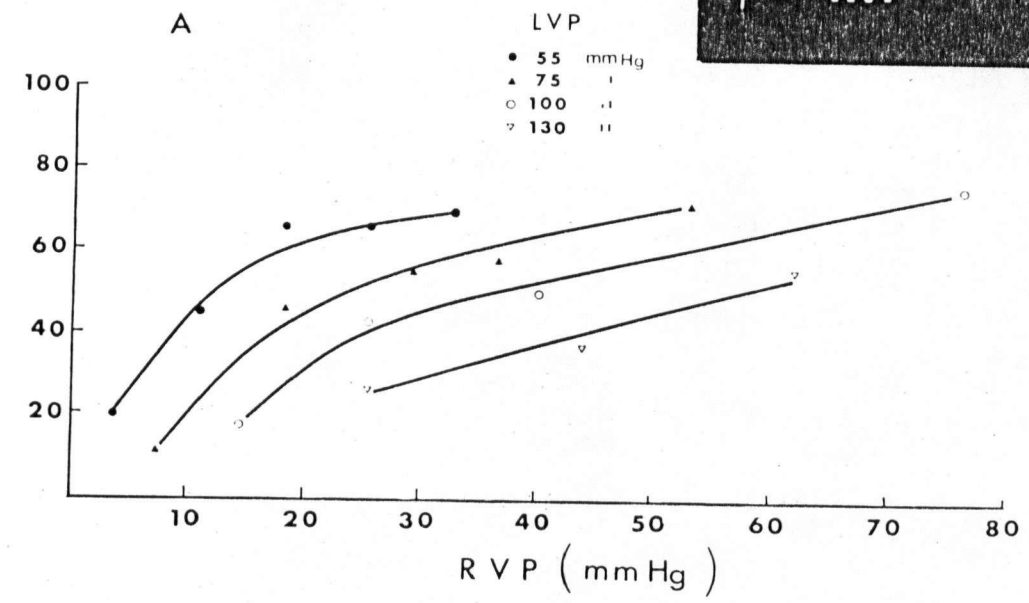
A
LVP
55 mm Hg
75
100
130
100
80
60
40
20
10
20
30
40
50
60
70
80
RVP (mm Hg)

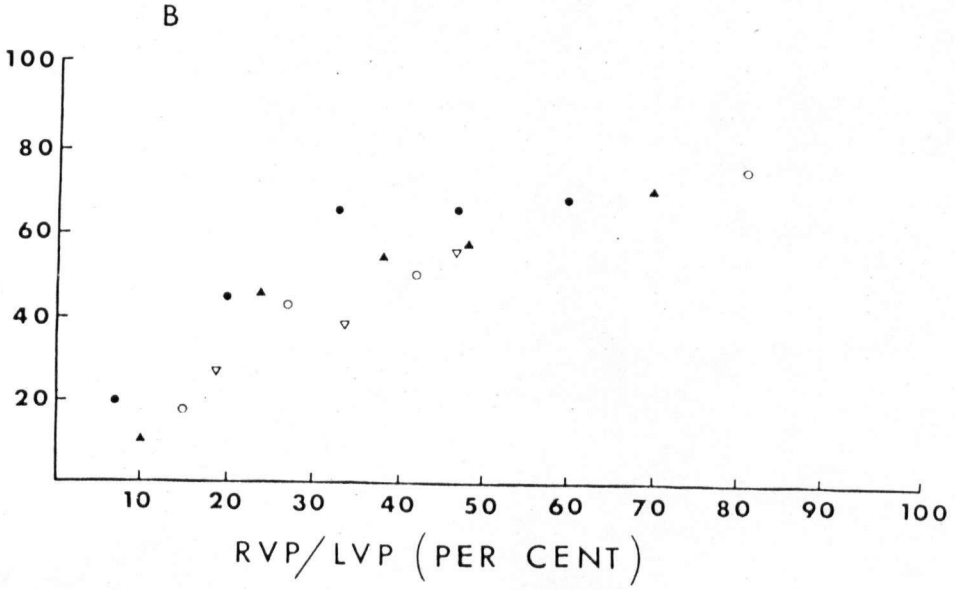
B
100
80
60
40
20
10
20
30
40
50
60
70
80
90
100
RVP/LVP (PER CENT)

held constant and the left ventricle inflated in steps, the degree of interaction closely matched that observed in vivo when 60 Hz oscillations were imposed on LVP. Step increases in RVP were about 1/4 - 1/5 the size of the increases in LVP throughout the physiological range of RVP and LVP. When high frequency (60 Hz) perturbation were applied to the left ventricle, at a mean LVP of 75 mm Hg, the oscillations in LVP were of the same magnitude as the systolic oscillations observed when this perturbation was applied to the ventricle in vivo. This confirmed that the mechanical state of the myocardium approximated that observed during systole.

Discussion

The present results have established that the left and right ventricles do not function independently of one another in respect to pressure generation. However, the degree of interaction which occurs in the intact animal and it physiological significance remains to be elucidated. There can be no doubt that marked changes in left ventricular afterload, accompanied by increased LVP, will promote an increase in the time derivative and absolute pressure generated in the right ventricle. This effect has been noted previously (Oboler et al, 1973), but the present data shows that the effects of increasing left ventricular afterload are transferred to the right ventricle throughout ejection and are not restricted to early systole (Oboler et al, 1973).

Since RVP responds to changes in LVP induced by altering left ventricular afterload but not by altering preload it is unlikely that the left to right interaction represents a direct transfer of intra-cavity pressure but is probably a reflection of a change in the mode of left ventricular contraction following aortic occlusion. During normal contraction the left ventricle initially shortens along the apex to base length with a coincident increase in circumference (Rushmer, 1956; Mitchell et al, 1965; Salisbury et al, 1965) and some septal protrusion

into the right ventricle is likely to occur. The fact that high frequency pressure oscillations were transferred from the left to the right ventricle during systole suggests that these geometrical changes of the left ventricle are responsible for the interaction observed during aortic occlusion. During the imposed oscillations the pressure increments would tend to make the left ventricle more spherical, in order to minimize stretch of the elastic components of the myocardium, and septal swelling would cause pressure transference to the right ventricle; the pressure decrements would cause the cavity to become more elliptical as the ventricle moved towards its unloaded geometry. This conclusion is supported by the fact that no interaction was observed when LVP was changed by altering the preload for Liedtke et al (1972) report that changes in preload affect only end-diastolic dimensions whereas increases in afterload tend to augment the shortening and circumferential swelling of the left ventricle. Although the present data has suggested a mechanism for left to right ventricular interaction the moderate changes in right ventricular pressure during severe alterations in left ventricular function do not appear sufficient to support the theory that the left ventricle plays a predominant role in generating right ventricular pressure (Starr et al, 1943; Bakos, 1950; Kagan, 1952).

The influence of right ventricular pressure on the left

ventricle, unlike the reverse interaction, does not depend on the pattern of contraction of the ventricles since pressure transfer occurred in the excised heart in rigor. This suggests that right ventricular pressures are, in part, directly superimposed on LVP. Since the right ventricle partially encapsulates the left it should be expected that RVP will contribute to the extramural pressure over which the left ventricle contracts. Certainly during pulmonary hypertension the septum is displaced to the left and becomes less convex (Dennis et al. 1974; Stool et al. 1974) further suggesting that the right ventricle compresses the left ventricular cavity. The present results obtained on excised hearts in rigor showed that as the right ventricle was distended or the left deflated, situations that will lead to the right more completely surrounding the left ventricle, a predictable increase in right to left pressure transference was obtained. At large relative distension of the right ventricle almost total right to left pressure transfer should occur and this was in fact observed in vivo during systemic hypotension.

The fact that these interactions were observed after surgical and chemical denervation of the heart further supports the suggestion that these instantaneous changes are due to a mechanical interaction. Furthermore, β blockade with propranolol was chosen over surgical sympathectomy since

homeometric autoregulatory mechanisms, intrinsic myocardial adaptations to alterations in load (Sarnoff et al., 1960), are known to be sharply diminished by this drug (Monroe et al.,1963) and were therefore shown to be of little importance in ventricular interplay. Consequently the present results show that, due to this mechanical interaction, the ventricles cannot be regarded as independent moieties. Fortunately, because of the insensitivity of peak left ventricular dP/dt to right ventricular function, these interactions do not argue against the usefulness of indices of myocardial contractility based upon time derivatives of left ventricular pressure. The independence of left ventricular dP/dt presumably results from the slightly asynchronous contraction of the two ventricles since right ventricular pressures are comparatively low when peak left ventricular dP/dt is attained.

General Discussion

The development of wave transmission models of arterial haemodynamics has advanced rapidly in the last two decades largely as a result of the inability of the windkessel approach to explain fundamental aspects of pressure flow relationships in arterial systems and as a consequence there has been a tendency to regard the windkessel model as outmoded (e.g., see Attinger, 1968). There is no doubt that the reason for rejection of the windkessel approach is that it assumes that the effects of cardiac ejection occur simultaneously throughout the arterial tree (McDonald and Taylor, 1959) a situation apparently never approximated in mammalian systems. However this situation is encountered in the bullfrog and there is reason to believe that the circulations of other species are also well described by such an approach. Consideration of the cardiovascular features conducive to generation of wave transmission phenomena have indicated that low heart rates and short arterial trees are prerequisites for a windkessel approach. In homeotherms higher heart rates of smaller species offset the effects of shorter arterial lengths (Kenner, 1970) and undoubtedly this largely accounts for the unsuitability of a windkessel model; thus it would appear that small poikilotherms are the most likely candidates for this approach. It is

generally believed that wave transmission effects, specifically wave reflections, are advantageous and contribute to circulatory efficiency. Changes in impedance patterns caused by reflections result in a reduction in work expended in producing the pulsatile component of blood flow (Taylor, 1964; O'Rourke, 1967) although this factor is a relatively small contributor to total cardiac work. In addition, however, reflections result in a node of the pressure wave occurring at the heart for normal heart rates (McDonald, 1974) and the resulting decrease in pulse pressure implies that the systolic pressures against which the heart ejects are lower. As a result there must be a concomitant reduction in the tension-time integral (total work) of the contracting myocardium. All other things being equal it would be expected that the pressures of natural selection would result in heart rates and pulse wave velocities in poikilotherms which would generate these wave reflection phenomena, and therefore it must be concluded that the costs of such adaptions in these species outweigh the advantages.

While models of arterial systems permit description of arterial pressure-flow interrelationships a complete understanding of arterial pressures and flows requires a knowledge of the ejection pattern of the heart. Conversely this ejection pattern is highly dependent on the hydraulic load presented by the arterial system (Milnor, 1975) and thus investigations of

the mechanics of cardiac contraction and of the physical properties of the arterial bed must be viewed as complementary, rather than independent studies and a major facet of the present study has been an extension of this approach to non-mammalian vertebrates. Integration of studies on cardiac pumping and arterial haemodynamics in mammals is highly complicated owing to the complex dynamic properties of the arterial beds and the non-linear connection between the heart and arteries, i.e. via the aortic and pulmonic valves (Milnor, 1975). Results of the present study, which indicate that some vertebrate arterial systems are well described by simple windkessel models, suggest that a more tractable approach to this problem may be gained by examining non-mammalian species.

Summary

1. Pressure-flow relationships in the arterial system of the bullfrog were well described in terms of a two component windkessel model whereas wave transmission effects were negligible.
2. During apnoea blood flow redistribution away from the lungs was accomplished by vasomotion of the peripheral circulations. No 'active shunting' role could be ascribed to the conus arteriosis.
3. Contraction of the conus arteriosis generated a significant portion of pulmocutaneous arterial flow while making only a minor contribution to systemic ejection. Contraction also served to draw the synangial and pylangial valves of the conus sufficiently close together to ensure competency. Since the conus did not refill before the next ventricular contraction the conus presents undistended valves to the ventricle and arterial arches during diastole. Occlusion of the coronary blood supply resulted in a complete loss of contractility of the conus arteriosis.
4. The compliance of the dorsal aorta of the cod is not negligible and as a result dynamic interaction between the gill and systemic circulations is complex. Pulsatility of gill blood flow was augmented and a marked 'damping'

of the pressure pulse distal to the gills observed.

5. Mean arterial pressure (143 ± 2 mm Hg) and cardiac output (219 ml/min per kg.) of the duck, Anas platyrhynchos, were high compared with those of mammals of similar size and 75% of this cardiac output is delivered to the wings, flight muscles and head by the brachiocephalic arteries.

6. Wave transmission effects, specifically wave reflections, had a marked effect on systemic pressure-flow relations in the duck indicating that this arterial system is not well described by a windkessel model.

7. In the rabbit, artificially induced discrete reflections from the abdominal aorta closely mimicked the effects of peripheral vasoconstriction and masked those of vasodilation; thus the suggestion that the major sites of reflection in the mammalian arterial system are in the arteriolar resistance vessels was supported. Distributed reflections from continuous variations in arterial wall stiffness also contribute to the total reflected wave although this contribution does not appear to be predominant.

8. The immediate effect of abrupt alteration in the function of either ventricle on pressures in both ventricles has been examined in rabbits. Maximal increases in left ventricular afterload (aortic occlusion) caused not only a near doubling of peak left ventricular pressure (195%

± 5% but also an immediate significant increase (13.2% ± 1.3 %) in right ventricular pressure. On the other hand when similar increases in left ventricular pressure were induced by sudden changes in preload no alteration in right ventricular pressure was seen. High frequency oscillatory infusion of saline into the left ventricle produced co-incident oscillations in both ventricular pressures during systole. These findings were interpreted in terms of present knowledge of the asynchronous patterns of contraction of the mammalian heart.

9. Left ventricular pressure generation was altered by all interventions with right ventricular performance and although this interaction was minimal at normal physiological pressures it was greatly potentiated by systemic hypotension or pulmonary hypertension. A direct transference of pressure from right to left ventricle was also observed when the ventricles of excised hearts in rigor mortis were inflated with saline and the degree of this transference was comparable with that observed in the normally beating hearts.

BIBLIOGRAPHY

Attinger, E.O. (1968). Analysis of pulsatile blood flow. Advan. Biomed. Eng. Med. Phys. 1: 1-59.

Attinger, E.O., Anne, A. and McDonald, D.A. (1966). Use of Fourier series for the analysis of biological systems. Biophys. J. 6: 291-304.

Attinger, E., Anne, A., Mikami, T. and Sugawara, H. (1966). Modelling of pressure - flow relations in arteries and veins. In Hemorheology, ed A.L. Copley. Oxford: Pergamon.

Bakos, A.C.P. (1950). The question of function of the right ventricular myocardium: an experimental study. Circulation 1: 724-732.

Barnard, A.C.L., Hunt, W.A., Timlake, W.P. and Varley, E. (1966a). A theory of fluid flow in compliant tubes. Biophys. J. 6: 717-724.

Barnard, A.C.L., Hunt, W.A., Timlake, W.P. and Varley, E. (1966b). Peaking of the pressure pulse in fluid-filled tubes of spatially varying compliance. Biophys. J. 6: 735-746.

Bauer, D.J. (1938). Effect of asphyzia upon the heart rate of rabbits at different ages. J. Physiol. 93: 90-103.

Bemis, C.E., Serur, J.K, Borkenhagen, D., Sonnenblick, E.H., and Urschel, C.W. (1974). Influence of right ventricular filling pressure on left ventricular pressure and dimen-

sion. Circulation Res. 34: 498-504.

Bergel, D.H. (1961a). The static elastic properties of the arterial wall. J. Physiol. 156: 445-457.

Bergel, D.H. (1961b). The dynamic elastic properties of the arterial wall. J. Physiol. 156: 458-469.

Bergel, D.H. (1964). Arterial viscoelasticity. In: Pulsatile Blood Flow, ed E.O. Attinger. New York: McGraw.

Bergel, D.H. and Milnor, W.R. (1965). Pulmonary vascular impedance in the dog. Circulation Res. 16: 401-415.

Brady, A.J. (1964). Physiology of the amphibian heart. In Physiology of the Amphibia, ed J.A. Moore. New York, London: Academic.

Brucke, E. von (1852). Beitrage zur vergleichenden Anatomic und Physiologie des Gefass - Systemes. Denkschr. Adad. Wiss. Wien 3: 335-367.

Burton, R.R. and Smith, A.H. (1968). Blood and air volumes in the avian lung. Poultry Sci. 47: 85-91.

Caro, C.G. and McDonald, D.A. (1961). The relation of pulsatile pressure and flow in the pulmonary vascular bed. J. Physiol. 157: 426-453.

Case, R.B., Roselle, M.A. and Nassar, M.E. (1966). Simplified method for calibration of electromagnetic flowmeters. Med. Res. Eng. 5: 38-34.

Cleary, E.G. (1961). Elastin, collagen and calcium content of

the human aorta (abst). Med. Res. 1: 12.

Cleary, E.G. (1963). Comparative and correlative study of the non-uniform arterial wall. M.D. Thesis. University of Sydney.

Cleary, E.G. and McCloskey, D.I. (1962). Aortic elastin and collagen: Age changes in the rabbit and species differences due to posture (abst.) Aust. J. Sci. 25: 111.

Cooley, J.W. and Tukey, J.W. (1965). An algorithm for the machine calculation of complex Fourier series. Math. of Comput. 19: 297-301.

Dawes, G.S., Handler, J.J. and Mott, J.C. (1957). Some cardiovascular responses in foetal, newborn and adult rabbits. J. Physiol. 139: 123-136.

DeLong, K.T. (1962). Quantitative analysis of blood circulation through the frog heart. Science 138: 693-694.

Emilio, M.G. and Shelton, G. (1972). Factors affecting blood flow to the lungs in the amphibian, Xenopus laevis. J. Exp. Biol. 56: 67-77.

Elzinga, G., van Grondell, R., Westerhof, N. and van den Bos, G.C. (1974). Ventricular interference. Am. J. Physiol. 226: 941-947.

Fich, S. and Welkowitz, W. (1967). A tapered reflectionless model of the aorta. Dig. 7th Int. Conf. Med. Biol. Eng. 51.

Fich, S. Welkowitz, W., and Hilton, R. (1966). Pulsatile blood flow in the aorta. Biomedical Fluid Mechanics Symposium. New York: ASME.

Folkow, B., Nilsson, N.J. and Yonce, L.R. (1967). Effects of 'diving' on cardiac output in ducks. Act. physiol. scand. 70: 347-361.

Fox, H. (1933). Arteriosclerosis in lower mammals and birds. In Arteriosclerosis, ed E.V. Cowdry. New York: Macmillan.

Foxon, G.E.H. (1947). The mode of action of the heart of the frog. Proc. Zool. Soc. London 116: 565-574.

Foxon, G.E.H. (1955). Problems of the double circulation in vertebrates. Biol. Rev., 30: 196-228.

Foxon, G.E.H. (1964). Blood and Respiration. Physiology of the Amphibia, ed J.A. Moore. New York and London: Academic Press.

Frank, O. (1899). Die Grundform des arteriellen Pulses. Erste Abhandlung. Mathematische Analyse. Z. Biol., 37: 483-526.

Franklin, D.L., Van Citters, R.L. and Rushmer, R.F. (1962). Balance between right and left ventricular output. Circulation Res. 10: 17-26.

Gessner, F.B. (1973). Hemodynamic theories of atherogenesis. Circulation Res. 33: 259-266.

Gessner, U. and Bergel, D.H. (1964). Frequency response of electromagnetic flowmeters. J. appl. Physiol. 19: 1209-1211.

Gillespie, J.A. and Rae, R.M. (1972). Constrictor and compliance responses of some arteries to nerve or drug stimulation. J. Physiol. 223: 109-130.

de Graaf, A.R. (1957). Investigations into the distribution of blood in the heart and aortic arches of Xenopus laevis (Daud.). J. Exp. Biol. 34: 143-172.

Greenfield, J.C., Patel, D.J., Mallos, A.J. and Fry, D.H. (1966). Evaluation of the Kolin type electromagnetic flowmeter and the pressure gradient technique. J. appl. Physiol. 17: 372-374.

Haberich, F.J. (1965). The functional separation of venous and arterial blood in the univentricular frog heart. An. N.Y. Acd. Sci. 127: 459-476.

Harkness, M.L.R., Harkness, R.D. and McDonald, D.A. (1957). The collagen and elastin content of the arterial wall in the dog. Proc. Roy. Soc. B. 146: 541-551.

Hepp, A., Gradistanic, G., Kissling, G. and Jacob, R. (1973). Influence of catheter position on blood pressure values in the pulmonary artery of the dog. Bas. Res. Cardiol. 68: 470-479.

Holeton, G.F. and Randall, D.J. (1967a). Changes in blood pressure in the rainbow trout during hypoxia. J. Exp. Biol. 46: 297-305.

Holeton, G.F. and Randall, D.J. (1967b). The effect of hypoxia

upon the partial pressure of gases in the blood and water afferent and efferent to the gills of rainbow trout. J. Exp. Biol. 46: 317-327.

Hughes, G.M. (1966). The dimension of fish gills in relation to their function. J. Exp. Biol. 45: 177-195.

Hutchison, V.H., Whitford, W.G., and Kohl, M. (1968). Relation of body size and surface area to gas exchange in anurans. Physiol. Zool. 41: 65-85.

Johansen, K. (1962). Cardiac output and pulsatile flow in the teleost Gadus morhua. Comp. Biochem. Physiol. 7: 169-174.

Johansen, K. and Ditadi, A.S.F. (1966). Double circulation in the giant toad, Bufo paracnemis. Physiol. Zool. 39: 140-150.

Jones, D.R. (1972). The effect of thermal acclimation on heart rate and oxygen consumption of frogs during submergence. Comp. Biochem. Physiol. 41A: 97-104.

Jones, D.R. (1972). Anaerobiosis and the oxygen debt in an anuran amphibian, Rana esculenta (L.). J. comp. Physiol. 77: 356-382.

Jones, D.R. and Holeton, G. (1972a). Cardiac output of ducks during diving. Comp. Biochem. Physiol. 41A: 629-645.

Jones, D.R. and Holeton, G. (1972b). Cardiovascular and respiratory responses of ducks to hypocapnic hypoxia. J. exp. Biol. 56: 657-666.

Kagan, A. (1952). Dynamic responses of the right ventricle following extensive damage by cauterization. Circulation 5: 816-823.

Katz, L.N. and Stamler, J. (1953). Experimental Atherosclerosis. Springfield (U.S.A.): Thomas.

Kenner, T. (1970). Flow and Pressure in Arteries. In Biomechanics, ed Y.C. Fung, N. Perrone and M. Anliker. Englewood Cliffs (U.S.A.): Prentice-Hall.

Keys, A. and Bateman, J.B. (1932). Branchial responses to adrenalin and pitressin in the eel. Biol. Bull. 63: 327-336.

Kolder, H., Horres, A.D. and Brecher, G.A. (1963). Influence of temperature on development of rigor mortis in dog hearts. Circulation Res. 13: 218-222.

Laks, M.M., Garner, D. and Swan, H.J.C. (1967). Volumes and compliances measured simultaneously in the right and left ventricle of the dog. Circulation Res. 20: 565-569.

Lander, J. (1964). The Shark Circulation (B.Sc. Med. Dissertation). Sydney: University of Sydney.

Learoyd, B.M. and Taylor, M.G. (1966). Alterations with age in the visco-elastic properties of human arterial walls. Circulation Res. 18: 278-292.

Liedtke, A.J., Pasternac, A., Sonnenblick, E.H. and Gorlin, R. (1972). Changes in canine ventricular dimensions with

acute changes in preload and afterload. Am. J. Physiol. 223: 820-827.

McCloskey, D.I. and Cleary, E.G. (1974). Chemical composition of the rabbit aorta during development. Circulation Res. 34: 828-835.

McDonald, D.A. (1955). The relation of pulsatile pressure to flow in arteries. J. Physiol. 127: 533-552.

McDonald, D.A. (1968). Regional pulse-wave velocity in the arterial tree. J. appl. Physiol. 24: 73-78.

McDonald, D.A. (1974). Blood Flow in Arteries. Baltimore, Williams and Wilkins.

McDonald, D.A. and Gessner, U. (1968). Wave attenuation in visco-elastic arteries. In Hemorheology, ed A.L. Copley. Oxford: Pergamon Press.

McDonald, D.A. and Taylor, M.G. (1959). The hydrodynamics of the arterial circulation. Progr. Biophys. 9: 107-173.

Middleton, C.C. (1965). Naturally occurring atherosclerosis in broad-breasted bronze turkeys. In Comparative Atherosclerosis ed J.C. Roberts jr. and R. Straus. New York: Harper & Row.

Milnor, W.R., Bergel, D.H. and Bargainer, J.D. (1966). Hydraulic power associated with pulmonary blood flow and its relation to heart rate. Circulation Res. 19: 467-480.

Milnor, W.R. (1975). Arterial impedance as ventricular after-

load. Circulation Res. 36: 565-570.

Mitchell, J.H., Mullins, C.B., Gupta, D.N., Payne, R.M., and Harris, M.D. (1965). Dimension and volume changes of the left ventricle. Federation Proc. 24: 146.

Monroe, R.G., LaFarge, C.G., Gamble, W.J., Rosenthal, A. and Honda, S. (1968). Left ventricular pressure volume relations and performance as affected by sudden increases in developed pressure. Circulation Res. 22: 333-344.

Morris, R.W. (1974). Function of the anuran conus arteriosis. J. Exp. Biol, 61: 503-520.

Mott, J.C. (1957). The cardiovascular system. In "The Physiology of Fishes" ed M.E. Brown. New York: Academic Press.

Moulopoulos, S.D., Sarcas, A., Stametolopoulos, A., and Arealis, E. (1965). Left ventricular preformance during by-pass or distension of the right ventricle. Circulation Res. 17: 484-491.

Murdaugh, H.v., Robin, E.D., Millen, J.E. and Drewry, W.F. (1965). Cardiac output determinations by the dye dilution method in Squalus acanthias. Am. J. Physiol. 209: 723-726.

Noble, G.K. (1925). The integumentary, pulmonary and cardiac modifications correlated with increased cutaneous respiration in the Amphibia: A solution to the 'hairy

frog' problem. J. Morph. 40: 341-416.

Noordergraaf, A. (1969). Hemodynamics. In "Biological Engineering." ed H.P. Schwan. New York: McGraw-Hill.

Oboler, A.A., Keefe, J.F., Gaasch, W.H., Banas, J.S. jr. and Levin, H.J. (1973). Influence of left ventricular isovolumic pressure upon right ventricular pressure transients. Cardiology 58: 32-44.

O'Rourke, M.F. (1967a). Steady and pulsatile energy losses in the systemic circulation under normal conditions and in simulated arterial disease. Cardiovas. Res. 1: 313-326.

O'Rourke, M.F. (1967b). Pressure and flow waves in systemic arteries and the anatomical design of the arterial system. J. appl. Physiol. 23: 129-149.

O'Rourke, M.F. and Taylor, M.G. (1966). Vascular impedance of the femoral bed. Circulation Res. 18: 126-139.

O'Rourke, M.F. and Taylor, M.G. (1967). Input impedance of the systemic circulation. Circulation Res. 20: 365-380.

O'Rourke, M.F., Blazek, J.V.,,Morreels, C.L. jr. and Krovetz, L.J. (1968). Pressure wave transmission along the human aorta. Circulation Res. 23: 567-579.

Ostlund, E. and Fange, R. (1962). Vasodilation by adrenaline and noradrenaline and the effects of some other substances on perfused gills. Comp. Biochem. Physiol. 5: 307-309.

Pace, J.B., Cox, R.H., Alvarez-Vara, F. and Karreman, G. (1972).

Influence of sympathetic nerve stimulation on pulmonary hydraulic input power. Am. J. Physiol. 222: 196-201.

Patel, D.J., de Freitas, F.M. and Fry, D.L. (1963). Hydraulic input impedance to aorta and pulmonary artery in dogs. J. appl. Physiol. 18: 134-140.

Peterson, L.H., Jensen, R.E. and Parnell, J. (1960). Mechanical properties of arteries in vivo. Circulation Res. 8: 622-639.

Pierce, D.E., Morrow, A.G. and Braunwald, E. (1964). Intra-operative studies of the mechanism of obstruction and its haemodynamic consequences. Circulation 30 Suppl. 4: 152-213.

Prichard, R.W. (1965). Spontaneous atherosclerosis in pigeons. In Comparative Atherosclerosis, ed J.C. Roberts jr. and R. Straus. New York: Harper and Row.

Randall, D.J. (1968). Functional morphology of the heart in fishes. Am. Zool. 8: 179-189.

Remington, J.W. (1960). Contour changes of the aortic pulse during propagation. Am. J. Physiol. 199: 331-334.

Remington, J.W. and O'Brien, L.J. (1970). Construction of the aortic flow pulse from pressure pulse. Am. J. Physiol. 218: 437-447.

Reuben, S.R., Swadling, J.P., Gersch, G.J. and Lee, G. de. J. (1971). Impedance and transmission properties of the

pulmonary arterial system. Cardiovas. Res. 5: 1-9.

Rushmer, R.F. (1956). Initial phase of ventricular systole: asynchronous contraction. Am. J. Physiol. 184: 188-194

Sabatier, A. (1873). Etudes sur le coeur et la circulation centrale dans la serie des vertebres. Paris: Montpellier.

Salisbury, P.F., Cross, C.E. and Rieben, P.a. (1965). Phasic dimensional changes in the left ventricle. Arch. Intern. Physiol. Biochim. 73: 188-208.

Sarnoff, S.J. Mitchell, J.H., Gilmore, J.P., and Remensnyder, J.P. (1960). Homeometric autoregulation in the heart. Circulation Res. 8: 1077-1091.

Satchell, G.H. (1971). Circulation in Fishes. Cambridge: Cambridge Univ. Press.

Satchell, G.H. and Jones, M.P. (1967). The function of the conus arteriosus in the Port Jackson shark, Heterodontus portusjacksoni. J. Exp. Biol. 46: 373-382.

Sharma, H.L. (1957). The anatomy and mode of action of the heart of the frog, Rana tigrinia. J. Morph. 100: 303-334.

Sharma, H.L. (1961). The circulatory mechanism and anatomy of the heart of the frog, Rana pipiens. J. Morph. 109: 323-349.

Shelton, G. (1970). The effect of lung ventilation on blood flow to the lungs and body of the amphibian, Xenopus

laevis. Resp. Physiol. 9: 183-196.

Shelton, G. and Jones, D.R. (1965a). Central blood pressure and heart output in surfaced and submerged frogs. J. Exp. Biol. 42: 339-357.

Shelton, G. and Jones, D.R. (1965b). Pressure and volume relationships in the ventricle, conus, and arterial arches of the frog heart. J. Exp. Biol. 43: 479-488.

Shelton, G. and Jones, D.R. (1968). A comparative study of central blood pressures in five amphibians. J. Exp. Biol. 49: 631-643.

Simons, J.R. (1959). The distribution of blood from the heart in some amphibia. Proc. Zool. Soc. London, 132: 51-64.

Speckmann, E.W. and Ringer, R.K. (1963). The cardiac output and carotid and tibial blood pressure of the turkey. Can. J. Biochem. Physiol. 41: 2337-2341.

Spector, W.S. (1956). Handbook of Biological Data. Philadelphia: Saunders.

Spencer, M.P. and Greiss, F.C. (1962). Dynamics of ventricular ejection. Circulation Res. 10: 274-279.

Starling, E.H. (1915). The Linacre lecture on the law of the heart. London: Longman's Green.

Starr, L., Jaffers, W.A., and Meade, R.H. (1943). The absence of conspicuous increments of venous pressure after severe damage to the right ventricle of the dog, with a discus-

sion of the relation between clinical congestive failure and heart disease. Am. Heart J. 26: 291-301.

Stevens, E.D. (1968). The effect of exercise on the distribution of blood in various organs in rainbow trout. Com. Biochem. Physiol. 25: 615-625.

Stevens, E. Don, and Randall, D.J. (1967a). Changes in blood pressures, heart rate and breathing rage during moderate swimming activity in rainbow trout. J. Exp. Biol. 46: 307-315.

Stevens, E. Don, and Randall, D.J. (1967b). Changes in gas concentrations in blood and water during moderate swimming activity in rainbow trout. J. Exp. Biol. 46: 329-337.

Stool, E.W., Mullins, C.B., Leshin, S.J. and Mitchell, J.H. " (1974). Dimensional changes of the left ventricle during acute pulmonary arterial hypertension in dogs. Am. J. Cardiol. 33: 868-875.

Sturkie, P.D. (1966). Cardiac output in ducks. Proc. Soc. exp. Biol. Med. 132: 487-488.

Sturkie, P.D. and Vogel, J.A. (1959). Cardiac output, central blood volume and peripheral resistance in chickens. Am. J. Physiol. 197: 1165-1166.

Taylor, M.G. (1959). An approach to an analysis of the arterial pulse wave. II; Fluid oscillations in an elastic pipe.

Phys. Med. Biol. 1: 321-239.

Taylor, M.G. (1964). Wave travel in arteries and the design of the cardiovascular system. In Pulsatile Blood Flow, ed E.O. Attinger. New York: McGraw-Hill.

Taylor, M.G. (1965). Wave travel in a non-uniform transmission line, in relation to pulses in arteries. Phys. in Med. Biol. 10: 539-550.

Taylor, M.G. (1966). The input impedance of an assembly of randomly branching elastic tubes. Biophys. J. 6: 29-51.

Taylor, R.R., Covell, J.W., Sonnenblick, E.H. and Ross, J. jr. (1967). Dependence of ventricular distensibility on filling of the opposite ventricles. Am. J. Physiol. 213: 711-718.

Templeton, G.H., Mitchell, J.H., Ecker, R.R., and Blomqvist, G. (1970). A method for the measurement of dynamic compliance of the left ventricle in dogs. J. Appl. Physiol. 29: 742-745.

Toews, D.P., Sheltong, G. and Randall, D.J. (1971). Gas tensions in the lungs and major blood vessels of the urodele amphibian, Amphiuma tridactylum. J. Exp. Biol. J. Exp. Biol. 55: 47-61.

Toews, D.P. (1969). Respiration and Circulation in Amphiuma Tridactylum. Ph.D. thesis, University of British Columbia.

Tsien, H.S. (1954). Engineering Cybernetics. New York: McGraw-

Hill.

Vandervael, F. (1933). Recherches suh le mecanisme de la circulation du sang dans le coeur des Amphibiens anoures. Archs. Biol., Paris 44: 571-606.

Westerhof, N. Sipkema, P., Van Den Bos, G.C. and Elzinga, G. (1972). Forward and backward waves in the arterial system. Cardiovas. Res. 6: 648-656.

White, F.N. (1968). Functional anatomy of the heart of reptiles. Am. Zool. 8: 211-219.

Womersley, J.R. (1958). The mathematical analysis of the arterial circulation in a state of oscillatory motion. Wright Air Development Center, Technical Report WADC-TR56-614.

Appendix

To demonstrate the applicability of Fourier transform techniques in determining frequency dependent parameters of a physical system the amplitude response of a manometer system was evaluated as follows. The manometer system to be tested and a very high frequency manometer system capable of accurately recording pressure signals throughout the range over which the test system is to be examined (0-60 Hz) were connected to the same pressure source. The pressure source applied a transient pressure to both manometers and Fig. A-1A illustrates the distorted pressure signal recorded by the test manometer and 'true' profile recorded by the reference manometer. Fig. A-1B illustrates the frequency response for the test manometer determined by comparing the Fourier transforms of the two pressure signals. A'pop-test' was also applied to the test manometer to determine its resonant frequency and damping coefficient so that a theoretical frequency response curve could be predicted from manometer theory (see McDonald, 1974). This curve is also shown in Fig. A-1B. A limitation of this Fourier transform approach is that the transient input to the system of interest, e.g. the pressure pulse in the above example, must exhibit a frequency spectrum which overlaps the frequency range one wishes to examine. Although for arbitrary transients this spectrum cannot be precisely determined until

Figure A-1. A. Output of reference (upper trace) and test (lower trace) manometers in response to a transient pressure pulse.

B. Test manometer frequency response curve calculated from Fourier transforms of the signals illustrated in (A) (dots) and according to manometer theory (solid line).

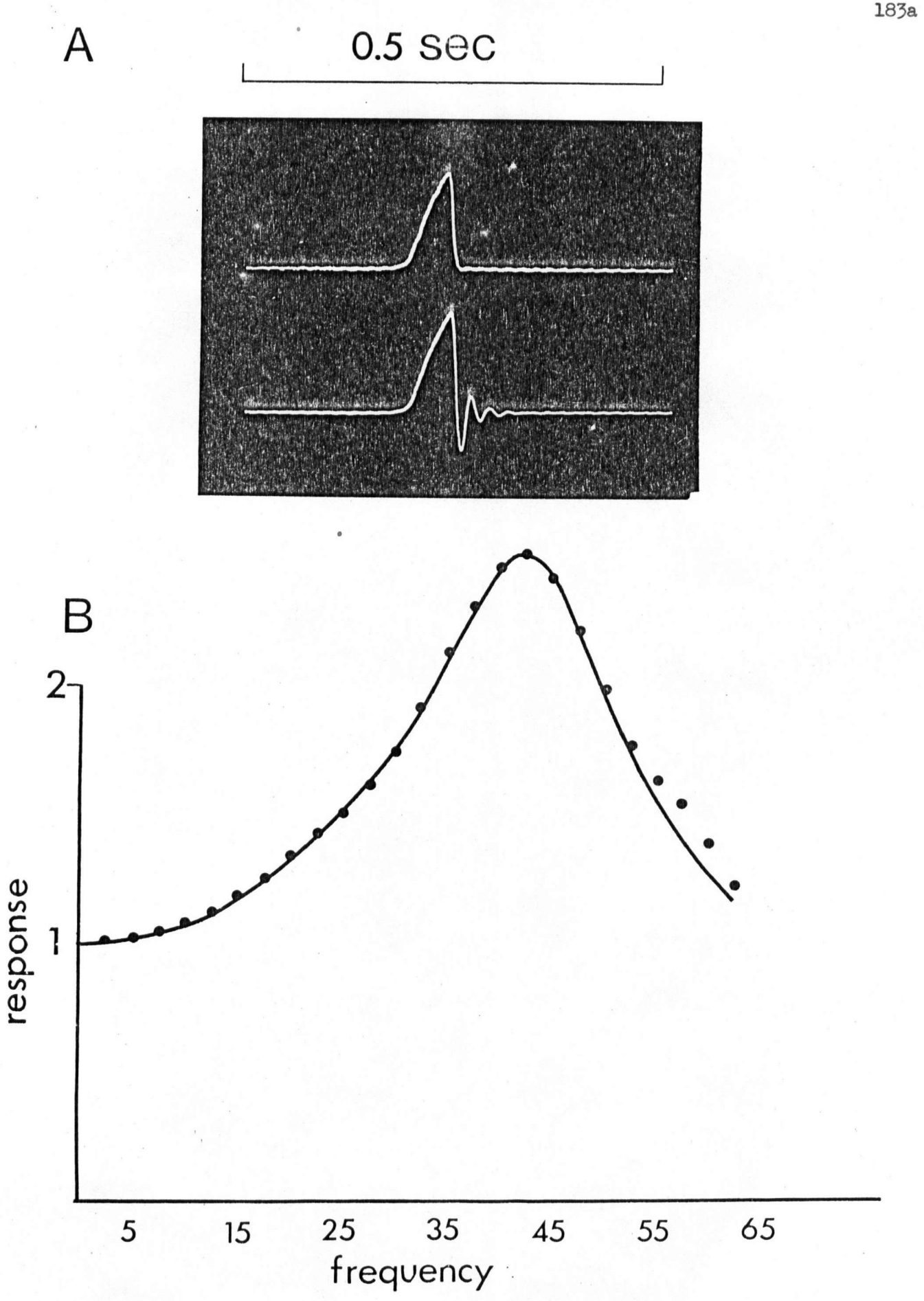
A
0.5 sec
B
2
1
response
5
15
25
35
45
55
65
frequency

data analysis has been completed most unidirectional transient signals (as opposed to transient oscillations) exhibit a flat amplitude spectrum up to frequencies which approach 1/T, where T is the duration of the transient. Thus in Section IV by applying unidirectional pressure pulses lasting at most 0.2 sec. to the hydraulic model an appropriate input spectrum for examining the frequency range, 1-10 Hz, was always attained. Additional precautions are required to avoid 'aliasing' errors (Blackmand and Tukey, 1959) which are errors that result from recording frequencies too high to be detected at the sampling rate of the A-D conversion system. Such errors can be avoided by sampling at a rate far above the highest frequency of interest and electronically filtering out all signals oscillating more rapidly than half the sampling frequency.

Bibliography

Blackman, R.B. and Tukey, J.W. (1959). The Measurement of Power Spectra. New York: Dover.

McDonald, D.A. (1974). Blood Flow in Arteries. Baltimore: Williams and Wilkins.